

# ResearchOnline@JCU

This file is part of the following reference:

**Zou, Huibin (2011) *Characterization of selenium containing proteins in the coral *Acropora millepora**. PhD thesis, James Cook University.**

Access to this file is available from:

<http://eprints.jcu.edu.au/29162/>

*The author has certified to JCU that they have made a reasonable effort to gain permission and acknowledge the owner of any third party copyright material included in this document. If you believe that this is not the case, please contact [ResearchOnline@jcu.edu.au](mailto:ResearchOnline@jcu.edu.au) and quote <http://eprints.jcu.edu.au/29162/>*

**Characterization of selenium containing proteins in  
the coral *Acropora millepora***

**Thesis submitted by**

**Huibin ZOU, Master of Science, Ocean University of China**

**In April 2011**

**For the degree of Doctor of Philosophy**

**In the School of Pharmacy and Molecular Sciences**

**at James Cook University**



## **Statement of Access**

I, the undersigned, author of this work, understand that James Cook University will make this thesis available for use within the University Library and, via the Australian Digital Theses network, for use elsewhere.

I understand that, as an unpublished work, a thesis has significant protection under the Copyright Act.

Huibin ZOU

Date

## **Statement of Sources**

I declare that this thesis is my own work and has not been submitted in any form for another degree or diploma at any university or other institution of tertiary education. Information derived from the published or unpublished work of others has been acknowledged in a Statement of Contribution of others and a list of references is given.

Huibin ZOU

Date

# Acknowledgements

## Supervision support

I gratefully thank the following experts for providing the academic support:

- Prof. David Miller: as my supervisor, David gave me the opportunity to do the PhD in his lab. Without his support and direction, I could not get my project done.
- Prof. Ross Crozier: as my co-supervisor, Ross gave lots of academic suggestion in the beginning of my PhD study. I am sorry to lose him in the middle of my candidature.
- Dr. Murray Davies and Dr. Suzanne Smith: as my co-supervisors, Murray and Suzanne gave the academic supervision for the binding experiments in chapter 5.
- Dr. Eldon Ball and Dr. David Hayward: thanks for their fruitful discussion about coral genomics and developmental biology.
- Dr. Tracy Ainsworth: as my co-supervisor, Tracy gave the academic supervision for the immune-histology experiments in chapter 4.

## Technical support

I appreciate the following technical help from other research staff and students:

- Chapter 2: bioinformatics support from Brent Knack and Dr. Sylvain Foret.
- Chapter 3: sampling support from Marcelo Visentini-Kitahara and Dr. Zoe Richards; qPCR technical support from Francois Seneca and Yvonne Weiss.
- Chapter 4: experimental support from Brent Knack and Dr. Chuya Shinzato.
- Chapter 5: experimental support from Dr Eskenda Mume, Dr Yi Hu, Dr. Gary Perkins.

## Funding support

My project was funded by:

- China Scholarship Council Scholarship
- School of Pharmacy and Molecular Science Scholarship, JCU
- Coral Reef center, Austrian Research Council
- Australian Institute of Nuclear Science and Engineering
- Australian Nuclear Science and Technology Organization

## Family support

Thanks my wife, parents and sisters. They gave the spiritual support and encouraged me to persist on the project.

## Abstract

Selenium (Se) and Se-containing proteins are believed to be involved in many physiological processes. Recent studies have revealed complex repertoires of Se containing proteins in mammals, of which some (known as selenoproteins) contain selenocysteine (Sec; encoded by in-frame UGA codons) and others in which the selenium is bound (selenium binding proteins; SeBPs) without selenoproteins. There have been few studies to date on the selenium protein complements of non-Bilateria animals, and many of the non-Bilateria selenoprotein genes in the public sequence databases are mis-annotated. The main objective of the work described in this thesis was to describe the selenoprotein and selenium-binding protein repertoire of the coral *Acropora millepora*, a representative non-Bilateria animal and to investigate aspects of the expression of some of the corresponding genes. These studies should not only provide evolutionary insights into selenium biology, but also be relevant to the physiology of coral stress.

To achieve these goals, phylogenetic tools were used to survey the repertoires of selenium-containing proteins in *A. millepora* and other model organisms, qPCR and immunohistochemistry employed to follow changes in the expression of genes encoding non-enzymatic selenium containing proteins under experimental manipulation, bioinformatics tools used to model the structure of proteins of interest, and chemical tools employed to analyze the Se binding ability of recombinant selenium binding protein towards the inorganic Se *in vitro*.

The evolutionary studies summarized in Chapter 2 show that in the known invertebrates which have been studied their selenium components, the coral *A. millepora* has the most complex selenium repertoire (21 Sec-containing selenoproteins and 2 selenium binding proteins); other cnidarians also contain complex selenium repertoires. These results suggest that most of the known

selenium components seen in bilaterian animals predate the bilaterian-cnidarian split. In Chapter 3 we report that the expression of several non-enzymatic selenium containing proteins in the coral *A. millepora* is highly up-regulated by oxidants, suggesting physiology roles for these selenium components in redox regulation.

Studies in Chapter 4 and 5 focused on the *A. millepora* 56 kDa SeBPs (*amSeBPs*). Sequence analysis and structure modeling revealed that the conserved cysteine residues that are characteristic of these proteins, together with nearby motifs, cluster at the centre of the monomer protein models. The *amSeBPs* were ubiquitously expressed and markedly up-regulated at the planula and presettlement stages. Immunolocalisation experiments imply that the *amSeBPs* are enriched in adult *A. millepora* gastrodermal tissue that is adjacent to *Symbiodinium*. The *in vitro* selenite/*amSeBP* binding assays showed that the binding of inorganic selenium by *amSeBP* is dependent on the redox state. These studies imply that the positions of the redox sensitive cysteine residues and nearby motifs are critical for *amSeBP* function; these constraints presumably underlie the high level of sequence conservation of the 56 kDa SeBP sequences among animals, plants and even microorganisms.

In summary, these results imply important roles for the selenium containing proteins that are abundant in *A. millepora*. Although some of these proteins have been systematically characterized and implicated in redox metabolism, the mechanistic details remain unclear. To date, functional studies have focused mainly on mammalian Se proteins. Functional analyses in non-Bilateria animals could shed some light on the significance of Se-proteins and selenium biology more broadly.

# Table of contents

Statement of Access .....	i
Statement of Sources .....	ii
Acknowledgements.....	iii
Abstract .....	iv
Table of contents.....	vi
List of figures .....	x
List of tables.....	xii
<b><u>Chapter 1</u> General Introduction .....</b>	<b>1</b>
1.1 The reef building coral <i>Acropora millepora</i> as a representative cnidarian .....	1
<b><i>1.1.1 Basic profiles</i></b> .....	<b>1</b>
<b><i>1.1.2 Physiology</i></b> .....	<b>5</b>
<b><i>1.1.3 Bleaching and oxidative theory</i></b> .....	<b>8</b>
1.2 Selenium (Se) biochemistry .....	10
<b><i>1.2.1 The trace element selenium has similar chemical properties to sulfur</i></b> .....	<b>10</b>
<b><i>1.2.2 The physiological roles of selenium</i></b> .....	<b>11</b>
<b><i>1.2.3 Se geographical distribution</i></b> .....	<b>12</b>
1.3 Selenium containing proteins: general points.....	14
<b><i>1.3.1 The forms of Se in vivo</i></b> .....	<b>14</b>
<b><i>1.3.2 Selenoproteins</i></b> .....	<b>15</b>
<b><i>1.3.3 Selenium binding proteins</i></b> .....	<b>18</b>
1.4 Project aims .....	20
<b><u>Chapter 2</u> Evolutionary insights into ancestral selenium components .....</b>	<b>22</b>
2.1 Introduction .....	22
2.2 Materials and Methods .....	26

2.2.1 Sequence Datasets.....	26
2.2.2 Sequence analyses and phylogeny construction.....	26
2.2.3 Secondary structure analysis.....	27
2.3 Results .....	27
2.3.1 The GPx family .....	27
2.3.2 The TR like genes .....	31
2.3.3 Other selenoproteins and related factors .....	33
2.3.4 Selenium binding proteins .....	38
2.4 Discussion .....	39
<b>Chapter 3 Changes in the expression of genes encoding non-enzymatic selenium proteins during oxidative stress in the coral <i>Acropota millepora</i> .....</b>	<b>42</b>
3.1 Introduction .....	42
3.2 Materials and methods.....	44
3.2.1 Collection and maintenance of corals.....	44
3.2.2 Experimental conditions .....	44
3.2.3 Total RNA extraction and first strand cDNA synthesis .....	45
3.2.4 Real time qPCR .....	46
3.2.5 Normalization and data processing.....	48
3.3 Results .....	49
3.3.1 The expression of GOIs in control samples .....	49
3.3.2 Rapidly induced GOIs associated with H <sub>2</sub> O <sub>2</sub> treatment .....	50
3.3.3 BSO+H <sub>2</sub> O <sub>2</sub> treatment results in elevated expression of five GOIs after 24 hours .....	51
3.3.4 Genes encoding the selenium-binding proteins amSeBP17 and amSeBP23 behave differently under oxidative stress .....	52
3.4 Discussion .....	54
3.4.1 The scleractinian coral <i>A. millepora</i> has an complex antioxidant network.....	54

<b>3.4.2 Hypothesis regarding the redox-sensitive selenium containing proteins in <i>A. millepora</i></b> .....	<b>54</b>
<b>Chapter 4 Two members of the 56 kDa selenium binding protein family from the coral <i>Acropora millepora</i></b> .....	<b>57</b>
<b>4.1 Introduction</b> .....	<b>57</b>
<b>4.2 Materials and methods</b> .....	<b>58</b>
<b>4.2.1 Sequence analysis and protein modeling</b> .....	<b>58</b>
<b>4.2.2 Temporal transcript levels of <i>amSeBP17</i> and <i>amSeBP23</i> genes</b> .....	<b>59</b>
<b>4.2.3 Expression and purification of recombinant <i>amSeBP23</i> in <i>E. coli</i></b> .....	<b>60</b>
<b>4.2.4 Western blotting</b> .....	<b>61</b>
<b>4.2.5 Immunohistochemistry</b> .....	<b>61</b>
<b>4.3 Results</b> .....	<b>63</b>
<b>4.3.1 Sequence analysis and protein modeling</b> .....	<b>63</b>
<b>4.3.2 Characterization of <i>amSeBP17</i> and <i>amSeBP23</i> transcripts</b> .....	<b>67</b>
<b>4.3.3 Production of recombinant <i>amSeBP23</i> and its recognition on western blots by heterologous antibody</b> .....	<b>67</b>
<b>4.3.4 Localization of immunoreactive <i>amSeBP</i></b> .....	<b>70</b>
<b>4.4 Discussion and Hypothesis</b> .....	<b>73</b>
<b>4.4.1 Conserved cysteine residues and nearby motifs form the redox centre of the 56 kDa <i>SeBP</i></b> .....	<b>73</b>
<b>4.4.2 <i>amSeBP</i> expression suggests high metabolic rates in <i>A. millepora</i> planula and pre-settlement stages</b> .....	<b>74</b>
<b>4.4.3 <i>amSeBPs</i>, may be involved in transport or metabolism between the host <i>A. millepora</i> and the <i>Symbiodinium</i></b> .....	<b>75</b>
<b>Chapter 5 <i>In vitro</i> selenite binding by a recombinant form of the <i>Acropora millepora</i> selenium binding protein (<i>ramSeBP</i>) produced in <i>Escherichia coli</i></b> .....	<b>77</b>
<b>5.1 Introduction</b> .....	<b>77</b>
<b>5.2 Experimental methods</b> .....	<b>78</b>

<b>5.2.1 Large (milligram) scale ramSeBP/selenite binding assay.....</b>	<b>78</b>
<b>5.2.2 HPLC (High-Performance Liquid Chromatography) assay of low levels (microgram) of ramSeBP .....</b>	<b>79</b>
<b>5.2.3 Dithiothreitol (DTT) treatment .....</b>	<b>79</b>
<b>5.2.4 Small (microgram) scale ramSeBP/selenite (<math>^{75}\text{SeO}_3^{2-}</math>) binding assay .....</b>	<b>80</b>
<b>5.3 Results .....</b>	<b>81</b>
<b>5.3.1 Selenite binding ability of high level ramSeBP23 in vitro.....</b>	<b>81</b>
<b>5.3.2 HPLC of native and DTT modified ramSeBP23 .....</b>	<b>83</b>
<b>5.3.3 <math>^{75}\text{SeO}_3^{2-}</math> binding ability of low level native and DTT-modified ramSeBP23 in vitro.....</b>	<b>85</b>
<b>5.4 Discussion and Hypothesis.....</b>	<b>85</b>
<b>5.4.1 The potential selenite binding sites of the ramSeBP23 .....</b>	<b>85</b>
<b>5.4.2 The selenite binding towards ramSeBP23 is depending on the redox status ..</b>	<b>86</b>
<b>5.4.3 The amSeBP is an ideal selenium stock protein .....</b>	<b>87</b>
<b><u>Chapter 6</u> General conclusion .....</b>	<b>89</b>
<b>6.1 To be or not to be: evolutionary insight into ancestral Se components .....</b>	<b>89</b>
<b>6.2 The nonenzymatic Se components: candidate antioxidants in Acropora millepora .....</b>	<b>90</b>
<b>6.3 The 56kD SeBP in Acropora millepora: not simple, not well known .....</b>	<b>91</b>
<b>6.4 Future directions .....</b>	<b>91</b>
<b>References .....</b>	<b>94</b>
<b>Supplementary file.....</b>	<b>109</b>
<b>Abbreviations .....</b>	<b>111</b>

## List of figures

Figure 1.1 Phylogenetics of Cnidaria.....	2
Figure 1.2 Morphology of adult <i>Acropora millepora</i> .....	3
Figure 1.3 Major developmental stages of <i>Acropora millepora</i> .....	4
Figure 1.4 The diffusion based physiology in <i>Acropora millepora</i> .....	7
Figure 1.5 Bleached <i>Acropora millepora</i> .....	8
Figure 1.6 The oxidative theory of coral bleaching .....	10
Figure 1.7 The large coal fired-power stations (production ability more than 1000 megawatts) may affect the Se distribution in the GBR protecting area.....	14
Figure 1.8 Different forms of selenium containing proteins <i>in vivo</i> .....	15
Figure 1.9 The hypothetical mechanism of selenocysteine biosynthesis and incorporation into selenoproteins .....	16
Figure 1.10 X-ray structure of monomeric 56 kDa SeBP from <i>Sulfolobus tokodaii</i> ..	19
Figure 1.11 Project aims .....	20
Figure 2.1 Phylogenic analysis of GPx Family .....	30
Figure 2.2 Phylogeny and C-terminal sequences of TR like proteins from representative animals .....	32
Figure 2.3 SECIS elements in cnidarian selenoprotein W, T genes.....	34
Figure 2.4 Phylogenic analysis of SeBP proteins .....	39
Figure 3.1 The relative expression levels of all the GOIs in control samples of both colonies before chemical treatments.....	49
Figure 3.2 The mean fold changes towards control samples Rc for the seven GOIs in four testing groups.....	52-53
Figure 3.3 Hypothetical antioxidant network of <i>A. millepora</i> .....	56
Figure 4.1 Sequence analysis and protein modeling of the 56kD SeBP.....	65-66
Figure 4.2 <i>amSeBP17</i> and <i>amSeBP23</i> transcripts during the major developing stages of <i>A. millepora</i> .....	67

Figure 4.3 Cloning strategy for production of recombinant <i>amSeBP23</i> and western blotting experiments.....	69
Figure 4.4 Immunolocalisation of <i>amSeBP</i> in <i>A. millepora</i> at the early planula stage.....	71
Figure 4.4 Immunolocalisation of <i>amSeBP</i> in section of adult <i>A. millepora</i> .....	72
Figure 5.1 ITLC assay .....	80
Figure 5.2 Selenium and protein content in the flow through mixtures off the affinity column .....	82
Figure 5.3 Chromatography A206 nm peak area/protein content curve .....	84
Figure 5.4 Chromatography profiles of <i>ramSeBP</i> after different periods of DTT treatment .....	84

## List of tables

Table 1.1 Effects of selenium supplementation on the mammalian immune system .....	12
Table 1.1 Selenoenzymes and non-enzymatic selenoproteins .....	17-18
Table 2.1 Overview of ancestral selenium components identified .....	35-37
Table 2.2 Summary of selenoprotein data for the animals studied .....	38
Table 3.1 Primers for ICGs and GOIs .....	47-48
Table 3.2 The up-regulated GOIs in all groups 4 hours after H <sub>2</sub> O <sub>2</sub> treatment .....	50
Table 3.3 The GOIs remained high expression level 24 hours after BSO + H <sub>2</sub> O <sub>2</sub> treatment .....	51
Table 5.1 The binding ratio between selenium and <i>ramSeBP</i> in Fig. 5.2 A. ....	83
Table 5.2 The binding ratio between <sup>75</sup> Se and <i>ramSeBP</i> in ITLC binding assay .....	85
Supplimentary Table 1 Unpublished Se components of <i>A. millepora</i> .....	109

# Chapter 1

## General Introduction

### 1.1 The reef building coral *Acropora millepora* as a representative cnidarian

#### 1.1.1 Basic profiles

**Taxonomy.** The Cnidaria is one of the earliest diverging phyla of Eumetazoa, and is believed to have diverged from the bilaterian lineage prior to or during the early Cambrian (Budd 2008). Although the vast majority of cnidarians are marine animals, examples being corals, jellyfish, sea anemones and box jellyfish, some cnidarians such as *Hydra* live in fresh water. The phylum comprises four classes: Cubozoa, Scyphozoa, Hydrozoa and Anthozoa (Fig 1.1). The largest class, Anthozoa, which includes corals and sea anemones, diverged first (Collins 2002; Ball et al., 2002; Miller et al., 2005; see Fig. 1.1). Members of the genus *Acropora* (Class Anthozoa, subclass Hexacorallia, Order Scleractinia, suborder Astrocoeniina, Family Acroporidae) are the dominant reef-building corals of the Indo-Pacific. *Acropora millepora* is a typical member of this large coral genus, and generally occurs on reef flats or on upper reef slopes, particularly where the water is clear.

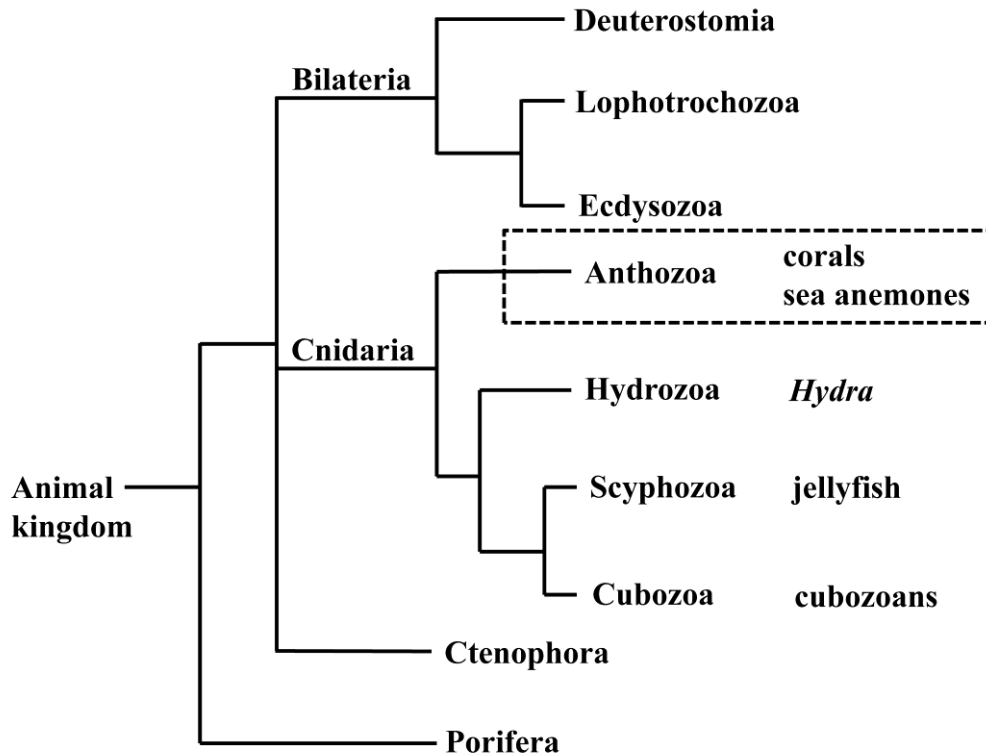


Fig. 1.1 Phylogenetics of Cnidaria. The largest class, Anthozoa, which includes corals and sea anemones, diverged first. *Acropora millepora* is a member of the Anthozoa (labeled in the box), subclass Hexacorallia, Order Scleractinia, suborder Astrocoeniina, family Acroporidae and genus Acropora. The figure is adapted from Ball et al. 2002 and Miller et al. 2005.

**Morphology of adult *A. millepora*.** Adult *A. millepora* colonies have short and uniform branches (also called corallites). Axial branches are distinctive and tubular in shape while radial branches are usually highly compacted (Fig. 1.2 A). Each branch has a scale like appearance with small and evenly separated polyps; tentacles are extended from the oral end of polyps (Fig. 1.2 B). Each polyp is anchored to the skeleton with its oral end up. As in other cnidarians, the *A. millepora* polyps give the appearance of near radial symmetry along the oral/aboral (O/A) axis, but there are subtle asymmetries in a second axis perpendicular to this *A. millepora* has no true organs. Each polyp has a gastrodermal cavity (or "stomach") with a mouth, a two layer-tissue wall with outer epidermis and inner gastrodermis, between which is a jelly-like mesogloea. The gastrodermal cavity or the mesogloea can be connected to other polyps (Fig. 1.2 C). The coral skeleton is extracellular, located below the aboral epidermis layer of each polyp.

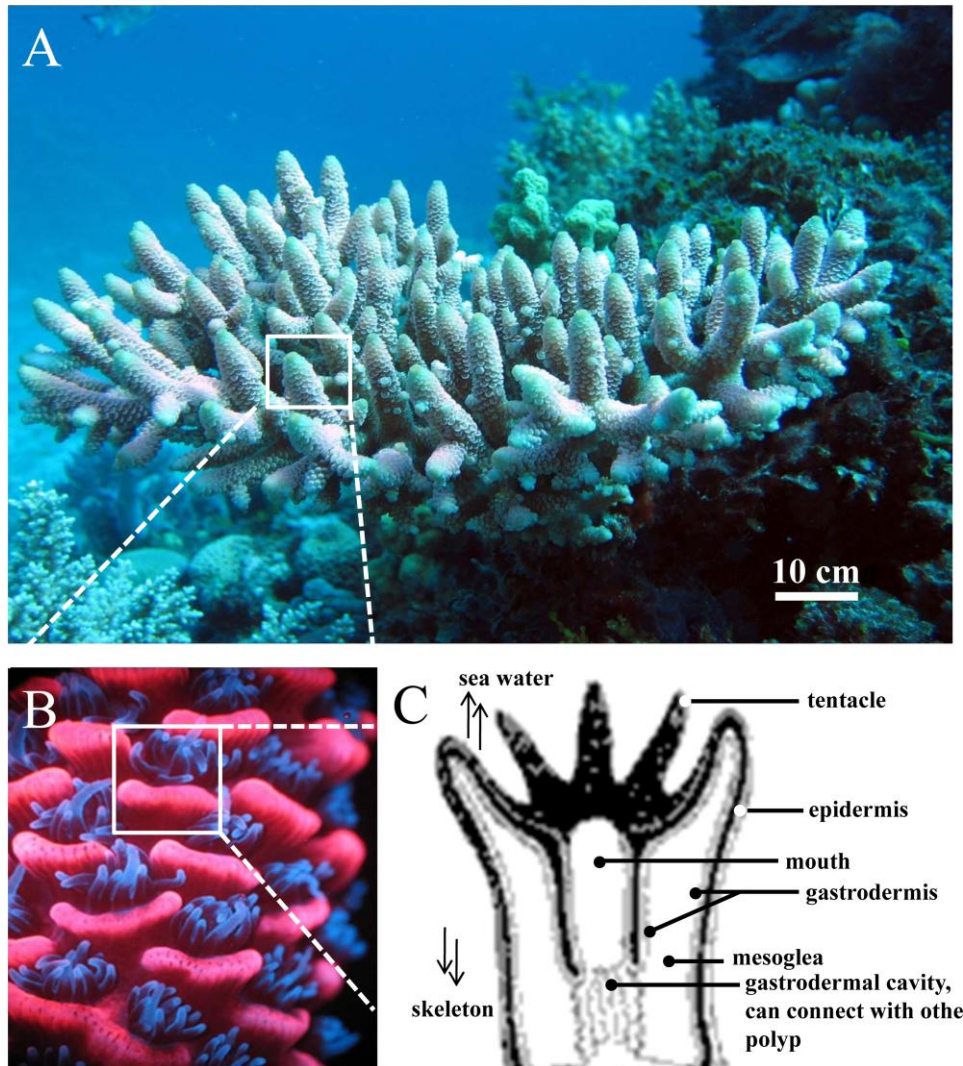


Fig 1.2 Morphology of adult *A. millepora*. (A) A typical adult colony of *A. millepora*, photograph: by Dr Madeleine van Oppen (Australian Institute of Marine Science). (B) An axial branch of the adult *A. millepora*, photograph: from scholarpedia website ([www.scholarpedia.org](http://www.scholarpedia.org)). (C) Polyp structure of *A. millepora* with oral end up towards sea water and aboral end down towards coral skeleton, each polyp has a gastrodermal cavity with a mouth, a two layer-tissue wall with outer epidermis and inner gastrodermis.

**Early development.** The availability of large amounts of early embryonic material is one advantage of *A. millepora* over the text-book cnidarian, *Hydra* (Miller et al., 2000), although availability is limited to the naturally occurring mass spawning events. The early development of *A. millepora* has not yet been described in great detail, although overviews have been published (Ball et al., 2002; Ball et al., 2004), as summarized below. A few nights after a full moon in late spring, egg/sperm bundles that are essentially self-incompatible are released into the water, float to the surface where they break apart and cross-fertilize with gametes from other colonies.

The fertilized eggs undergo unilateral cleavage, resulting in the formation of blastomeres. Approximately 13 h post-fertilization, the irregular-shaped ‘prawnchip’ stage appears which may be unique to some corals. Gastrulation typically occurs at 22 to 36 h post-fertilization, and results in the formation of endoderm and ectoderm; the edges of the prawnchip appear to fold upward and a cavity is formed at the centre of the embryo. Due to the shape of the embryo, the gastrula stage of *Acropora* is often referred to as the ‘donut’ stage. Approximately 28 h post-fertilization, the blastopore begins to close, marking the transition from embryo to larva. After blastopore closure, the larva becomes pear-shaped and cilia ultimately develop; the pear-shaped early larvae become motile spindle-shaped planulae (Fig. 1.3). Extensive cellular differentiation, including the elaboration of a complex nerve net, is apparent in late planulae. Planulae actively seek appropriate substrates for settlement by swimming aboral-end first. When triggered by appropriate cues, planulae settle to the substratum at the aboral end and become flattened along their O/A axis. Following settlement, the primary polyps adopt a rather different morphology to the planulae; a gastrodermal cavity appears within the flattened disc, and tentacles begin to form in the area surrounding the oral pore. Typically, symbionts are acquired 6-12 days after settlement (Baird et al., 2006), and eventually, a new colony of *A. millepora* is formed (Fig. 1.3).

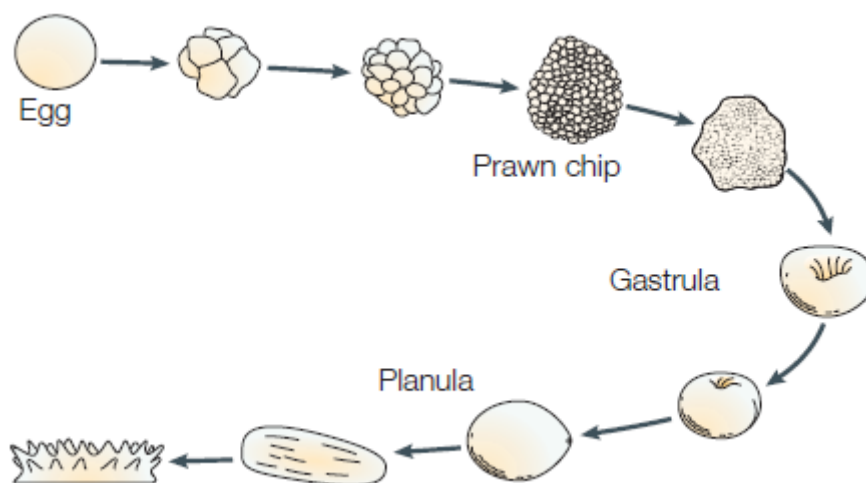


Fig. 1.3 Major developmental stages of *A. millepora* (Ball et al., 2004). Approximately 13 h post-fertilization, the irregular-shaped ‘prawnchip’ stage appears; approximately 22 h post-fertilization, the gastrula stage occurs;

approximately 28 h post-fertilization, the blastopore begins to close, marking the transition from embryo to larva, the pear-shaped early larvae become motile spindle-shaped planulae and seek appropriate substrates for settlement.

**Unexpected genetic complexity.** Whereas anthozoan cnidarians are morphologically simple animals, *A. millepora* and *Nematostella vectensis* (sea anemone) have been shown to have complex gene complements (Kortschak et al., 2003; Miller et al., 2005; Putnam et al., 2007) that include many genes previously thought to be restricted to vertebrates because they had been characterized in the context of vertebrate-specific traits and are absent from *Drosophila* and *Caenorhabditis*. Not only are all of the major developmentally-regulated signaling pathways known in Bilateria animals (Wnt, TGF $\beta$ , Hedgehog, Ras-MAPK and Notch) present in anthozoans, but the differentiation of these families of signaling molecules clearly predates the cnidarian/bilaterian split (Technau et al., 2005, Kusserow et al., 2005; Guder et al., 2006). The present study is consistent with this idea of “ancestral genetic complexity” (Technau et al., 2005), as complex repertoires of genes encoding selenium containing proteins were found complex in the three cnidarians examined (Chapter 2). Although *A. millepora* is good comparator for evolutionary comparisons of this kind, there are limitations in working with this animal; because it is not a laboratory organism, functional analyses are impossible or difficult to perform. Nevertheless, there is a need to understand the molecular bases of many aspects of coral biology, so it is important that attempts are made to link the genetic information with corresponding physiological roles, and one way to approach this is to infer gene function from gene expression data, an approach pursued here.

### **1.1.2 Physiology**

*‘Day and night, year after year, generation by generation, the way tiny corals fix inorganic carbon to build up reef is one of the most amazing works of nature which approves the power of life.’* (Charles Darwin, 1845).

**The diffusion based physiology of corals.** Diffusion is an efficient means of

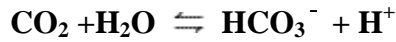
exchange of materials only over short distances (e.g. over about 1 mm for oxygen exchange). The main physiological activities of corals, including respiration, digestion and elimination rely largely on diffusion. This diffusion based physiology, restricts corals to water and is facilitated by the large surface area provided by polyps with long thin tentacles. In scleractinian corals including *A. millepora*, the two main interfaces through which the material based diffusion (Zoccola et al., 1999; Irigaray et al., 1996) can occur within the water/coral /skeleton sandwich (Fig. 1.4.) are: (1) the oral ectoderm/water or endoderm/water interface, or (2) the aboral ectoderm/skeleton interface. Moreover, diffusion based physiological activities occur at the intracellular level, between the endodermal cells of the coral and the symbiotic dinoflagellates (*Symbiodinium spp*), which supply the host cells the main nutrition and energy (Muscatine and Porter, 1977; Papina et al., 2003).

**Biomineralisation.** Complex physiological metabolisms are involved in the biomineralisation process and the underlying molecular mechanisms are still largely unknown (reviewed by Allemand et al., 2004). In order to build the skeleton, which is composed of calcium carbonate (CaCO<sub>3</sub>) crystallized largely as aragonite (orthorhombic system), scleractinian corals have not only to supply calcium and inorganic carbon from ambient seawater (through the coral/sea water interface, Fig 1.4.) to the calcification site (through coral/coral skeleton interface, Fig. 1.4.), but also to eliminate the protons (through coral/coral skeleton interface, Fig. 1.4.) that result from the mineralising process:



This process requires the movement of charged Ca<sup>2+</sup> across the coral/sea water interface, presumably via calcium channels (B énazet-Tambutt é 1996; Zoccola et al., 1999) and its transport across the coral/skeleton interface against a chemical gradient (Fig. 1.4), presumably requiring a Ca<sup>2+</sup>-ATPase (Zoccola et al., 2004). The

predominant form of dissolved inorganic carbon is as  $\text{HCO}_3^-$  which is present in sea water as well as in coral tissues at much higher concentration than are  $\text{CO}_3^{2-}$  and  $\text{CO}_2$ . The availability of  $\text{HCO}_3^-$  in coral tissue is ensured by the presence of the enzyme carbonic anhydrase (Allemand et al., 2004), which facilitates the following equilibrium:



The rate of biomineralisation may also modified by the photosynthetic activities of the symbiotic dinoflagellates. Photosynthetic activities in the symbiont can consume inorganic carbon, thus favoring carbonate precipitation. In addition, the liberation of  $\text{OH}^-$  during photosynthesis can effectively neutralize protons arising from  $\text{CaCO}_3$  precipitation, thus facilitating calcification (Fig. 1.4; reviewed by Allemand et al., 2004).

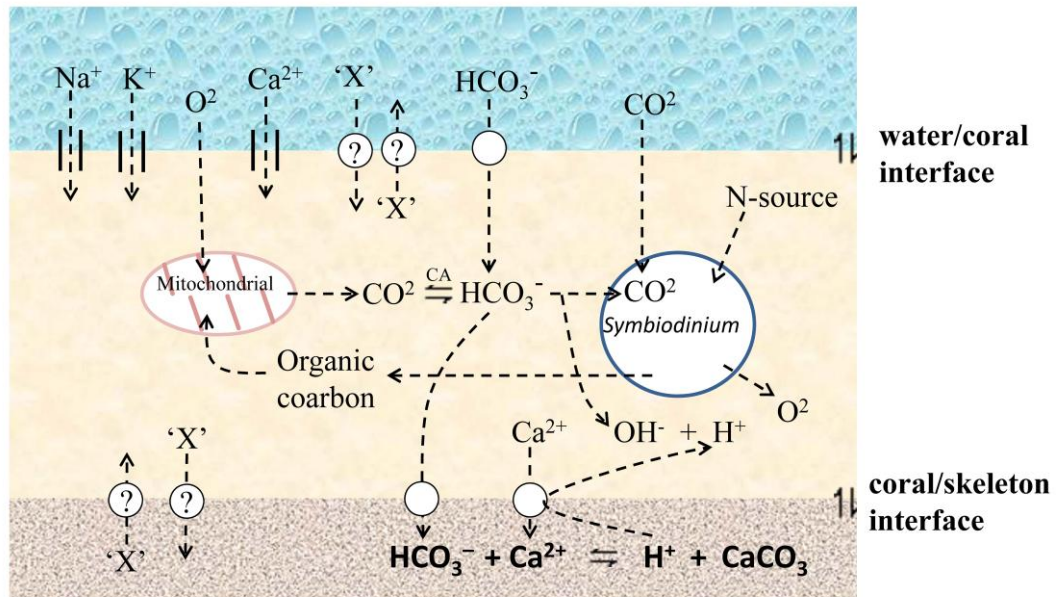


Fig. 1.4 The diffusion based physiology of *A. millepora*. Materials can move within the water/coral /skeleton sandwich through diffusion interfaces (water/coral interface, coral/skeleton interface, coral/ *Symbiodinium* interface). X: other diffused materials like Se, Sr, Ba etc, and their distribution/movement in corals remain largely unclear. CA: carbonic anhydrase. The figure is adapted from Allemand et al., 2004.

The application of isotope flux kinetics and X-ray microanalysis indicates that the

distribution of many elements (Na, Mg, P, S, Cl, K, Ca, Sr, Ba) in coral tissues, symbiotic dinoflagellates and skeletons and the kinetics of movement of these elements between different compartments are under biological control (reviewed by Marshall and McCulloch, 2002). However, the biological roles of these elements and the significance of their distribution/movement in scleractinian corals remain largely unclear.

### ***1.1.3 Bleaching and oxidative theory***

Because of their diffusion-based physiology, corals are particularly susceptible to physical (Lesser et al., 1990), chemical (Piniak 2007) and biological (reviewed by Rosenberg et al., 2007) stresses imposed from the living environments. For example, under elevated sea water temperatures, the symbiotic relationship between corals and their endosymbiotic dinoflagellates can breakdown, leading to the bleaching (loss of endosymbiotic dinoflagellates ) in a variety of scleractinian coral species (Downs et al., 2002; Hughes et al., 2003; Abrego et al., 2008) including *Acropora millepora* (Fig. 1.5). Over the last two decades, temperature-induced bleaching events have increased in both frequency and severity (Coles & Brown 2003; Hughes et al., 2003).



Fig 1.5 Bleached *A. millepora*. Photograph: by Dr Ray Berkelmans (Australian Institute of Marine Science). The

symbiotic relationship between corals and their endosymbiotic dinoflagellates can breakdown, leading to the bleaching in a variety of scleractinian coral species including *Acropora millepora*.

The physiological mechanisms underlying coral bleaching remain unclear despite extensive investigation over the last few years. A number of studies (Downs et al., 2002; Abrego et al., 2008) suggest that oxidative stresses imposed on the coral by the symbiotic dinoflagellates play important roles in the process of sea-surface temperature-induced coral bleaching. The basic idea is that heat stress combined with intense ultraviolet irradiation destabilizes the Photosystem II-catalyzed electron transfer, resulting in increased production of reactive oxygen species (ROS) such as  $H_2O_2$  (Giardi et al., 2001). It is proposed that  $H_2O_2$  arising in this way in the dinoflagellate can diffuse into the coral cytoplasm (Fig. 1.6, Downs et al., 2002), where it may overload antioxidant buffering systems and potentially cause extensive tissue damage. To prevent this occurring, the theory goes, corals sense oxidative damage and move to eradicate the dominant source of ROS production by expelling their endosymbiotic dinoflagellates. Thus, the bleaching may be a last ditch attempt by the coral (Fig. 1.6, “*Oxidative Theory of Coral Bleaching*” Downs et al., 2002) to deal with environmental stress. Several studies are consistent with this theory; for example, more temperature tolerant dinoflagellate strains (*Symbiodinium* type D) impose less ‘oxidative damage’ on their coral hosts during acute temperature stress, and may thus facilitate adaptation of corals to warmer environments (Van Oppen et al., 2005; Abrego et al., 2008).

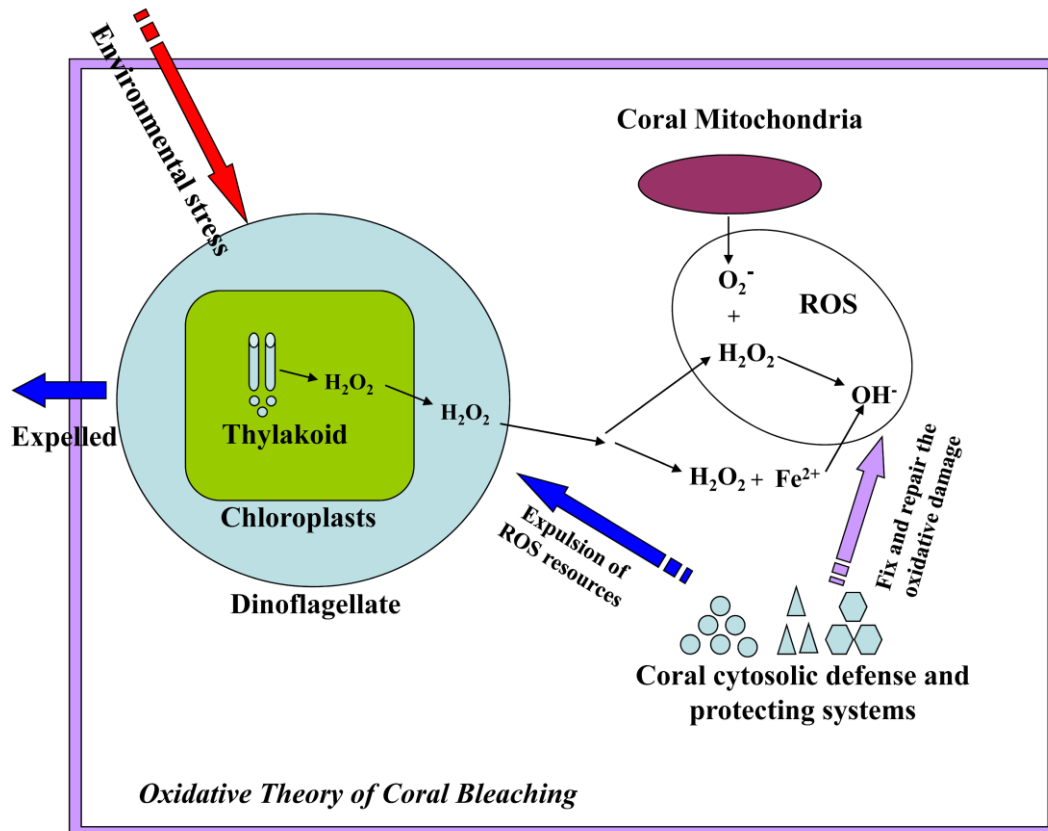


Fig. 1.6 The oxidative theory of coral bleaching (adapted from Downs et al., 2002). Environmental stresses like heat and UV accelerate the production of hydrogen peroxide ( $H_2O_2$ ) in the chloroplasts of the algal symbionts either by damaging the thylakoid membrane or disrupting the Calvin cycle.  $H_2O_2$  arising in the dinoflagellate can diffuse into the coral cytoplasm, and some of the ROS products like hydrogen peroxide can be accumulated in the host cell, where they activate a cellular protecting response, which results in expulsion of symbionts and leads to the coral bleaching.

## 1.2 Selenium (Se) biochemistry

### 1.2.1 The trace element selenium has similar chemical properties to sulfur

The trace element selenium was discovered and named after Selene, the Greek goddess of the moon, in 1817 by Swedish chemist Jons Jacob Berzelius. In the periodic table, selenium ( $Se^{34}$ ) is in the same group (16# group) as sulfur ( $S^{16}$ ) and shares with them a number of chemical properties (Rosenberg et al., 1966). Because compounds of selenium and sulfur can act as reversible and specific oxidation agents to a variety of organic chemicals, they are important in biological redox regulation (Driscoll and Copeland, 2003). Replacement of S for Se tends to make the species

more reducing under physiological conditions (Stadtman 1996), thus many enzymes whose active sites contain selenium catalyze oxidation/reduction reactions *in vivo* (Stadtman 2000).

### ***1.2.2 The physiological roles of selenium***

Due to its chemical properties, selenium was historically regarded as a toxic agent, but is now known to be an essential trace element with a number of important physiological roles (reviewed by Rayman, 2000). The biological activities of selenium as a nutrient or a toxicant depend not only on the dose, but also on its chemical form (Ip et al., 1991). The most obvious biological role of selenium is as an antioxidant, as many selenium-containing enzymes including glutathione peroxidases and thioredoxin reductases, are antioxidants (Rotruck et al., 1973).

The recommended dietary intake (RDI) for Se in the UK is 75 mg/day for adult males and 60 mg/day for adult females (reviewed by McKenzie et al., 1998), and there is a considerable body of evidence linking Se-deficiency with a variety of disorders. These include Keshan disease, which occurs in areas of China with low Se soil (Chen et al., 1980), cardiovascular disease (Clark et al., 1996), cancer (Ip et al., 1991; Clark et al., 1996), rheumatoid arthritis and cataracts (Reviewed by Lockitch, 1989). The importance of Se in the mammalian immune system has been described at both the cellular (Table 1.1, reviewed by McKenzie et al., 1998) and molecular levels (reviewed by Arthur et al., 2003). Moreover, Se can protect human keratinocytes against the cytotoxic effects of ultraviolet (UV) irradiation and hydrogen peroxide treatment (Shisler et al., 1998).

Table 1.1 Effects of selenium supplementation on the mammalian immune system

	<b>Tests</b>	<b>Research models</b>
<i>In vivo</i>	Increased high-affinity of IL-2 receptor	Mouse
	Increased T-cell proliferation	Mouse
	Increased activity of natural killer cell	Mouse, Human
	Increased cytotoxic T-cell activity	Mouse
	Enhanced T-cell response to pokeweed mitogen	Cow
	Increased activity of lymphokine activated killer cell	
	Enhanced vaccine induced immunity	Mouse
	Decreased cell death following paraquat exposure	Rat
	Decreased skin cancer and mortality induced by UV	Mouse
	Decreased erythema following UV exposure	Human, mouse
<i>In vitro</i>	Enhanced antibody response to virus	Cow
	Increased apoptosis in tumours	Human, mouse
	Enhanced response in lymphocytes	Human
	Increased killing by macrophages	Human
	Increased killing by cytotoxic T cells	Human
	Decreased HIV replication in T cells	Human
	Decreased NF-kB activation	Human
	Decreased B cell lipoxigenase activity	Human
	Decreased skin cell death following UV exposure	Mouse, human
	Decreased DNA damage of skin cell following UV exposure	Mouse, human
	Decreased IL-6,8 and TNF mRNA following UV exposure	Human
	Decreased apoptosis in skin cell following UV exposure	Human

### 1.2.3 Se geographical distribution

**Terrestrial distribution of Se.** The geographical distribution of Se in soils is a function not only of the parent materials (Ure and Berrow, 1982) but also other soil properties including the loss on ignition (LOI) value and C concentration (Shand et al., 2010). Thus the terrestrial distribution of Se is highly variable. In general, organic-rich soils have higher Se concentrations. The variability of Se levels in soils leads to significant geographical differences in Se levels in crops; for example, American-grown wheat grain generally has a higher Se content than UK-grown grain (Adams et al., 2002).

**Se contamination of aquatic ecosystems.** Because inorganic selenium salts and

compounds are soluble, mobile in the water column and tend to accumulate in organic-rich sediments, over long time periods environmental input of Se can result in local contamination of aquatic ecosystems. One major source of Se contamination of aquatic systems is agricultural irrigation drainage containing organic wastes, which is known to have caused severe teratogenesis in wild populations of aquatic birds in central California (Heinz et al., 1987). The other main contributors of aquatic Se contamination are coal-fired power plants, which often pollute nearby water bodies with Se-rich fly ash. This kind of pollution has been reported in lakes of central Alberta, Canada (Donahue et al., 2006), in Belews Lake, North California (Lemly 2002) and in Lake Macquarie, NSW, Australia (Kirby et al., 2001), frequently causing teratogenesis in fish and other aquatic organisms. To protect aquatic organisms, a water quality criterion of  $<2 \mu\text{g/l}$  for selenium has been recommended based on extensive review of the toxicology literature (reviewed by Hamilton and Lemly, 1999).

**Potential Se pollution risks to the GBR.** In Queensland, Se toxicity has been reported in some regions as a result of livestock feeding on Se accumulative plant species like *Neptunia amplexicaulis* (Peterson and Butler 1967). In addition, anthropogenic activities such as disposal of fly ash, raising of economic crops and mining operations have the potentiality to contribute substantially to the redistribution and cycling of Se in Queensland (reviewed by Tinngi, 2003). The issue of Se levels and distribution in the GBR (Great Barrier Reef) marine protected area is of urgent concern because there have been no base line studies and extensive risks exist in the forms of both agricultural run-off associated with sugarcane production and as the presence of large coal-fired power stations (Fig. 1.7). A priority should be widespread surveying and monitoring of Se levels across the whole GBR, but of particular concern are areas proximal to power stations such as that at Gladstone (Fig. 1.7 B).

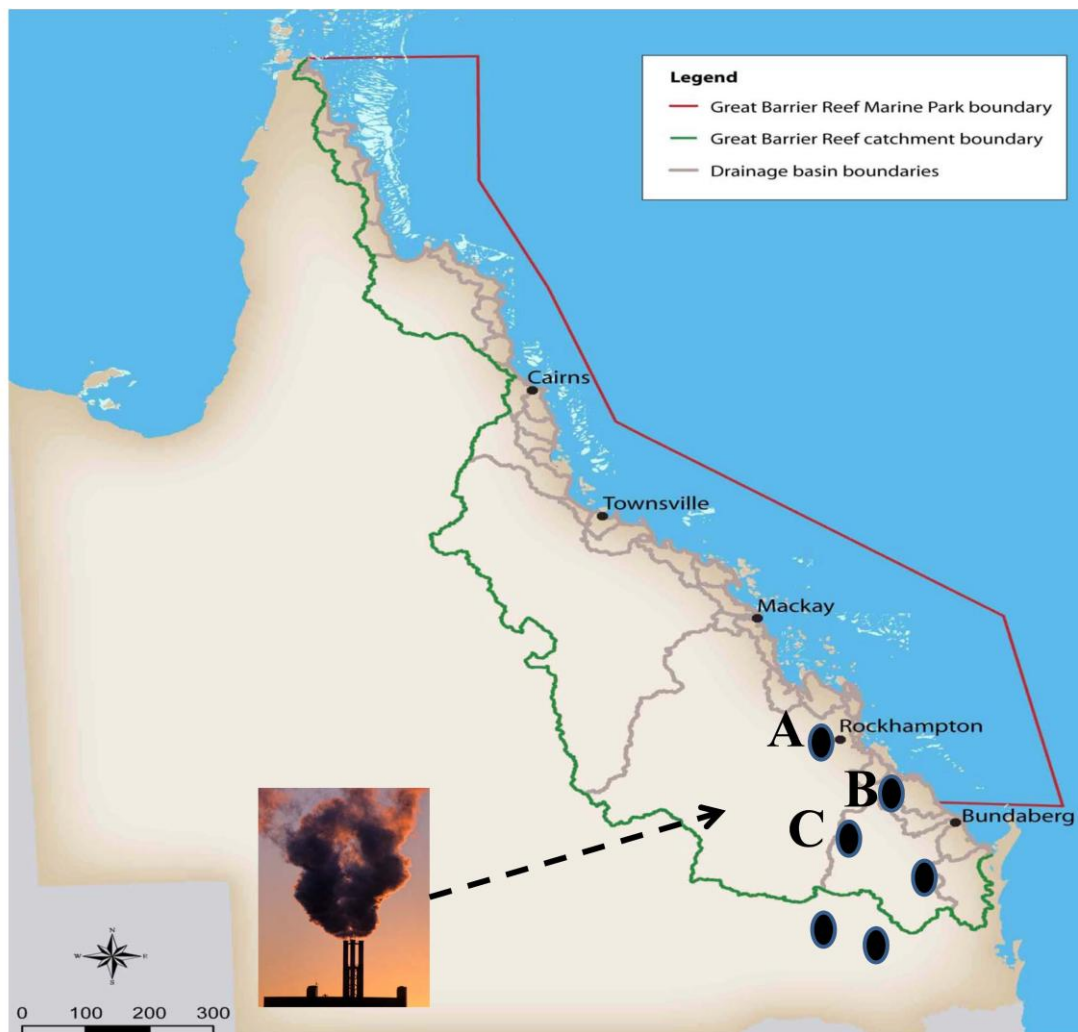


Fig 1.7 The large coal fired-power stations (production ability more than 1000 megawatts) may affect the Se distribution in the GBR protecting area. A: Stanwell power station (1440 megawatts); B: Gladstone power station (1650 megawatts); C: Callide power station (1700 megawatts). Information is adapted from Department of Mines and Energy, Queensland Government, Australia.

## 1.3 Selenium containing proteins: general points

### 1.3.1 The forms of Se in vivo

After ingestion of normal levels of selenite, selenate, or selenocysteine, nearly all of the element is metabolized via an intermediary pool and incorporated into specific Se-containing proteins (reviewed by Behne et al., 1991). The known Se-containing proteins (reviewed by Behne and Kyriakopoulos, 2001) can be divided into three groups: (1) proteins into which the element is incorporated nonspecifically, (2)

proteins that specifically bind selenium, and (3) proteins that contain selenium in the form of selenocysteine (Sec); this latter category are defined as selenoproteins, and in this case the Sec is encoded by a UGA codon. The incorporation of dietary selenium into the different types of selenium containing proteins is summarized in Figure 1.8.

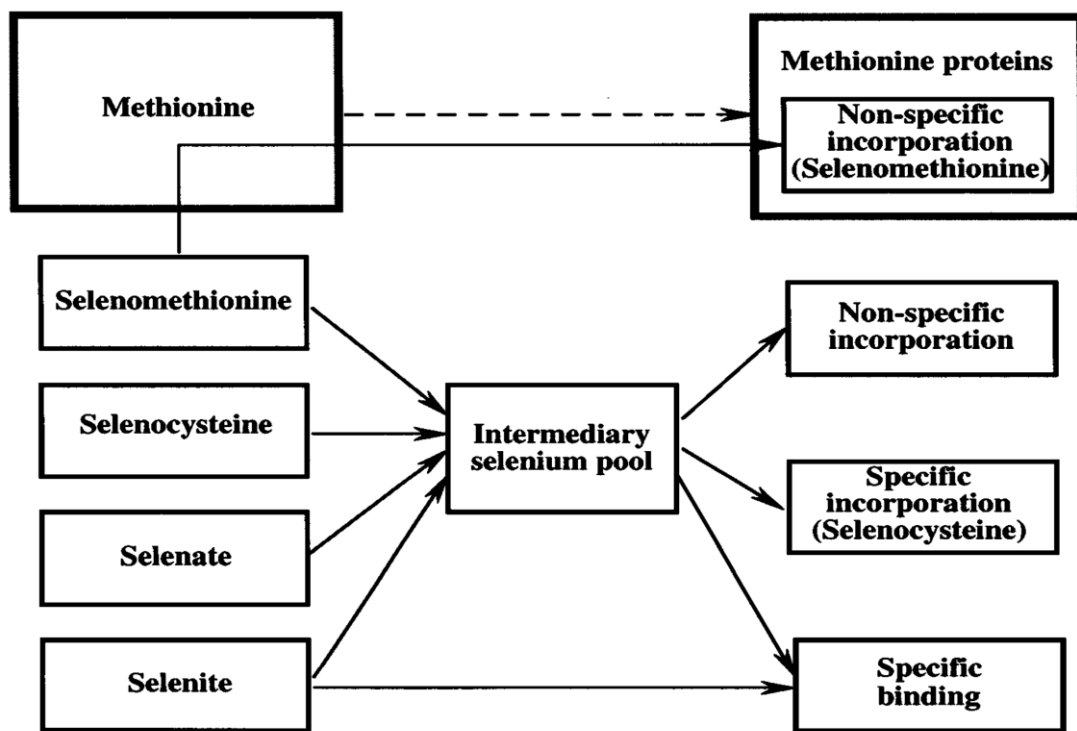


Fig 1.8 The forms and kinetics of selenium *in vivo* (reviewed by Behne and Kyriakopoulos, 2001).

### 1.3.2 Selenoproteins

**The mechanism of Sec incorporation.** The unique feature in the incorporation of selenocysteine is the use of the UGA codon, which normally serves as a termination signal. The Sec codon of UGA needs specific stemloop structures located in the untranslated region of the mRNAs termed selenocysteine insertion (SECIS) elements, and trans-acting factors that associate with the SECIS elements (reviewed by Squires and Berry, 2008) which include the Sec elongation factor (EFSec) and the SECIS binding protein 2 (SBP2). Several models to describe the mechanism of Sec incorporation have been proposed in the past few years (reviewed by Papp et al., 2007), however, a clear and detailed picture is still lacking. In the commonly

recognized model, SBP2 stimulates Sec incorporation by associating with SECIS elements and recruiting the selenocysteyl-tRNA complexes to the ribosome. A simplified diagram illustrating the proposed complexes and their subcellular distribution is presented in Fig. 1.9.

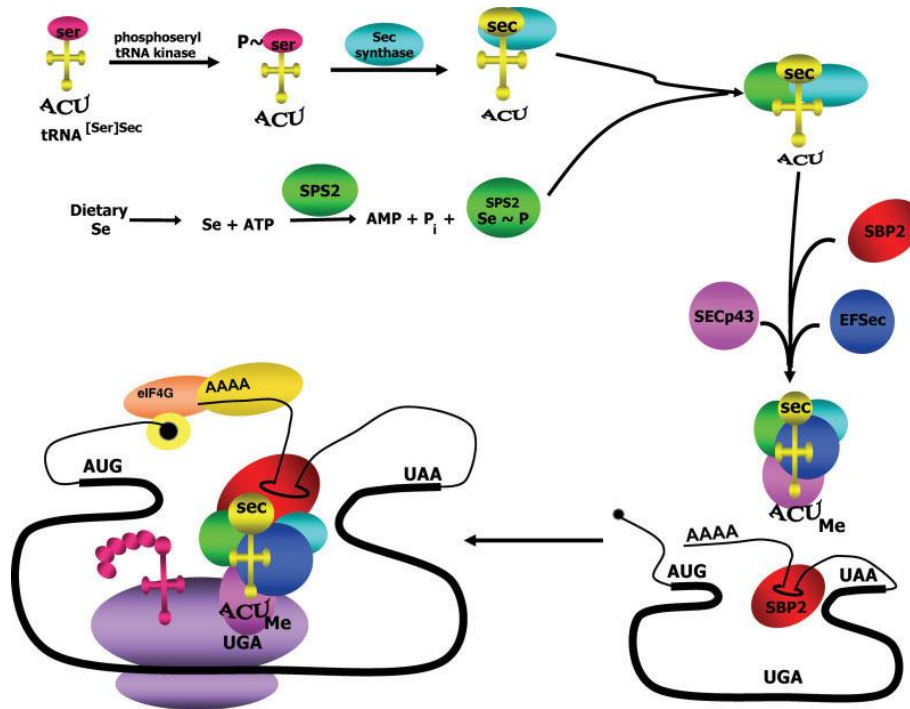


Fig 1.9 The hypothetical mechanism of selenocysteine biosynthesis and incorporation into selenoproteins (reviewed by Squires and Berry, 2008). In the process, a selenocysteyl-tRNA complex was synthesized and its insertion to the ribosome was bridged through the SECIS elements and the trans-acting factors.

**Selenoproteins with known enzymatic functions.** Most of the well characterised selenoproteins are enzymes, with the selenocysteine residue responsible for catalytic functions. The known selenoenzymes are listed in Table 1.2. Amongst the most widely distributed and best characterised selenoproteins are the glutathione peroxidases (GPx's), iodothyronine deiodinases, and the thioredoxin reductases (TR's). These selenoenzymes are catalytically active in redox processes as electron donors. Although their enzymatic functions have been established (Flohé et al., 1973; Tamura and Stadtman, 1996) for most of them the information on metabolic role and biological significance is far from complete.

**Non-enzymatic selenoproteins.** In addition to the selenoenzymes, a large number of other selenoproteins have been identified on the basis of <sup>75</sup>Se labeling, including selenoprotein P, selenoprotein W, 15KD selenoprotein and selenophosphate synthetase 2 (SPS2; Low and Berry, 1996; Behne et al., 1988; Behne et al., 2000). Recently, computer programs have been developed that allow the identification of genes encoding selenoproteins by scanning the nucleotide sequence databases for the selenocysteine insertion sequence elements necessary for decoding UGA as selenocysteine. Novel selenoproteins discovered in this way include SelH, SelI, SelK, SelM, SelN, SelO, SelR, SelS SelT SelV SelW and 18 KD Selenoprotein (see Table 1.2; Kryukov et al., 1999; Kyriakopoulos et al., 1996; Kryukov 2003; Saijoh et al., 1995). For many of these selenoproteins, the function is unknown. In the cases of selenoprotein P (Hill et al., 1991), selenoprotein W (Vendeland et al., 1993) and the 15KD selenoprotein (Kalcklosch et al., 1995; Gladyshev et al., 1998), antioxidant functions have been suggested, but not confirmed, and mechanistic details are lacking.

Table 1.2 Selenoenzymes and non-enzymatic selenoproteins

<b>Selenoprotein</b>	<b>Abbreviations used</b>	<b>Significant studies</b>
Glutathione peroxidases	GPxs	
Cytosolic or classical GPx	cGPx, GPx1	Flohe et al., 1973
Gastrointestinal GPX,	GI-GPx, GPx2	Chu et al., 1993
Plasma GPx	pGPx, GPx3	Takahashi et al., 1987
Phospholipid hydroperoxide GPx	PHGPx, GPx4	Ursini et al., 1985
Sperm nuclei GPx	snGPx	Pfeifer et al., 2001
Thioredoxin reductases	TRs	
Thioredoxin reductase 1	TR1	Tamura and Stadtman, 1996
Thioredoxin reductase 2	TR2	Gasdaska et al., 1999
Thioredoxin reductase 3	TR3	Sun 1999
Iodothyronine deiodinases		
Type 1 deiodinase	D1, 5'DI	Behne et al., 1990
Type 2 deiodinase	D2, 5'DII	Davey et al., 1995
Type 3 deiodinase	D3, 5'DIII	Croteau et al., 1995
Difulfide bond formation protein A	DsbA	Jiang et al., 2010
Methionine sulfoxide reductase	MsrA	Castellano et al., 2005
15KD selenoprotein	Sel15	Gladyshev et al., 1998
18KD selenoprotein	Sel18	Kyriakopoulos et al., 1996
Selenoprotein H	SelH	Mendelev et al., 2010

Selenoprotein I	SelI	Kryukov et al., 2003
Selenoprotein J	SelJ	Castellano et al., 2005
Selenoprotein K	SelK	Kryukov et al., 2003
Selenoprotein L	SelL	Shchedrina et al., 2003
Selenoprotein M	SelM	Kryukov et al., 2003
Selenoprotein N	SelN	Kryukov et al., 2003
Selenoprotein O	SelO	Kryukov et al., 2003
Selenoprotein P	SelP	Hill et al., 1991
Selenoprotein R	SelR	Kryukov et al., 2003
Selenoprotein S	SelS	Kryukov et al., 2003
Selenoprotein T	SelT	Kryukov et al., 2003
Selenoprotein U	SelU	Castellano et al., 2004
Selenoprotein V	SelV	Kryukov et al., 2003
Selenoprotein W	SelW	Vendeland et al., 1993
Selenoprotein Z	SelZ	Lescure et al., 1999

---

### ***1.3.3 Selenium binding proteins***

Selenium binding proteins (SeBP) do not contain selenocysteine but selectively and specifically bind selenium (Bansal et al., 1989<sup>a</sup>). Two major families of selenium binding proteins are distinguished based on molecular mass, the 14 kDa SeBP first identified in mouse liver as a fatty acid-binding protein which was mainly distributed in mammalian research models (Bansal et al., 1989<sup>b</sup>); the 56 kDa SeBP type that is both highly conserved and widely distributed (Song et al., 2006; Bevan et al., 1998). It was found that the chemopreventive effects of selenium could be mediated by selenium-binding proteins other than glutathione peroxidase (Bansal 1989<sup>a</sup>). The chemical form of selenium present in SeBPs is not known, but the absence of selenocysteine implies that the association is non-covalent.

**The 14 kDa SeBP.** The mouse 14 kDa SeBP specifically binds selenite both in *vitro* or in *vivo* (Sani et al., 1988). Although its function is not known, it has been suggested to be active in the intracellular Se transport (Bansal et al., 1989<sup>a</sup>). Another suggestion is that it may act as a growth regulatory molecule and that by modulating its function selenium may inhibit cell growth (Bansal et al., 1989<sup>b</sup>).

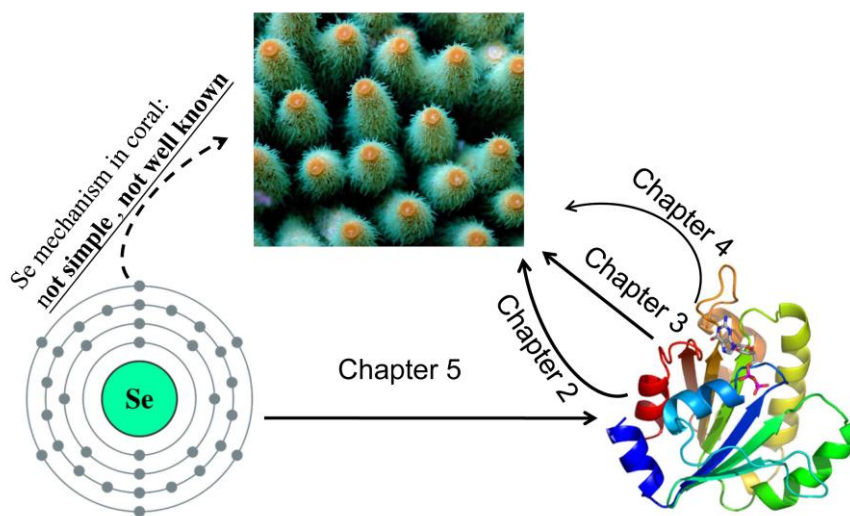
**The 56 kDa SeBP.** Levels of the 56 kDa SeBP in rat liver are significantly increased following administration of aryl hydrocarbon (Ah)-receptor ligands, pentachlorobiphenyl (PCB126) and 3-methylcholanthrene (MC) (Ishii et al., 1996; Chang et al., 1997). There have been suggestions that the 56 kDa SeBP could also be induced by oxidative stress (Song et al., 2006). Involvement in anticarcinogenic growth regulation (Morrison et al., 1988; Yang and Sytkowski, 1998), reduction/oxidation modulation (Jamba et al., 1997), detoxification (Ishii et al., 1996<sup>a</sup>), and intra-Golgi protein transport (Porat et al., 2000) has been suggested, but the physiological functions, mode of induction and mechanism are still largely unclear. The known structure of the *Sulfolobus tokodaii* SeBP indicate that the 56 kDa SeBPs are typically monomeric (Fig. 1.9, Yamada et al., PDB: 2ECE, unpublished). It has recently been suggested (Jeong et al., 2009) that selenite can be specifically bound to the 56 kDa SeBP, but binding constant data were not provided. Whether or not the 56 kDa SeBP binds selenite through Cys(S)-Se bonds remains to be seen.



Fig 1.10 X-ray structure of monomeric 56 kDa SeBP from *Sulfolobus tokodaii* (Yamada et al., 2ECE in protein data bank, unpublished).

## 1.4 Project aims

As discussed above, the trace element Se and many of the proteins in which it occurs play crucial roles in many physiological processes. Unfortunately, most of what we know about selenium biology is from studies based on Bilateria models, and many aspects of the Se biochemistry of non-Bilateria animals need further research. Significant issues here are that many selenoprotein genes are incorrectly annotated, and there have been very few systematic analyses of non-enzymatic selenoproteins and selenium binding proteins. As a representative anthozoan cnidarian, characterization of the selenium protein repertoire of *A. millepora* may help clarify nature of the ancestral gene set as well as the importance of Se-proteins for the biology of reef animals. My project aims to carry out systematic research towards three key terms: Se, Se containing proteins and *A. millepora* (Fig. 1.11).



- Aim 1: Chapter 2 **Se components** in the coral and other cnidarians
- Aim 2: Chapter 3 Se components **responded towards oxidative** stress
- Aim 3: Chapter 4 **Characterization of the 56KD SeBP** in the coral
- Aim 4: Chapter 5 **Binding mechanism of the 56KD SeBP** towards inorganic Se

Fig 1.11 Project aims: systematic research towards Se mechanism in the coral *A. millepora*.

To achieve these goals: (Aim 1, in Chapter 2) bioinformatics tools were used to survey the repertoires of selenium-containing proteins in cnidarians and other model

organisms; (Aim 2, in Chapter 3) the expression of non-enzymatic selenoproteins and SeBP in *A. millepora* under oxidative stress was studied; (Aim 3, in Chapter 4) the 56 kDa *A. millepora* SeBP was characterized; and (Aim 4, in Chapter 5) the Se-binding mechanism of the *A. millepora* 56 kDa SeBP was investigated.

## Chapter 2

### Evolutionary insights into ancestral selenium components

#### 2.1 Introduction

Selenium (Se) has similar redox properties to sulfur (S), while under physiological conditions it is of higher biochemical reactivity than sulfur. In a similar manner to the utilization of cysteine as the redox catalytic center in thiol (R-SH) proteins (Winterbourn and Hampton, 2008), selenium-containing proteins (R-SeH) often use selenocysteine or selenium to catalyze oxidation/reduction reactions *in vivo*. For example, the glutathione peroxidase (GPx) family of selenoproteins catalyze the reduction of peroxides (Rotruck et al., 1973). The specific selenium containing proteins known so far can be divided into two groups: the (specific) selenium binding proteins (SeBPs), and the selenoproteins, the latter of which contain selenium in the form of selenocysteine encoded by an in-frame UGA codon (Behne and Kyriakopoulos, 2001). Both selenium binding proteins and selenoproteins play important roles in a variety of physiological processes.

Based on the application of traditional  $^{75}\text{Se}$  labeling methods (Low and Berry, 1996; Behne et al., 1988; Behne et al., 2000) and bioinformatics-based approaches (Kryukov et al., 2003), large numbers of selenium-containing proteins have recently been reported from a wide range of organisms (Refer to Chapter 1 – Table 1.1). Among these, mammalian members of the GPx and TR (thioredoxin reductase) families have been highly studied in terms of their enzymatic properties, and their catalysis in redox processes. GPx proteins catalyze the reduction of hydrogen peroxide and organic hydroperoxides and thus protect cells from oxidative damage. To date, eight mammalian members of the GPx family have been identified, five of

which are selenoproteins (i.e. contain selenocysteine) and the remainder cysteine based thio-proteins. GPx1, which is also known as cytosolic GPx (cGPx), was the first selenoprotein to be identified (Flohe et al., 1973; Rotruck et al., 1973) and contributes to antioxidant defense against reactive molecules and free radicals. GPx2, originally known as gastrointestinal GPx (GI-GPx), is a tissue-specific selenoenzyme that was found in rats only in the GI tract and in humans only in the GI tract and liver (Chu et al., 1993); because of its tissue specificity, GI-GPx may be an important component of the defense system against ingested lipid hydroperoxides (Esworthy et al., 1998) and is thus of interest in the context of the prevention of colon cancer (Chu et al., 1997). GPx3, also known as Plasma GPx (pGPx), was identified as a secreted selenoprotein (Takahashi et al., 1987). GPx4, known as Peroxidase Phospholipid hydroperoxide GPx (PHGPx), has activity specifically on phospholipid/cholesterol hydroperoxides (Ursini et al., 1985; Thomas et al., 1990) and functions in mammalian spermatogenesis (Behne et al., 1982), has thus been considered the primary selenoprotein component of the system protecting biomembranes against oxidative damage (Roveri et al., 1994). The subcellular localization of GPx4 is dependent on specific promoters (Pushpa-Rekha et al., 1995; Arai et al., 1996), three different transcripts encoding cytosolic, mitochondrial (Calvin et al., 1981) and nuclear forms of the protein (Ursini et al., 1999). GPx-6, the fifth mammalian selenoprotein, is specifically expressed in the olfactory epithelium and was previously known as olfactory-metabolizing protein (OMP) (Dear et al., 1991). The other three members of the mammalian GPx superfamily, GPx-5 (Berry et al., 1997), GPx-7, GPx-8 (Reviewed by Toppo et al., 2008) are cysteine-based thio-proteins other than selenocysteine-based selenoproteins.

The thioredoxin reductase (TR) selenoprotein family was named for their ability to catalyze the NADPH-dependent reduction of oxidized thioredoxin. Thioredoxin reductase 1 (TR1), purified from <sup>75</sup>Se-labeled human lung cancer cells, was the first mammalian selenocysteine-containing thioredoxin reductase to be identified (Tamura and Stadtman, 1996). A second such protein, the mitochondrial thioredoxin

reductase 2 (TR2), was described by four groups in 1999; TR2 cDNAs were cloned from human prostate and liver (Gasdaska et al., 1999), human adrenal (Miranda-Vizueté et al., 1999), rat liver (Li et al., 1999), and the amino acid sequence of bovine TR2 determined after purification of the protein from adrenal cortex (Watabe et al., 1999). The biological role of TR2 in mitochondria is unknown, but it is likely to be involved in protection against mitochondrial-mediated oxidative stress. A third Sec-containing thioredoxin reductase, known here as thioredoxin reductase 3 (TR3), was purified from <sup>75</sup>Se labeled mouse testis, where it is preferentially expressed (Sun et al., 1999). The deduced sequence of the human enzyme shows 70% identity to that of TR1.

Whereas selenoproteins contain selenocysteine, the chemical form of selenium present in selenium binding proteins (SeBPs) is not known, but the absence of selenocysteine codons (TGA) in the coding sequences and the independence of levels of the two proteins on dietary selenium supply, imply that the element is strongly but non-covalently bound to the proteins. The physiological function of the 56 kDa SeBP has been intensively researched. Levels of the protein in rat liver significantly increased following administration of various xenobiotics (Ishii et al., 1996; Ishida et al., 1998; Chang et al., 1997; Rushmore et al., 1991). These and other experiments led to the realization that the chemo-protective effects of selenium could be due at least in part to selenium-binding proteins other than glutathione peroxidase (Bansal et al., 1989<sup>a</sup>). A number of reports indicate that the expression of the 56 kDa SeBP is induced by oxidative stress (Song et al., 2006; Hassan et al., 1983). Roles have been proposed for SeBP in anti-oncogenic growth regulation (Morrison et al., 1988; Yang and Sytkowski, 1998), reduction/oxidation modulation (Jamba et al., 1997), detoxification (Ishii et al., 1996), and intra-Golgi protein transport (Porat et al., 2000), but its physiological functions in vivo and molecular mechanisms are still largely unknown.

By comparison with mammals, few studies have focused on selenium-containing

proteins from early-diverging animals, but data are accumulating at a rapid rate. The 56 kDa SeBP is the most highly conserved of known selenium-containing proteins, invertebrate, plant and microbial (Bansal et al., 1989<sup>b</sup>; Bevan et al., 1998) members of this family having high levels of similarity with their mammalian counterparts. Selenoproteins are also known from a wide range of organisms, including bacteria (Bock, 1994; Bock, 2000; Zhang et al., 2005). Both selenoproteins and the Sec insertion machinery are present in green algae but have been entirely lost in higher plants and fungi (Lobanov et al., 2007). In actinopterygian fishes and early-diverging chordates, a number of selenoproteins have been identified which include some restrictedly distributed selenoproteins like selenoprotein J (Castellano et al., 2005), selenoprotein L (Shchedrina et al., 2007) and disulfide bond formation protein A (DsbA, Jiang et al., 2010). In the insects, a Sec-containing TR is present in *Caenorhabditis elegans* (Gladyshev et al., 1999), and *Drosophila melanogaster* selenoprotein K (which was named by G-rich selenoprotein) and selenoprotein H (which was named by BthD) both contain Sec (Martin-Romero et al., 2001). The literature on cnidarian selenoproteins is very limited: a selenocysteine-containing protein most like GPx4 is known from *Hydra* (Dash et al., 2006).

An interesting aspect of selenoprotein evolution is that most of these proteins have homologs in which the selenocysteine catalytic center is replaced by cysteine. Examples include the GPx6 proteins, where the Sec present in (for example) the human sequence is replaced by Cys in the case of the rodent GPx6 genes (Kryukov et al., 2003), and the TR proteins, where the Sec present in the human protein is replaced by Cys in both *D. melanogaster* (Kanzok et al., 2001) and *C. elegans* (Lacey and Hondal, 2006).

The research summarized above indicates that selenium-containing proteins are widespread throughout the living world, but there have been few attempts to systematically survey their distribution and evolution. The recent availability of whole genome sequences and large EST datasets for a range of animals now permits

a systematic survey of the selenoprotein and selenium-binding protein complements of representative metazoans, and provides new perspectives on the evolution of the animal selenoproteome. In this chapter, we specifically address the evolution of the selenium-containing proteins GPx, TR and the 56 kDa SeBP, focusing particularly on the Sec/Cys switch in selenoproteins. For comparative purposes, the cephalochordate *B. floridae*, the ecdysozoans *D. melanogaster* and *C. elegans*, the cnidarians *N. vectensis*, *H. magnipapillata* and *A. millepora*, the poriferan *Amphimedon queenslandica* (sponge) were selected, as in every case except the last, whole genome sequences were available.

## 2.2 Materials and Methods

### 2.2.1 Sequence Datasets

*B. floridae* and *N. vectensis* genome and protein datasets were downloaded from the Joint Genome Institute website (<http://genome.jgi-psf.org/>). The *H. magnipapillata* and *A. millepora* datasets were obtained from the COMPAGEN platform (<http://compagen.zoologie.uni-kiel.de/>), in the latter case supplemented by 454/Illumina transcriptome assemblies generated locally by Sylvain Foret. Other sequences were obtained from the public database at NCBI. The SelenoDB 1.0 tool (Castellano et al., 2008) was used to manipulate some *D. melanogaster* and *C. elegans* datasets.

### 2.2.2 Sequence analyses and phylogeny construction

The local Blast platform (<http://compagen.zoologie.uni-kiel.de>) and the public NCBI Blast platform were used for Blast analyses. Matches of selenoproteins identified in the original datasets were scrutinized for the presence of potential Sec encoding in-frame UGA codons. This process led to the identification of several mis-annotated selenoproteins, as indicated by asterisks against sequence identifiers in Table 2.1. Protein sequences were aligned using ClustalW version 2 (Larkin et al., 2007) and

maximum likelihood phylogenetic analyses were performed in SeaView version 4 package (Gouy et al., 2010) with PhyML version 3 (Guindon and Gascuel, 2003) using the LG substitution matrix (Le and Gascuel, 2008). The SH-like values calculated by PhyML were used as branch-support values in the constructed phylogenetic trees.

### ***2.2.3 Secondary structure analysis***

Sec insertion sequence (SECIS) elements were analyzed using the SECISearch 2.19 program (Kryukov et al., 2003), and graphics of the stem-loop structures in the corresponding mRNAs also generated in this program.

## **2.3 Results**

### ***2.3.1 The GPx family***

In mammals, some GPxs are expressed ubiquitously and have general roles, whereas the expression of others is restricted to specific tissues and associated with particular physiological processes. Based on phylogenetic analysis of these diversified GPxs, mammalian GPx sequences generally fall into four groups: GPx1, 2 as group A; GPx3, 5, 6 as Group B; GPx7, GPx8 as Group D; GPx4 as Group C (Toppo et al., 2008). By comparison with mammals, the animals included in this study have much simpler morphologies, however, a range of GPx isoforms were identified corresponding to each of the mammalian GPx groups (Fig. 2.1).

Based on the genome sequence database available via the JGI and NCBI website, fifteen predicted GPx sequences were identified in the cephalochordate *Branchiostoma floridae* (Table 2.1). Phylogenetic analysis grouped three of the *Branchiostoma* sequences with mammalian GPx1 and 2 counterparts, seven *Branchiostoma* sequences grouped with mammalian GPx3, 5 and 6, one grouped with mammalian GPx4 counterparts and the remaining four lancelet sequences were

grouped with mammalian GPx7 and 8 (Fig 2.1). One particularly interesting aspect of the *Brachiostoma* data is that most of the predicted lancet GPx sequences contain cysteine rather than selenocysteine, despite the fact that the *Brachiostoma* GPxs cluster with the mammalian selenocysteine-containing proteins.

The GPx repertoire of ecdysozoans varied considerably – whereas the genome of *C. elegans* encodes eight predicted GPx sequences, that of *D. melanogaster* encodes only one (Table 2.1). In phylogenetic analysis, three of the *C. elegans* sequences were grouped with the mammalian GPx3/5/6 type and the other five others most resemble the mammalian GPx7/8 type. The sequence from *D. melanogaster* appeared to be highly diverged and did not cluster with any of the mammalian GPx groups (Fig 2.1). As in *Brachiostoma*, all of the predicted GPx sequences from *C. elegans* and *D. melanogaster* contained cysteine as opposed to selenocysteine.

Despite the absence of any selenocysteine-containing GPx forms in the model ecdysozoans, a GPx4 has previously been reported in the cnidarian *Hydra vulgaris* (Dash et al., 2006), suggesting that cnidarians might be informative with respect to the ancestral GPx repertoire. Scanning the available data for *N. vectensis*, *H. magnipapillata* and *A. millepora* allowed the identification of surprisingly complex GPx inventories that included both selenocysteine- and cysteine-containing predicted proteins (Table 2.1). Phylogenetic analysis grouped two selenocysteine-containing *Nematostella* GPx like sequences (JGI:Nemvel|90698 and Nemvel|140021) with mammalian GPx 1 and 2 with high bootstrap support (Fig 2.1). One selenocysteine-containing sequence (Nemvel|63846) and two cysteine-containing sequences (Nemvel|81508 and Nemvel|238222) grouped with the mammalian GPx3/5/6-type. Two cysteine-containing *Nematostella* GPx like sequence grouped with the mammalian GPx 7/ 8-type and the remaining (selenocysteine-containing) sequence fell into the clade defined by mammalian GPx4 (Fig 2.1). Of the six GPx sequences identified in *H. magnipapillata*, only two contained selenocysteine. Two of the *Hydra* GPx sequences clustered together with the GPx4 type, but illustrate the

lability of the cysteine/selenocysteine character – the phylogeny implies that these are products of independent duplication events but only one of them contains selenocysteine. One *Hydra* sequence (DN246918) clustered with sequences from *Nematostella* (jgi|Nemvel93209) and *Acropora* (DY579918) within the larger GPx4 clade, suggesting that these might represent orthologs of a cnidarian GPx-type. One *Hydra* sequence (DT619601) containing seleocysteine fell into the GPx3/5/6 clade and the remaining two sequences from this organism group together, diverging close to the base of the clade comprising both group A and group B sequences.

Moreover, two GPx like sequences were found in the sponge *A. queenslandica*, one clustered with cnidarian GPx-type in Group C, the other fell into GPx7/8 clade (Fig 2.1). No sequences of GPx1/2 and GPx3/5/6 are present in the *A. queenslandica* genome.

The broad pattern of distribution of GPx like sequences suggests an early emergence of the GPx4 type despite the fact that no sequences of this type are present in ecdysozoans. Cnidarian and sponge *A. queenslandica* genomes encode members of both the GPx4 and GPx7/8 types; cnidarians also contain members of the larger clade that comprises mammalian GPx1/2 and GPx3/5/6.

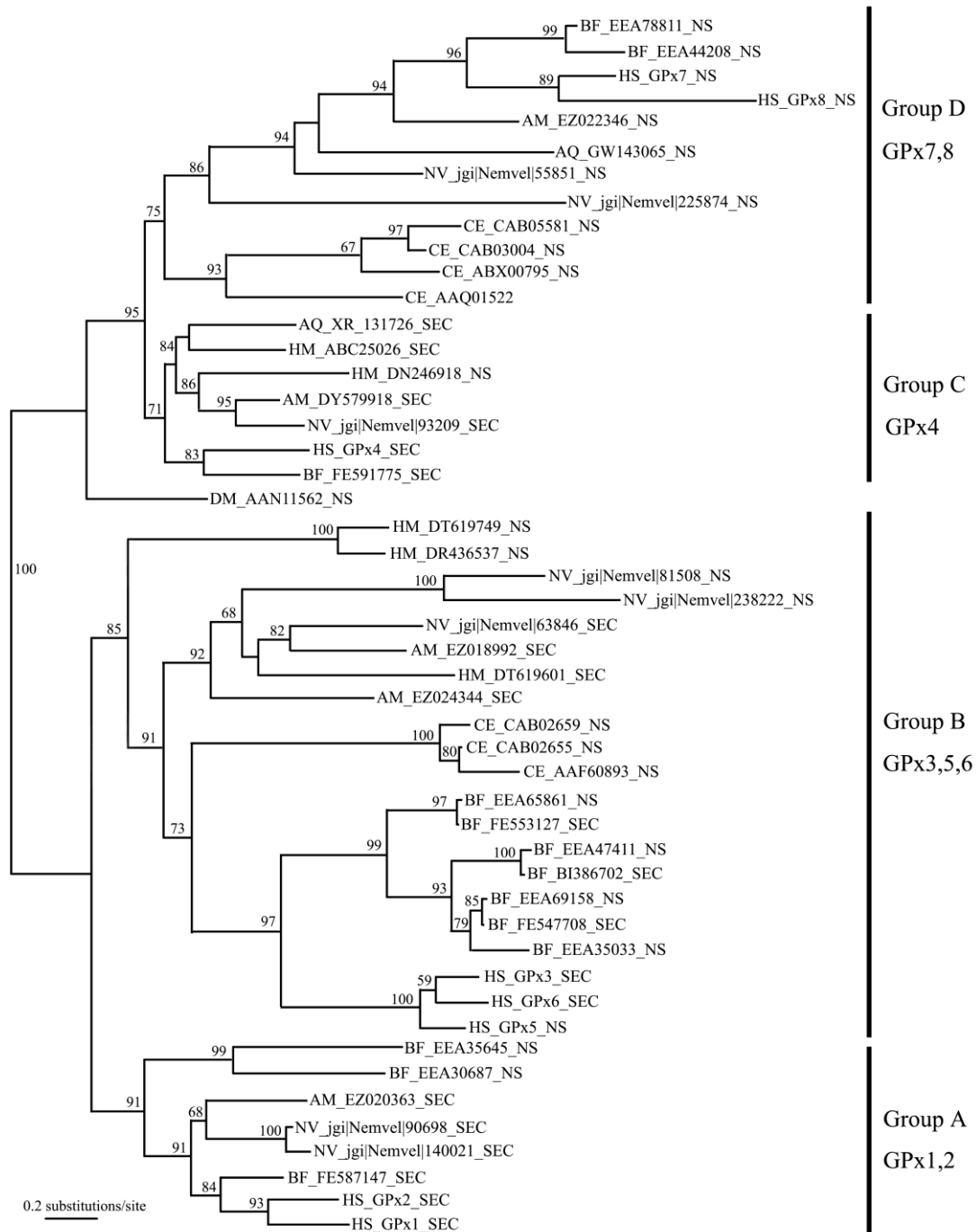


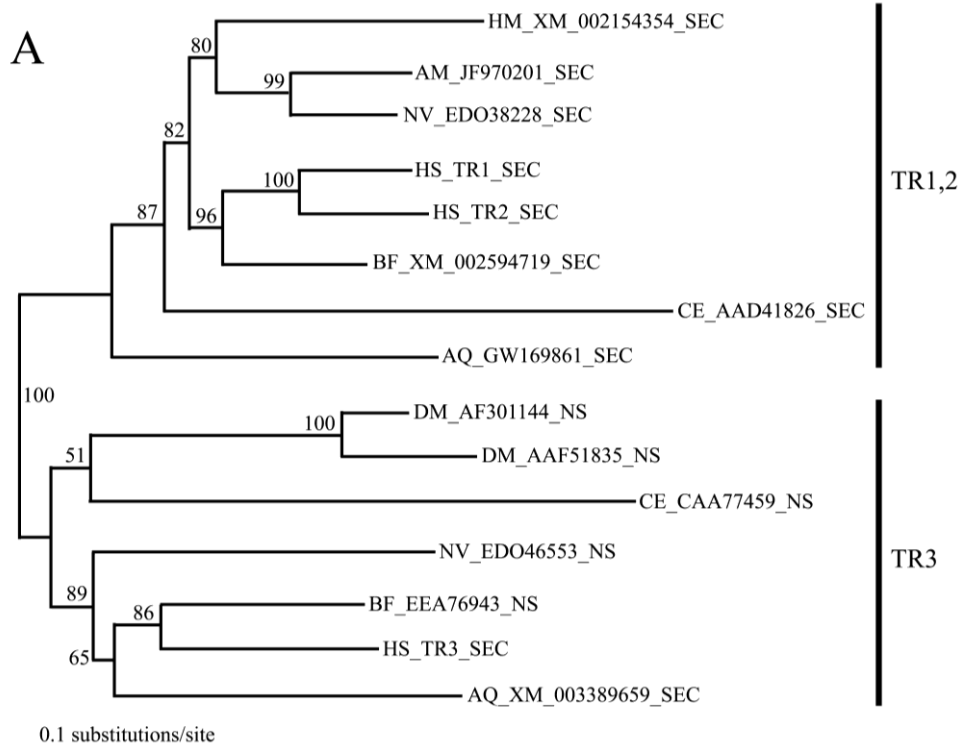
Fig. 2.1 Phylogenetic analysis of GPx Family. The maximum likelihood (ML) tree shown is the result of analysis of a ClustalW alignment of the GPx homologues from the cephalochordate ‘BF’ (*B. floridae*), two ecdysozoans ‘DM’ (*D. melanogaster*) and ‘CE’ (*C. elegans*), three cnidarians ‘NV’ (*N.vectensis*), ‘HM’ (*H. magnipapillata*), ‘AM’ (*A. millepora*), and the poriferan ‘AQ’ (*A. queenslandica*, sponge). The SH-like values were calculated to support the branches of the PhyML constructed ML tree. Four groups were resolved by this analysis, corresponding to the mammalian GPx1/2 (Group A), GPx3/5/6 (Group B), GPx4 (Group C) and GPx7/8 (Group D) types. ‘SEC’ indicates the presence of selenocysteine; ‘NS’ indicates the absence of selenocysteine.

### 2.3.2 The TR like genes

The amino acid sequence Gly-Cys-Sec-GlyOH (GCUG) located at the COOH termini of mammalian TRs functions as a redox centre (Kanzok et al., 2001). Due to Sec being encoded by an in-frame UGA, mis-annotation is common in the case of TR like sequences. To clarify the evolution of the TR protein family, candidate sequences were reevaluated in this study, leading to the finding that some sequences had been mis-annotated with respect to the UGA code (indicated in Table 2.1). After reevaluation of the available sequence data, Sec-containing TR like sequences were identified in each of the cnidarians *H. magnipapillata*, *N. vectensis*, and *A. millepora*. A second TR like sequence was identified in *N. vectensis*, but this lacks Sec (Table 2.1). The sponge *A. queenslandica* also have two mis-annotated TR like sequences (GW169861 and XM\_003389659), they were identified as Sec-containing TRs in this study (Fig 2.2).

Phylogenic analysis resolved two major groups of animal TRs, one of which is defined by mammalian TR3 (Fig 2.2), but it is interesting to note that most of the invertebrate members of this clade lack selenocysteine (except the sponge TR3 XM\_003389659). In contrast, those invertebrate TRs containing selenocysteine grouped with the mammalian TR1/TR2 type in phylogenetic analysis (Fig 2.2). Although the (selenocysteine-containing) TR1/TR2 type appears to have been lost in *D. melanogaster*, members of this clade are present in *C. elegans*, in sponge *A. queenslandica* as well as each of the three cnidarians, *H. magnipapillata*, *A. millepora*, and *N. vectensis* (Fig 2.2).

Comparison of the C-terminal sequences indicates that the invertebrate TR3-type sequences differ from their mammalian counterparts in that the GCUG (Gly-Cys-Sec-GlyOH) motif present in the vertebrate proteins is replaced by GC--, GCCG or SCCS. The invertebrate TR1/TR2 type proteins, on the other hand have the conserved GCUG at the C-terminus as in their mammalian counterparts.



**B**

<i>H. magnipapillata</i> XM_002154354	GIHPVCAEVFTTLSVTKRSG-ASILQAGCUG	TR1,2
<i>A. millepora</i> JF970201	GIHPTVSEVFTTLLSTTKRSG-KDVSAGGCUG	
<i>N. vectensis</i> EDO38228	GIHPTCSETFTLLDVTKRSG-ASIVSSGCUG	
<i>H. sapiens</i> TR1	GIHPVCAEVFTTLSVTKRSG-ASILQAGCUG	
<i>H. sapiens</i> TR2	GIHPTCGEVFTTLEITKSSG-LDITQKGCUG	
<i>B. floridae</i> XM_002594719	GIHPTNAEIFTTMDITKSG-EDPTKTGCUG	
<i>C. elegans</i> AAD41826	GIHPTVAENFTTLLLEKKEGDEELQASGCUG	
<i>A. queenslandica</i> GW169861	GIHPTCSETFTTLRVTKSSG-EDSSAGNCUG	
<i>D. melanogaste</i> AF301144	GIHPTTAEFTRLAITKRSG-LDPTPASCCS	TR3
<i>D. melanogaste</i> AAF51835	GIHPTTAEFTRLSITKRSG-RDPTPASCCS	
<i>C. elegans</i> CAA77459	AIHPCSSEEFVKLHITKRSG-QDPRTQGCGG	
<i>N. vectensis</i> EDO46553	GIHPTCAEEVVKLHITKRSG-EDPTVTGC--	
<i>B. floridae</i> EEA76943	GIHPTCAEEVVKMGITKRSG-LDPTVTGC--	
<i>H. sapiens</i> TR3	GIHPTCSEEVVKLRISKRSRSG-LDPTVTGCUG	
<i>A. queenslandica</i> XM_003389659	GIHPTVAEEVVKLHITKSSG-EDPTVTACUG	

Fig 2.2 Phylogeny and C-terminal sequences of TR like proteins from representative animals. A: The maximum likelihood (ML) tree shown is the result of analysis of a ClustalW alignment of all of the TR homologues listed in Table 2.1 from a cephalochordate ‘Bf’ (*B. floridae*), two ecdysozoans ‘DM’ (*D. melanogaster*) and ‘CE’ (*C. elegans*), three cnidarians ‘NV’ (*N. vectensis*), ‘HM’ (*H. magnipapillata*), ‘AM’ (*A. millepora*), and the poriferan ‘AQ’ (*A. queenslandica*, sponge). The SH-like values were calculated to support the branches of the PhyML constructed ML tree. ‘SEC’ indicates the presence of selenocysteine; ‘NS’ indicate the absence of selenocysteine. B: The alignment of C-terminal sequences shows the conservation of the Gly-Cys-Sec-GlyOH sequence (marked GCUG) in the invertebrate TR1/TR2 homologues.

### 2.3.3 Other selenoproteins and related factors

In addition to GPxs and TRs, other selenoprotein-like sequences were also surveyed in the available cnidarian sequence data. In some animals, many of the proteins are represented but have undergone loss of the selenocysteine residue. The most extreme example of this is *C. elegans*, in which a total of 20 selenoprotein-like sequences are present (this figure includes GPxs and TRs), but most of these lack Sec, only a single Sec-containing protein (a TR) was identified. Of the 14 selenoprotein-like sequences in *D. melanogaster*, only three contain Sec, and of the 40 selenoprotein-like sequences in *B. floridae*, only small portion of these proteins contain Sec (Table 2.1, 2.2). By comparison with these models, Cnidarians have maintained more selenoproteins than have the ecdysozoans, and a higher portion of these contain selenocysteine compared to the other invertebrates surveyed; 13 of 28 in *N. vectensis*, 21 of 27 in *A. millepora* and 12 of 21 in *H. magnipapillata*) selenoproteins identified contained Sec.

Patterns of retention and loss varied considerably across the range of invertebrates studied, which supports the mosaic evolution pattern of selenium elements in other research models (Castellano et al., 2005). Members of the 15 KD selenoprotein and Selenoprotein T families showed a conserved evolution pattern, which were present in each of the animals studied (Table 2.1). Selenoproteins P, S, V and W were present in amphioxus and cnidarians but appear to have been lost from the ecdysozoans studied. Conversely, selenoprotein K homologues were identified in both *Drosophila* and *Caenorhabditis* but were not found in either amphioxus or cnidarians. Homologues of selenoprotein N was found in cnidarians but were absent from both amphioxus and the ecdysozoans. More interestingly, some rare selenoproteins like selenoprotein L, J, U, DsbA (difulfide bond formation protein A), MsrA (methionine sulfoxide reductase) which are absent or only have Cys homologues in mammalian models were found in both amphioxus and cnidarians, indicated these selenoproteins

have diversified before the bilaterian-cnidarian split.

After sequence analysis using the program SECISearch 2.19 (Kryukov et al., 2003), Sec insertion sequence (SECIS) elements were found in the 3'-untranslated regions (3'-UTRs) of the cnidarian Sec-containing selenoproteins W and T (Fig. 2.3). These sequences each contain the ATGA\_AA\_GA pattern and are predicted to fold into a stem-loop structure in the corresponding mRNA.

Other related factors required for Sec biosynthesis (Kryukov et al., 2003), including Sec-specific elongation factor (eEFSec), SECIS binding protein and selenophosphate synthetase (SPS) were identified in *N. vectensis*, *B. floridae* and *D. melanogaster*, (Table 2.1), but in the case of *C. elegans* and *H. magnipapillata* the SECIS binding protein could not be identified.

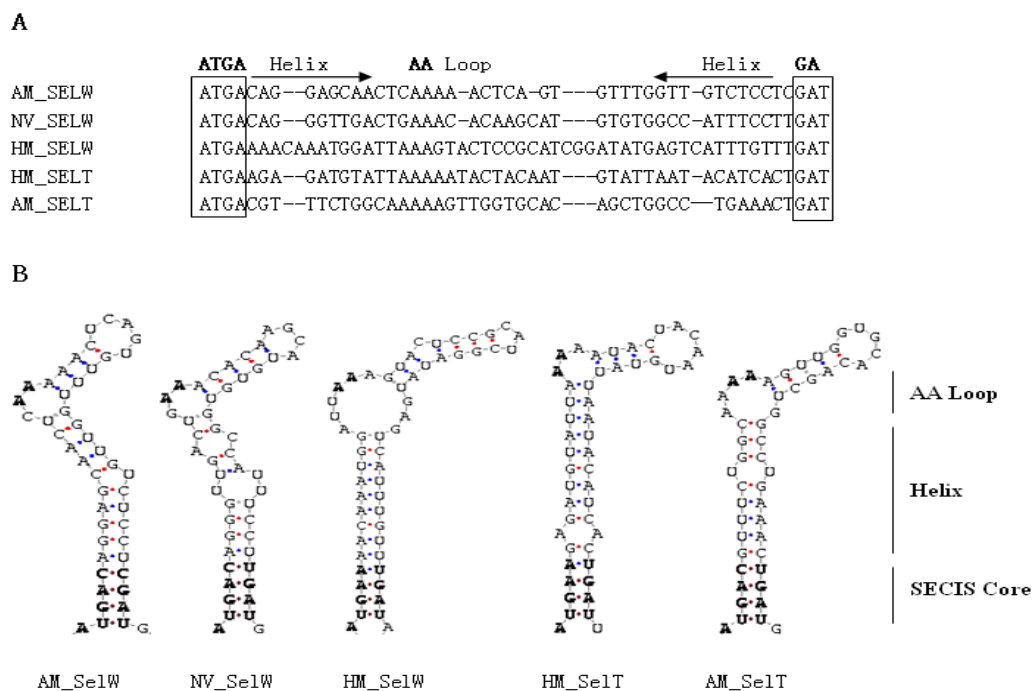


Fig 2.3 SECIS elements in cnidarian selenoprotein W and T genes. (A) The primary sequence of SECIS elements in 'NV' (*N.vectensis*), 'HM' (*H. magnipapillata*) and 'AM' (*A. millepora*) selenoprotein W, T genes; alignment of these SECIS elements shows a conserved ATGA\_AA\_GA pattern. (B) The predicted secondary stem-loop structure of these SECIS elements.

Table 2.1 Overview of selenium components identified.

Vertebrata		Cephalochordata		Ecdysozoa				Cnidaria						
<i>H. sapiens</i>		<i>B. floridae</i>		<i>D. melanogaster</i>		<i>C. elegans</i>		<i>N. vectensis</i>		<i>A. millepora</i>		<i>H. magnipapillata</i>		
GPx Family														
A	GPx1	SEC	gb EEA35645	NS				jgi Nemve1 90698	SEC	gb EZ020363	SEC			
	GPx2	SEC	gb EEA30687	NS				jgi Nemve1 140021	SEC					
			gb FE587147	SEC										
B	GPx3	SEC	gb EEA65861	NS		gb CAB02659	NS	jgi Nemve1 63846	SEC	gb EZ018992	SEC	gb DT619601	SEC	
	GPx5	NS	gb EEA47411	NS		qb CAB02655	NS	jgi Nemve1 81508	NS	gb EZ024344	SEC	gb DT619749	NS	
	GPx6	SEC	gb EEA69158	NS		gb AAF60893	NS	jgi Nemve1 238222	NS				gb DR436537	NS
				gb EEA35033	NS									
				gb FEA553127	SEC									
			gb BI386702	SEC										
			gb FE547708	SEC										
C	GPx4A	SEC	gb FE591775	SEC				jgi Nemve1 93209	SEC	gb DY579918	SEC	gb ABC25026	SEC	
	GPx4B	SEC										gb DN246918	NS	
	GPx4C	SEC										gb CN553521	NS	
D	GPx7	NS	gb EEA78811	NS	gb AAN11562	NS	gb CAB05581	NS	jgi Nemve1 55851	NS	gb EZ022346	NS		
	GPx8	NS	gb EEA44208	NS			gb CAB03004	NS	jgi Nemve1 225874	NS				
				gb EEA35486	NS			gb ABX00795	NS					
				gb EEA46801	NS			gb AAF39836	NS					
						gb AAQ01522	NS							
TR Family														
	TR1	SEC	gb XM_002594719*	SEC			gb AAD41826	SEC	gb EDO38228*	SEC	gb JF970201	SEC	gb XM_002154354*	SEC
	TR2	SEC												

TR3	SEC	gb EEA76943	NS	gb AF301144	NS	emb CAA77459	NS	gb EDO46553	NS				
				gb AAF51835	NS								
Other selenoproteins													
DI (iodothyronine deiodinase)	SEC	gb FE585018.1	SEC					gb FC285887.1	NS	gb EZ039538.1	NS		
										gb EZ016985.1	SEC		
DsbA (difulfide bond formation protein A)		gb BW705483.1	SEC					gb XM_001631934.1	NS	gb EZ027474.1	SEC	gb XM_002165149.1	NS
MsrA (methionine sulfoxide reductase)	NS	gb BW893558.1	SEC	gb BI607173.1	NS	gb EC019259.1	NS	gb FC285329.1	SEC	gb DY580633.1	SEC	gb XM_002165032.1	TBC
								gb FC241244.1	SEC				
15KD selenoprotein	SEC	gb EEA32674	NS	gb AAM51078	NS	gb AAF36064	NS	jgi Nemve1 98340	TBC	gb DY584261	SEC	gnl ti 795695620*	SEC
		gb EEA43749	NS										
Selenoprotein H	SEC	gb FE596030.1	SEC	gb AAK72982	SEC	emb AL110471.1	NS			am sepH	SEC		
				gb AAF53633	NS								
				gb AAF58585	NS								
Selenoprotein I	SEC	gb EEA32690	NS	gb AAL39243	NS	gb NM_059053.3	NS	jgi Nemve1 219181*	SEC	am sepI	SEC	gnl ti 221129191	TBC
Selenoprotein J		gb FE540968.1	NS							gb EZ042767.1	SEC	gb XM_002156793.1	NS
Selenoprotein K	SEC			gb AAF48111	SEC	gb CAB09004	NS						
Selenoprotein L		gb FE590577.1	SEC					gb XM_001630134.1	TBC	gb EZ015666.1	TBC	gb XR_053861.1*	SEC
Selenoprotein M	SEC	gb BW909508.1	SEC							gb EZ009555.1	SEC	gnl ti 1166535561*	SEC
Selenoprotein N	SEC							jgi Nemve1 108300	NS	gb EZ041633.1	TBC		
Selenoprotein O	SEC	gb EEA54826	NS	gb EC054401.1	TBC			jgi Nemve1 225263	TBC	gb DY584700	SEC	gb XM_002164928.1*	SEC
								gb XM_001640887.1*	SEC				
Selenoprotein P	SEC	gb EEA47179	NS					jgi Nemve1 240662	TBC	gb DY586647	TBC	gnl ti 1170393204	TBC
Selenoprotein R	SEC	gb FE550509.1	NS	gb AAF54569	NS	gb AAA28039	NS	jgi Nemve1 90236	TBC	am sepR	SEC	gb XM_002157802.1	TBC
Selenoprotein S	SEC	gb EEA36680	NS					gb EDO34836.1	TBC	am sepS	SEC	gnl ti 1243521569*	SEC

Selenoprotein T	SEC	gb EEA63693	NS	gb AAF52202	NS	gb CAB01692	NS	jgi Nemve1 139284	TBC	gb DY585317	SEC	gnl ti 1229906363*	SEC
		gb BW894722.1	SEC			gb CAA96637	NS						
Selenoprotein U	NS	gb BW887982.1	NS			gb NM_063753.2	NS	gb XM_001625464.1*	SEC	gb EZ041414.1	SEC	gb XR_053861.1*	SEC
Selenoprotein V	SEC	gb BW891156.1	SEC					gb XM_001627725.1*	SEC	gb EZ043112.1	SEC		
Selenoprotein W1	SEC	gb EEA68305	NS					jgi Nemve1 245929*	SEC	gb DY584383	SEC	gnl ti 908319051*	SEC
		gb BW841330.1	SEC										
Selenoprotein W2	SEC	gb EEA45698	NS							gb DY585128	SEC		
		gb FE581389.1	SEC										
Sec incorporation factors													
SPS1	NS	gb EEA72698	NS	gb AAB88790	NS					gb DY586785	NS	gnl ti 1170390503	NS
SPS2	SEC	gb FE558318.1	SEC	gb CAB93526	SEC	gb NM_070203.1	NS	jgi Nemve1 96658	SEC	gb EZ010392.1	TBC	gb XR_053622.1	SEC
eEFSec	NS	gb EEA35955	NS	gb AAF46721	NS	gb CAB16862	NS	jgi Nemve1 165791	NS	am eEFSec	NS	gnl ti 657480864	NS
SECIS binding protein	NS	gb EEA66162	NS	gb AAF50448	NS			jgi Nemve1 131390	NS	am SECIS-BP	NS		
Selenium binding proteins (SeBP)													
14 kDa SeBP	NS												
56 kDa SeBP	NS	gb EEA73516	NS	gb AAF54900	NS	gb CAA19490	NS	gb EDO41029	NS	am SeBP1	NS	gb CN772336	NS
		gb EEA68173	NS			gb CAB01239	NS			am SeBP2	NS	gb CN626781	NS

‘SEC’ indicates the presence of selenocysteine; ‘NS’ indicates the absence of selenocysteine; ‘TBC’ indicates that the Sec status of the sequence needs further investigation. ‘\*’ indicates the sequence is mis-annotated in the original datasets. ‘am|’ indicates the unpublished sequence of *A. millepora*, and the sequence is summarized in supplementary Table 1.

Table 2.2 Summary of selenoprotein data for the animals studied.

	Number of Sec-containing selenoprotein	Number of sequences without Sec	Number of unclear sequences*	Total Number	Percentage of Sec-containing sequences
<i>B. floridae</i>	17	23	0	40	42.5%
<i>D. melanogaster</i>	3	10	1	14	21.4%
<i>C. elegans</i>	1	19	0	20	5.0%
<i>N. vectensis</i>	13	9	6	28	46.4%
<b><i>A. millepora</i></b>	<b>21</b>	<b>2</b>	<b>4</b>	<b>27</b>	<b>77.8%</b>
<i>H. magnipapillata</i>	12	6	4	21	57.1%

\* indicates that the Sec status of the sequence needs further investigation.

### 2.3.4 Selenium binding proteins

By comparison with selenoproteins, the selenium binding proteins (SeBPs) have received relatively little attention. The limited literature on SeBPs has been focused on mammals, despite the fact that SeBPs clearly play important roles in redox processes in all animals. The likely indispensability of the 56 kDa SeBP suggested by previous work was confirmed by the fact that 56 kDa SeBP sequences were identified in all of the animals studied here (Table 2.1, Fig 2.4). As in the case of mammals, two 56 kDa SeBP isoforms, were present in *B. floridae*, *H. magnipapillata* and *A. millepora*, but not in *A. queenslandica*, *N. vectensis*, *C. elegans* or *D. melanogaster*. In each case the two isotypes have high similarity with each other (Fig 2.4), suggesting independent duplication events in each lineage.

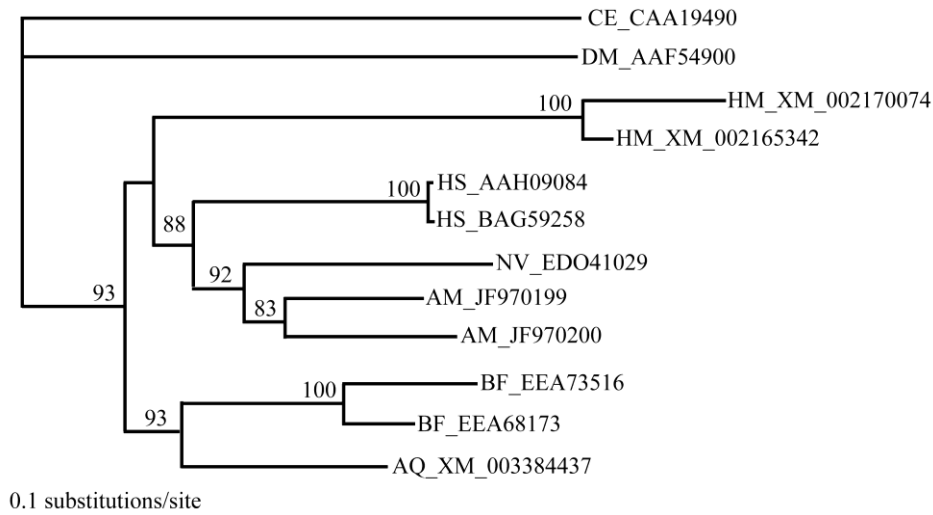


Fig 2.4. Phylogenetic analysis of SeBP proteins. The maximum likelihood (ML) tree shown is the result of analysis of a ClustalW alignment of all the 56kDa SeBP homologues from the cephalochordate ‘BF’ (*B. floridae*), two ecdysozoans ‘DM’ (*D. melanogaster*) and ‘CE’ (*C. elegans*), three cnidarians ‘NV’ (*N.vectensis*), ‘HM’ (*H. magnipapillata*), ‘AM’ (*A. millepora*), and the poriferan ‘AQ’ (*A. queenslandica*, sponge). The SH-like values were calculated to support the branches of the PhyML constructed ML tree.

## 2.4 Discussion

The selenium protein repertoires of morphologically simple animals (poriferan, cnidarians, cephalochordate) are comparable in complexity with those of mammals, and include selenoproteins, the components associated with Sec biosynthesis and selenium binding proteins, indicating the importance of selenium in the metabolism of the common ancestor of animals. The ancestral complements of Sec and non-Sec selenium proteins together nearly cover all the mammalian GPx, TR family and other selenoprotein types (Table 2.1, Fig 2.1, Fig 2.2, Fig 2.4), despite the fact that some of the mammalian GPx types are thought to have very restricted expression patterns and to be associated with specific physiological processes (Behne et al., 1982; Chu et al., 1993; Toppo et al., 2008). The results suggest that most of the known mammalian selenoproteins like GPxs and TRs have diversified before the bilaterian-cnidarian split.

Moreover, from the scenarios that the ancestral Gpx4 (Group C in Fig 2.1) and TR 1/2 types are more likely to keep their Sec components than other types, we suppose that and each of the GPx and TR types has a distinct evolutionary history under different evolutionary forces. One of the forces is the specific physiological role of the Sec in these selenoproteins.

During evolution, selenoproteins have been lost from specific lineages, and the Sec residue seems particularly labile, as many Sec-containing proteins have close homologues in which the Sec is replaced by Cys. Table 2.2 shows the diversity of predicted selenoproteins in the range of animals studied here: the majority of *B. floridae*, nematode and fruit fly homologues of mammalian selenoproteins have Cys substituted for Sec. Consistent with this, it has been reported that insects have much reduced selenoproteomes (Lobanov et al., 2008); surprisingly, many more of the selenoproteins in cnidarians appear have retained the Sec residue which include some rare Se elements like selenoprotein L, J, U, DsbA and MsrA. The reasons for this are unclear, but presumably relate to the selective balance between the enhanced catalytic properties of Sec versus the limited availability of selenium in some environments. The necessity to retain a relatively complex synthetic repertoire also imposes a selective cost, and most likely has been a factor in the complete loss of selenoproteins in some lineages. The conversion of Sec to Cys observed in some ancestral models gives the appearance of the work of ‘a skilled surgeon’, but presumably occurred in a stepwise fashion, rather than as a single event.

In animals, the mechanism ensuring that the appropriate in-frame UGA codons are effectively recoded as Sec requires the SECIS element in the 3'-UTR of the selenoprotein mRNA (Low and Berry, 1996), SECIS binding protein, Sec-specific elongation factor and selenophosphate synthetase. Recent research has identified derived SECIS elements present in nematode, fruit fly (Castellano et al., 2008) and *B. floridae* (Jiang et al., 2010) selenoproteins, and our results show that cnidarian selenoproteins W and T also have SECIS elements in the 3'-UTRs. Other components

of the Sec insertion system, including SECIS binding protein, Sec-specific elongation factor and selenophosphate synthetase are found in the ancestral models we studied here. It seems highly unlikely that *B. floridae* would only retain one selenoprotein (Jiang et al., 2010) with such a complex Sec insertion machinery. We further scan the *B. floridae* genome to search for other selenoproteins and have characterized 16 more selenoproteins (Table 2.1, 2.2). There are precedents for taxon-specific selenoproteins; for example, SelJ is restricted to actinopterygian fish and echinoderms, with Cys-containing versions present in cnidarians (Castellano et al., 2005). We also found the rare SelJ in the cnidarian *A. millepora* and its Cys homologue in *H. magnipapillata*. Moreover, other rare Se components like selenoprotein L, U and DsbA are found in amphioxus and cnidarians (Table 2.1) which indicates these rare selenoproteins have diversified from the common ancestors of bilaterian and cnidarian.

To systematically survey the whole status of Se utilization in the metazoan animals studied, we also research the selenium-binding protein in this study. In contrast to the complex and diverse patterns of evolution observed in the case of the animal selenoprotein repertoire, the 56 kDa selenium-binding protein family is evolutionarily stable (Table 2.1, Fig 2.4), highlighting the biological importance of selenium even in those organisms which have extensively ‘degraded’ their selenoprotein repertoires.

The major contribution of our study is the revealing of Se components in the early diverging animals (poriferan and cnidarians), which is not systematically analyzed before. The *A. millepora* has the most abundant selenium containing proteins (21 selenoproteins and 2 SeBP) in the invertebrates so far studied, indicating the importance of selenium utilization in coral biology.

## Chapter 3

# Changes in the expression of genes encoding non-enzymatic selenium proteins during oxidative stress in the coral *Acropota millepora*

### 3.1 Introduction

To neutralize the reactive oxidants that are continually produced from a variety of physiological processes and metabolic activities, most aerobic cells have developed a comprehensive network of antioxidants that include non-enzymatic components and metabolic enzymes. Due to the reversible oxidation/reduction (redox) activity of the element sulfur (S), the basic redox buffer is assumed to be composed primarily of small molecules and proteins containing the active thiol (-SH) group (reviewed by Winterbourn and Hampton 2008, Kemp et al., 2008), such as the tripeptide glutathione (GSH) and the protein thioredoxin (Trx). Moreover, the trace element selenium (Se) has similar redox properties to sulfur, and the selenol group (-SeH) is more active than the thiol group under normal physiological conditions (Stadtman 1996). Thus selenium containing proteins are now generally believed to also be key components of antioxidant network (Driscoll and Copeland 2003). For example, in mammals, the selenoenzymes glutathione peroxidase (GPx) (Flohé et al., 1973; Rotruck et al., 1973) and thioredoxin reductase (TR) (Gasdaska et al., 1995; Tamura and Stadtman 1996) appear to function in regulation of the redox state of the basic thiol components in the redox network.

The main form in which Se is present in proteins is as selenocysteine (Sec), the 21st amino acid, which is incorporated during selenoprotein synthesis (Stadtman 1996). Se can also be bound by proteins after translation, as in the selenium binding proteins

(SeBP) (Bansal 1989). Both selenoproteins (reviewed by Driscoll 2003) and SeBPs (Flemetaki 2002) are widely distributed across the three kingdoms of life: prokaryotes, eukaryotes and archaeobacteria. Amongst eukaryotes for which whole genome sequence data are available, vertebrates (and particularly mammals) have the most extensive Se protein repertoires; more than 20 selenoproteins (selenoproteome) and several selenium binding protein have been reported in some mammals (reviewed by Behne and Kyriakopoulos 2001; Kryukov 2003). By comparison, nematodes and insects have massively reduced selenoproteomes through gene loss and/or replacement of Sec with cysteine (Gladyshev et al., 1999; Martin-Romero et al., 2001; Lobanov et al., 2007). Higher plants have undergone complete selenoproteome loss, retaining only the highly conserved SeBPs (Flemetakis et al., 2002). Neither selenoproteins nor SeBPs have been found in yeasts but many algae have a number of selenoproteins (Lobanov et al., 2007). To better understand patterns of evolution of selenium containing proteins in the animal kingdom, we carried out a bioinformatic analysis (in Chapter 2) focusing on the cnidarians *Hydra magnipapillata*, *Nematostella vectensis* and *Acropora millepora* and found complex selenoproteomes and SeBP repertoires. The *A. millepora* selenoproteome (containing Sec site) includes two types of selenoprotein W (W1,W2), GPx, TR, Selenoprotein P, O, T, H, and the 15 kDa selenoprotein. In addition, two highly conserved SeBP homologs, amSeBP17, amSeBP23, were found in *A. millepora*. Thus, despite its early evolutionary position within Metazoa, the repertoire of Se-containing proteins in the cnidarian *A. millepora* is remarkably complex.

Whereas selenoenzymes such as GPx and TR have well-established redox functions, the roles of the non-enzymatic selenium containing proteins are much less clear. Most research on these latter has focused on the mammalian proteins, but has not clearly established their involvement in the redox network. In this study, we artificially exposed the coral *A. millepora* to oxidative stress by using hydrogen peroxide (H<sub>2</sub>O<sub>2</sub>) and L-buthionine-[S,R]-sulfoximine (BSO), a chemical which blocks the basic redox buffer GSH (Griffith and Meister 1979), and then monitored the expression of genes

encoding a number of Se-containing proteins. This study represents the first step in establishing which Se containing proteins are critical in the response of *A. millepora* to oxidative stress. In Chapter 4 of this thesis, further characterization of two candidate genes identified here is described.

## **3.2 Materials and methods**

### ***3.2.1 Collection and maintenance of corals***

Branches (about 5 cm in length) from three separate colonies of *A. millepora* were collected between 1.5 and 3 m depth on the reef flat of Nelly Bay (Magnetic Island, Townsville, Australia) at June 2008. All branches were attached firmly (with oral end up) on the racks in outdoor tank supplied with running seawater for 6 days to recover from damage during collection and transport. In this period, the environmental temperature was between 20 °C (night) and 25 °C (day), and sea water temperature in the tank was in the range 21-23 °C. The experiment was carried out in winter to avoid problems associated with the hot summer (December to April) climate and the physiological complications of spawning activity (September to November) which might impose thermal or physiological stresses on the coral. After six days in aquaria, two colonies were judged to be healthy on the basis of the following criteria: (1) the tentacles surrounding the oral end of the coral displayed normal feeding behaviour, and (2) the corals remained “normal” with respect to apparent symbiont density, no difference in level of colony coloration. By contrast, the third colony was judged not to be in good condition on the basis of these criteria, and was excluded from the experiment.

### ***3.2.2 Experimental conditions***

Previous studies (Seneca et al., 2009; Bay et al., 2009) have established that considerable heterogeneity exists in healthy coral colonies with respect to basal expression levels of a wide range of genes. To minimize the contribution of genetic

background, expression levels were compared within single colonies in the experiment described here - treatments ( $\text{H}_2\text{O}_2$ , BSO+ $\text{H}_2\text{O}_2$ ) were carried out on branches from the same colony and compared to controls from within the same colony. Prior to experimental treatment, three branches (selected at random) of each healthy colony were snap frozen in liquid nitrogen and stored at  $-80^\circ\text{C}$  freezer until required. Other healthy branches of each colony were randomly separated into two groups: groups A and B for colony 1, and groups C and D for colony 2. Samples B and D were separately treated with BSO (300  $\mu\text{M}$  in filtered sea water) for 20 h to block the basic redox buffer GSH. After BSO treatment, all four groups of samples were treated with  $\text{H}_2\text{O}_2$  (200  $\mu\text{M}$  in filtered sea water). At 4 h, 12 h, 24 h time points after  $\text{H}_2\text{O}_2$  treatment, three branches (selected at random) from each group were snap frozen in liquid nitrogen and then stored at  $-80^\circ\text{C}$ . All samples in each of the four treatment groups remained normal throughout the experiment in terms of the criteria outlined above.

### ***3.2.3 Total RNA extraction and first strand cDNA synthesis***

Total RNA was extracted from adult coral branches as previously described (Seneca et al., 2009) using a high pressure crushing process. Frozen coral branches (coral tissue with skeleton) were first crushed to a fine powder in liquid nitrogen. Aliquots (3 ml) of TRI reagent (Ambion, Australia) were then added to 150 mg of each powdered sample, and the slurry lightly vortexed for 5 mins. Well-mixed samples were then spun at 12,000 g for 10 min to pellet the skeleton. Total RNA was then extracted from the aqueous phase using a modification of the TRI reagent protocol in which chloroform was replaced with trimethylene chlorobromide (BCP, Sigma, USA). The total RNA preparations were then treated with DNase I, (Amp Grade, Invitrogen, USA) after which the integrity of the RNA was examined by electrophoresis and the concentration and purity determined by the use of an ND-1000 Spectrophotometer (NanoDrop Technologies). cDNA was generated for each sample using 1  $\mu\text{g}$  aliquots of the DNase-treated total RNA preparations as template for reverse-transcription

using the Superscript<sup>TM</sup> III First-Strand Synthesis System (Invitrogen, USA) using the supplier's protocol. cDNA samples were diluted 20-fold with ultra-pure PCR grade water (Bioline, Australia) prior to qPCR.

#### **3.2.4 Real time qPCR**

Four commonly used housekeeping genes (*amACTB*, *amGAPD*, *amSDHA*, *amUBC*, full name in Table 3.1) were selected as candidate internal control genes (ICGs), and the nine *A. millepora* genes of interest (GOIs) studied encoded a variety of selenium-containing proteins (*amSEP15kD*, *amSEPW1*, *amSEPW2*, *amSeBP17*, *amSeBP23*, *amSEPP*, *amSEPT*, *amSEPH*, *amSEPO*, full name in Table 3.1). Primer Premier 5.0 (PremierBiosoft, CA) was used to design primers with similar annealing temperatures (57-60 °C) for use in qPCR. Because the cDNA generated may contain *Symbiodinium* contamination (Mayfield et al., 2009; Seneca et al., 2009), it was necessary to test primers against not only coral but also *Symbiodinium* (Table 3.1; subclade C3 cDNA kindly provided by Lynda Boldt) in order to identify coral-specific primers. Reaction conditions (primers concentration; MgCl<sub>2</sub> concentration) were optimized for each primer combination prior to their use in qPCR.

Real time qPCR reaction mixtures were generated using a calibrated CAS-1200 loading robot (Corbett Research). Each 18 µl reaction mixture contained: 9 µl of 2 x SensiMixPlus SYBR green (Quantace Ltd) reagent, 0.2 µl additional 50 mM MgCl<sub>2</sub> (giving final concentration of 3.5 mM), 1 µl of each primer stock (final concentration 400 nM of each primer), 2 µl of 20 x diluted cDNA sample and 4.8 µl ultra-pure PCR grade water (Bioline Australia). Prior to the PCR phase, the reactions were held at 95 °C for 11 mins to activate the polymerase. The PCR phase consisted of 40 cycles of 95 °C for 15 secs/57 °C for 30 secs/72 °C for 20 secs, with a final melting phase (from 57 °C to 95 °C at a rate of 0.1 °C per sec) for detecting nonspecific amplification products or primer dimmers. Each qPCR assay run consisted of 100 individual reactions, 96 reactions tested four pair primers (at least one ICG; *amACTB*) on eight

cDNA samples in triplicate and four reactions tested the four pair primer on blank control (no cDNA in the reaction mixture). For each sample, raw expression levels were read as the threshold cycle (Ct) at the same threshold baseline (0.321) in all cases. For each assay, the mean Ct value of *amACTB* in the control samples was determined as Ct<sup>SD</sup>. Relative expression levels Cq (comparative quantity) for each reaction were then estimated as  $2^{\Delta Ct}$  ( $\Delta Ct = Ct - Ct^{SD}$ ). Ct<sup>SD</sup> values were calculated for each 96-well run, in order to minimize differences between qPCR runs.

Table 3.1 Primers for ICGs and GOIs

Symbol	Full name	Forward (F) and Reverse (R) primer sequences	Nonspecific amplification*
<b>ICGs</b>			
<i>amACTB</i>	Beta actin	F:TGTGATGGTTGGTATGGGTC R: ACCCTCGTAGATGGGAACT	Absence
<i>amGAPD</i>	Glyceraldehyde-3-phosphate dehydrogenase	F: CAGAAGACAGTGGATGGACCTA R: GTCTCCGATGCTTTCTTCAC	Absence
<i>amSDHA</i>	Succinate dehydrogenase	F: GGACTGCCAAACCAGGACAT R: GAGTGTCTCCGCTGGCAAAT	Absence
<i>amUBC</i>	Ubiquitin C	F:CGTACCTTGAGCGACTACAACA R:CATGCCGCCACGTAAACGCAAA	Absence
<b>GOIs</b>			
<i>amSEP15kD</i>	15 kDa Selenoprotein	F: TCTGAACTGACTCCCGAACA R: CAATGCTTAGGACCTCTTTGAC	Absence
<i>amSEPW1</i>	Selenoprotein W1	F:CAAGGTAGTTTATTGTGGTGCCTG R:TGGCATCCAAAATCCTCTGCATCT	Absence
<i>amSEPW2</i>	Selenoprotein W2	F: TCTGTGGAATATTGTGGTGCCTG R: GTGCAATTTCCATCACTTCGCG	Absence
<i>amSeBP17</i>	Selenium binding protein	F: GGACAGGTGTTTATTGGTGGCA R: ATCACCACCAGGATAGCGCAC	Absence
<i>amSeBP23</i>	Selenium binding protein	F: ACCAAGCCTGCTCCAATGG R: ATCAAACCTGGCATCTCGGG	Absence
<i>amSEPP</i>	Selenoprotein P	F: CTGGGGTTTTTCGGTCAACTTGC	Absence

---

		R: TGCTTAGGACCTCTTTGACCTCA	
<i>amSEPT</i>	Selenoprotein T	F: GCTACCGAAAGGTGTTTGAAGA R: ATTTGGGAGGCGACCTGATTC	Absence
<i>amSEPH</i>	Selenoprotein H	F: GAAAAAGTCCAGCGAAGAAAGC R: AACAACAGCATCAGGGAAGG	Absence
<i>amSEPO</i>	Selenoprotein O	F: AAGAACCTCCAAGCCATACC R: CATAACTTCAACCCGTTCTTT	Absence

---

\*: Primers were tested on *Symbiodinium* spp. cDNA (subclade C3)

### 3.2.5 Normalization and data processing

The cDNA samples from two parallel colonies were separately normalized to minimize the effects of inter-colony variability. For each colony, the non-normalized mean Cq values (mean of triplicate assays in each case) for the four ICGs to be used against six stressed samples (two treatments H<sub>2</sub>O<sub>2</sub>, BSO+H<sub>2</sub>O<sub>2</sub>; three time points 4 h, 12 h, 24 h) and one control sample were put into the Excel-based geNorm program (version 3.5) in order to determine the relative stability values (M) of each ICG (Vandesompele et al., 2002). Two of the most stable ICGs (i.e. smallest M values) *amACTB* and *amGAPD* were selected to calculate the normalization factors (NFs) to be applied to all the test and control cDNA samples. The normalized Cq values were calculated as non-normalized Cq/NF (NF values established for each individual cDNA template) and used in the data analysis. Normalized Cq values are represented as the mean  $\pm$  SD of triplicates. To examine the differences in gene expression levels between control and test samples, the fold change for each test sample R<sub>c</sub> is represented as the ratio between Cq<sup>t</sup> (Cq of test sample) and Cq<sup>c</sup> (mean Cq for control sample); R<sub>c</sub> also represents the mean  $\pm$  SD of triplicates. At each time point, we used SPSS 17.0 to evaluate the statistical significance within three groups: two experimental (H<sub>2</sub>O<sub>2</sub>, BSO+H<sub>2</sub>O<sub>2</sub>) and one control groups.

### 3.3 Results

#### 3.3.1 The expression of GOIs in control samples

The results (Fig. 3.1) showed most GOIs were expressed at measurable and consistent levels in the control samples, the exceptions being *amSEPH* and *amSEPO*, for which mRNA levels were very low in both coral colonies (Cq between 0.002-0.02 in control and test samples), effectively precluding examining changes in their expression during oxidative stress. Amongst the seven other GOIs, levels of *amSeBP17* and *amSeBP23* mRNAs were relatively stable between two colonies (Fig. 3.1); however, the expression of *amSBP15kD*, *amSEPW1* and *amSEPW2* varied significantly between healthy colonies; differences like this have previously been described for *AmSW* in bleaching corals (Seneca et al., 2009). Future studies of this sort should use larger sample sizes in order to better statistically support for patterns of change. However, the experimental design used here based on sampling within colonies minimizes the effects of inter-colony variability and was the most appropriate approach given the limitations of the experiment.

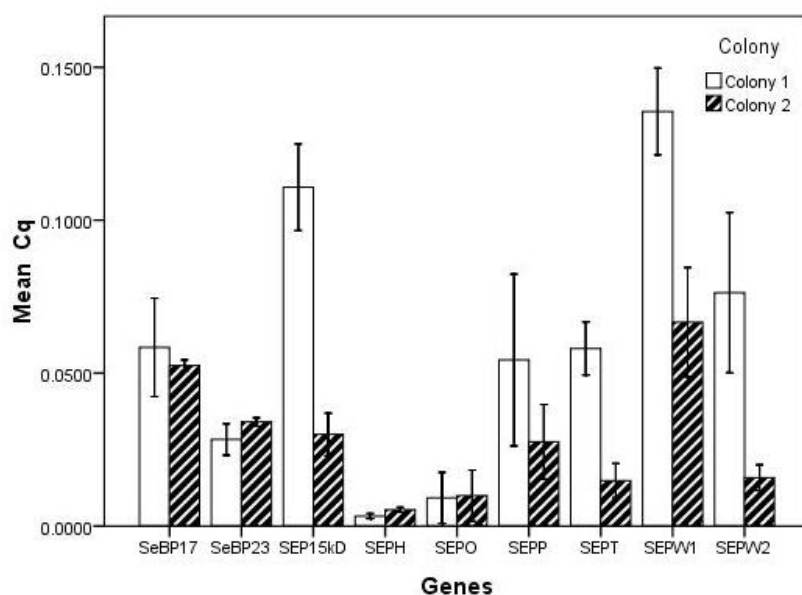


Figure 3.1 The relative expression levels of all the GOIs in control samples of both colonies before chemical treatments. The normalized Cq values were represented as the mean  $\pm$  SD.

### 3.3.2 Rapidly induced GOIs associated with H<sub>2</sub>O<sub>2</sub> treatment

*amSEPP*, *amSEPT*, *amSEPW1* and *amSEPW2* were up-regulated more than two fold at 4h after H<sub>2</sub>O<sub>2</sub> or BSO+H<sub>2</sub>O<sub>2</sub> treatment in all the groups (Fig. 3.2 A) relative to the controls (significance P<0.05, Table 3.2). For these GOIs, no obvious differences were observed between treatment groups (Table 3.2, P>0.05, *amSEPP* transcripts between Group A/B; *amSEPT* transcripts between Group A/B; *amSEPW1* transcripts between Group C/D), indicating that H<sub>2</sub>O<sub>2</sub> treatment was the main trigger of the acute up-regulation of these four GOIs.

Table 3.2 The up-regulated GOIs in all groups 4 hours after H<sub>2</sub>O<sub>2</sub> treatment

GOIs	Group	Treatments	Mean Rc	Statistic groups*	P (towards control)	P (between treatments)
<i>amSEPP</i>	A (4h)	H <sub>2</sub> O <sub>2</sub>	7.25±0.65	A, B, Con 1	0.002	0.587
	B (4h)	BSO+H <sub>2</sub> O <sub>2</sub>	6.27±0.44		0.004	
	C (4h)	H <sub>2</sub> O <sub>2</sub>	4.10±0.35	C, D, Con 2	1.21 x E <sup>-5</sup>	6.40 x E <sup>-5</sup>
	D (4h)	BSO+H <sub>2</sub> O <sub>2</sub>	1.77±0.02		0.020	
<i>amSEPT</i>	A (4h)	H <sub>2</sub> O <sub>2</sub>	5.48±0.14	A, B, Con 1	7.32 x E <sup>-6</sup>	0.933
	B (4h)	BSO+H <sub>2</sub> O <sub>2</sub>	5.38±0.44		8.30 x E <sup>-6</sup>	
	C (4h)	H <sub>2</sub> O <sub>2</sub>	4.78±0.19	C, D, Con 2	3.23 x E <sup>-5</sup>	0.017
	D (4h)	BSO+H <sub>2</sub> O <sub>2</sub>	3.61±0.47		2.65 x E <sup>-4</sup>	
<i>amSEPW1</i>	A (4h)	H <sub>2</sub> O <sub>2</sub>	3.32±0.22	A, B, Con 1	1.80 x E <sup>-5</sup>	2.37 x E <sup>-6</sup>
	B (4h)	BSO+H <sub>2</sub> O <sub>2</sub>	6.61±0.18		3.01 x E <sup>-7</sup>	
	C (4h)	H <sub>2</sub> O <sub>2</sub>	2.57±0.47	C, D, Con 2	0.007	0.125
	D (4h)	BSO+H <sub>2</sub> O <sub>2</sub>	3.33±0.30		0.001	
<i>amSEPW2</i>	A (4h)	H <sub>2</sub> O <sub>2</sub>	8.70±0.80	A, B, Con 1	1.20 x E <sup>-5</sup>	4.29 x E <sup>-4</sup>
	B (4h)	BSO+H <sub>2</sub> O <sub>2</sub>	4.58±0.34		0.001	
	C (4h)	H <sub>2</sub> O <sub>2</sub>	6.84±0.21	C, D, Con 2	3.13 x E <sup>-7</sup>	1.62 x E <sup>-5</sup>
	D (4h)	BSO+H <sub>2</sub> O <sub>2</sub>	4.32±0.22		3.27 x E <sup>-6</sup>	

\*: Three of the involved statistical groups (H<sub>2</sub>O<sub>2</sub>, BSO+H<sub>2</sub>O<sub>2</sub>, Control) were tested by Tukey method ( $\alpha=0.05$ , One-Way ANOVA). Con 1: control group of colony 1; con 2: control group of colony 2.

### 3.3.3 BSO+H<sub>2</sub>O<sub>2</sub> treatment results in elevated expression of five GOIs after 24 hours

After 24 hours, the BSO+H<sub>2</sub>O<sub>2</sub> treatment groups (B for colony 1, D for colony 2) displayed elevated expression of five GOIs (Fig. 3.2 C) relative to the control and H<sub>2</sub>O<sub>2</sub> treatment groups A and C (P<0.001, Table 3.3). The results suggest that pre-treatment with BSO may prolong the effects of oxidative stress in corals. Thus in the presence of BSO, elevated expression of the oxidative stress responding GOIs *amSeBP17*, *amSEP15kD*, *amSEPP*, *amSEPT* and *amSEPW2* is maintained after H<sub>2</sub>O<sub>2</sub> is degraded.

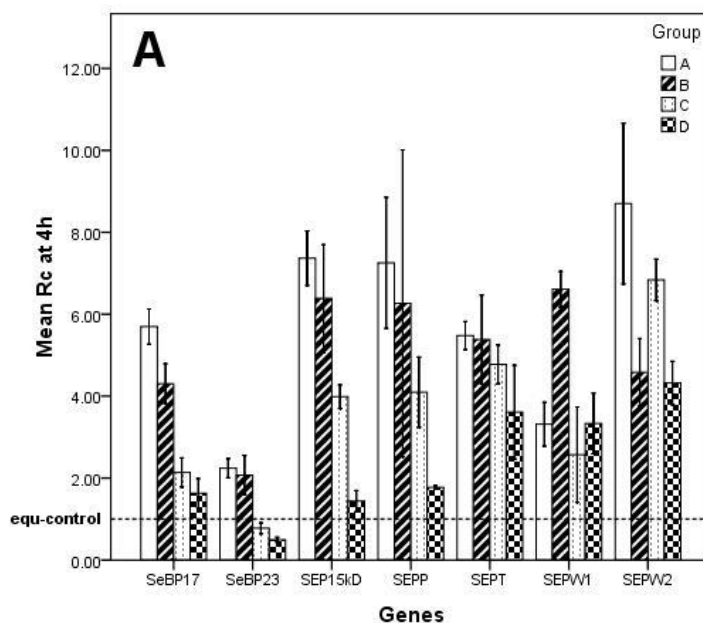
Table 3.3 Expression of the GOIs remained high 24 hours after BSO + H<sub>2</sub>O<sub>2</sub> treatment

GOIs	Group	Treatments	Mean Rc	Statistic groups*	P (towards control)	P (between treatments)
<i>amSeBP17</i>	A (24h)	H <sub>2</sub> O <sub>2</sub>	1.28±0.06	A, B, Con 1	0.897	5.58 x E <sup>-5</sup>
	B (24h)	BSO+H <sub>2</sub> O <sub>2</sub>	8.72±1.09		4.50 x E <sup>-5</sup>	
	C (24h)	H <sub>2</sub> O <sub>2</sub>	0.42±0.03	C, D, Con 2	0.037	3.79 x E <sup>-7</sup>
	D (24h)	BSO+H <sub>2</sub> O <sub>2</sub>	5.87±0.30		5.43 x E <sup>-7</sup>	
<i>amSEP15kD</i>	A (24h)	H <sub>2</sub> O <sub>2</sub>	3.73±0.07	A, B, Con 1	2.49 x E <sup>-7</sup>	3.33 x E <sup>-7</sup>
	B (24h)	BSO+H <sub>2</sub> O <sub>2</sub>	5.45±0.06		2.49 x E <sup>-7</sup>	
	C (24h)	H <sub>2</sub> O <sub>2</sub>	0.82±0.06	C, D, Con 2	0.721	0.001
	D (24h)	BSO+H <sub>2</sub> O <sub>2</sub>	2.53±0.38		0.001	
<i>amSEPP</i>	A (24h)	H <sub>2</sub> O <sub>2</sub>	3.52±0.28	A, B, Con 1	2.71 x E <sup>-4</sup>	0.012
	B (24h)	BSO+H <sub>2</sub> O <sub>2</sub>	4.73±0.41		2.89 x E <sup>-5</sup>	
	C (24h)	H <sub>2</sub> O <sub>2</sub>	0.97±0.04	C, D, Con 2	0.965	1.71 x E <sup>-5</sup>
	D (24h)	BSO+H <sub>2</sub> O <sub>2</sub>	2.61±0.19		1.90 x E <sup>-5</sup>	
<i>amSEPT</i>	A (24h)	H <sub>2</sub> O <sub>2</sub>	2.40±0.24	A, B, Con 1	0.001	3.88 x E <sup>-5</sup>
	B (24h)	BSO+H <sub>2</sub> O <sub>2</sub>	4.81±0.23		2.78 x E <sup>-6</sup>	
	C (24h)	H <sub>2</sub> O <sub>2</sub> ;	1.15±0.55	C, D, Con 2	0.345	3.31 x E <sup>-7</sup>
	D (24h)	BSO+H <sub>2</sub> O <sub>2</sub>	4.33±0.16		3.06 x E <sup>-7</sup>	
<i>amSEPW2</i>	A (24h)	H <sub>2</sub> O <sub>2</sub>	2.40±0.22	A, B, Con 1	1.30 x E <sup>-4</sup>	7.59 x E <sup>-6</sup>
	B (24h)	BSO+H <sub>2</sub> O <sub>2</sub>	4.70±0.09		6.09 x E <sup>-7</sup>	
	C (24h)	H <sub>2</sub> O <sub>2</sub> ;	1.29±0.11	C, D, Con 2	0.735	2.37 x E <sup>-4</sup>
	D (24h)	BSO+H <sub>2</sub> O <sub>2</sub>	4.80±0.66		1.51 x E <sup>-4</sup>	

\*: Three of the involved statistical groups (H<sub>2</sub>O<sub>2</sub>, BSO+H<sub>2</sub>O<sub>2</sub>, Control) were tested by Tukey method ( $\alpha=0.05$ , One-Way ANOVA). Con 1: control group of colony 1; con 2: control group of colony 2.

### 3.3.4 Genes encoding the selenium-binding proteins *amSeBP17* and *amSeBP23* behave differently under oxidative stress

Although the two major coral selenium-binding proteins have high similarity (chapter 2) and are expressed at similar levels in healthy corals (Fig. 3.1), their response towards oxidative stress differed markedly. In the case of *amSeBP17*, expression was elevated above the controls in all testing groups at 4 hours after oxidative stress (Fig. 3.2 A) and in the BSO+H<sub>2</sub>O<sub>2</sub> treatment groups (A/C) remained higher after 12 hours (Fig. 3.2 B); even after 24 hours expression remained significantly elevated above controls in the BSO+H<sub>2</sub>O<sub>2</sub> treatment groups ( $P < 0.001$ , Fig. 3.2 C, table 3.3). In complete contrast, expression of *amSeBP23* did not change significantly upon application of oxidative stress (Fig. 3.2 A, B, C).



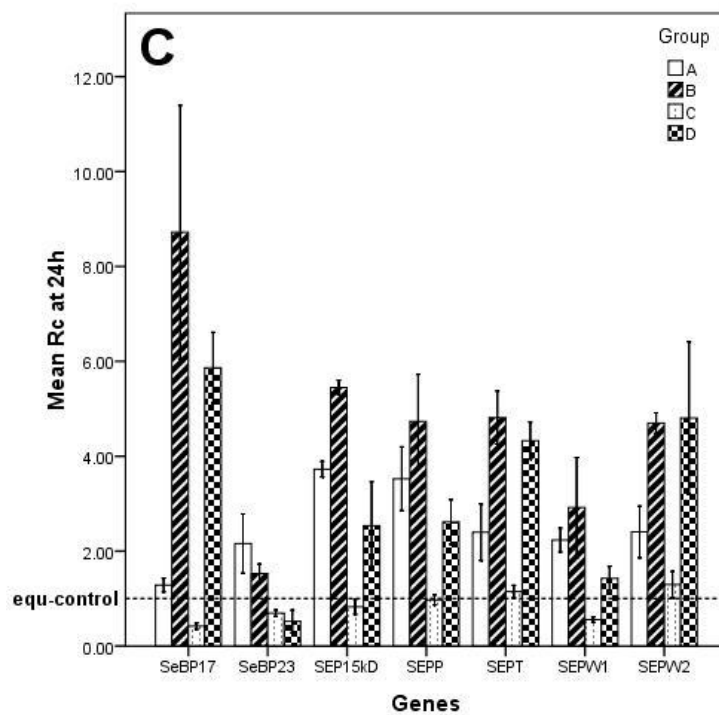
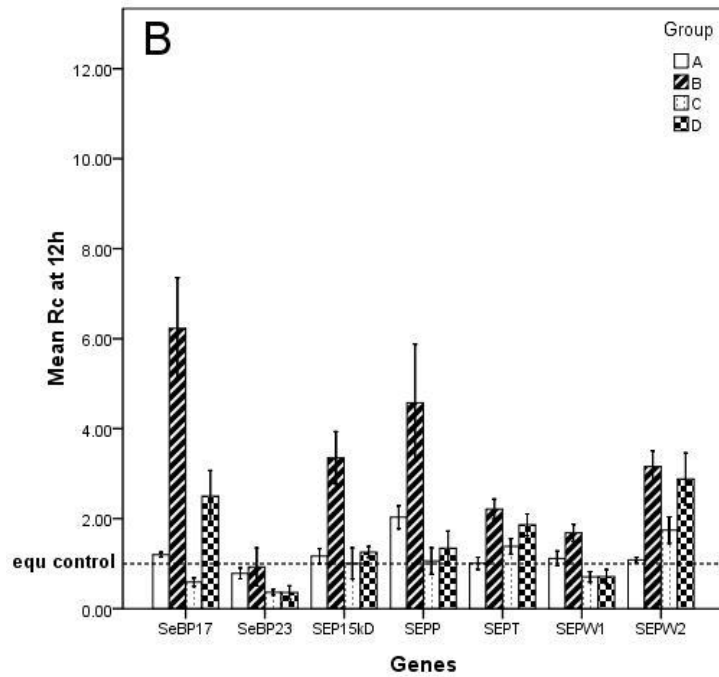


Figure 3.2 The mean fold changes relative to control samples Rc for the seven GOIs in four testing groups (Group A: Colony 1 with H<sub>2</sub>O<sub>2</sub> treatment; Group B: Colony 1 with BSO+H<sub>2</sub>O<sub>2</sub> treatment; Group C: Colony 2 with H<sub>2</sub>O<sub>2</sub> treatment; Group D: Colony 2 with BSO+H<sub>2</sub>O<sub>2</sub> treatment) at 4 hours (Fig. 3.2 A), 12 hours (Fig. 3.2 B) and 24 hours (Fig. 3.2 C) after treatments. The Rc values were represented as the mean  $\pm$  SD.

## 3.4 Discussion

### *3.4.1 The scleractinian coral *A. millepora* has an complex antioxidant network*

Several recent studies have established the presence of several known antioxidant systems in scleractinian corals and implicated these in responses to the oxidative stresses imposed by the symbiont (Downs et al., 2000) or environmental stress (Bierkens 2000). For example, superoxide dismutase (SOD) activity is elevated in the coral *Pocillopora capitata* after heat stress (Flores-Ramírez et al., 2007) and catalase (CAT) expression is up-regulated in *A. millepora* during the bleaching response (Seneca et al., 2009). It has been hypothesized that the GFP-like proteins that are particularly abundant in scleractinian corals have some protective functions (Dove et al., 1995; Dove et al., 2001; Mazel et al., 2003; Miyawaki 2002) against heat induced oxidative stresses. Elsewhere in this thesis (Chapter 2), other selenium-containing enzymatic antioxidants (GPx and TR) were identified in a bioinformatics analysis of *A. millepora*, as were a large number of non-enzymatic selenium-containing proteins. The results implied that the coral *A. millepora* has an advanced antioxidant network that includes the “usual suspects” – homologues of known antioxidants from other animals, as well as numerous selenium-containing proteins whose precise functions remain unknown.

### *3.4.2 Hypothesis regarding the redox-sensitive selenium containing proteins in *A. millepora**

In mammals, antioxidant roles for many of the non-enzymatic selenium-containing proteins have been proposed because they are highly expressed in specific tissues or organs which are the sites of relatively intensive redox metabolism; for example, the 56kD SeBP is highly expressed in liver (Bansal et al., 1989), SEPW (Vendeland et al., 1993; Sun et al., 1998; Gu et al., 1999) in skeletal muscle, SEP 15kD in prostate (Kalcklosch et al., 1995) and SEPP in liver and plasma (Motsenbocker and Tappel 1982; Read et al., 1990; Saijoh et al., 1995). Despite the much simpler morphology of

the coral, a surprisingly large number of selenium-proteins (*amSeBP*, *amSEP15kD*, *amSEPP*, *amSEPT* and *amSEPW(W1,W2)*) were responsive to oxidative stress in *A. millepora*. How do these proteins function in the antioxidant network of corals? We hypothesise here that they may act as an emergency redox buffer system that is able to effectively supplement the more basic (SH-group-based) redox buffer in the cases described in Fig. 3.3 Case 1: Under biological conditions, if oxidants overwhelm the basic redox buffer system then the selenium-based “emergency” redox buffer cuts in. In the study described in this chapter, *amSEPP*, *amSEPT*, *amSEPW1* and *amSEPW2* were induced after oxidative treatments (Fig 3.2, Table 3.2); other studies have established that SeBP and SEPW are highly induced by oxidative challenge in mammalian and marine mollusc models: the mice SEPW exhibited an immediate response to oxidative stress in proliferating myoblasts (Loflin et al., 2006), after exposure to hydrogen peroxide, similar to mollusc SeBP (Song et al., 2006). For SEPT, there is no direct evidence in other research models that it can be induced by oxidative stress; but the recent study (Tanguy et al., 2011) implied its crucial role in tissues where have relatively intensive redox metabolism. Case 2: When the GSH/Trx-based redox buffer system is compromised or inhibited: in the present study, the use of BSO to block the basic redox buffer GSH (Fig. 3.3) led to induction of the non-enzymatic proteins *amSeBP17*, *amSEP15kD*, *amSEPP*, *amSEPT* and *amSEPW2* (Fig. 3.2, Table 3.3). Case 3: The enzymatic support component of the basic redox buffer may be affected by the environmental factors such as temperature and chemicals (Fig 3.3); in this case, the comparatively stable non-enzymatic selenium-proteins may be involved. Further studies are required to support this model, and in particular to test Scenario 3.

The reason that *A. millepora* maintain such a complex antioxidant network including many redox sensitive selenium-proteins is unclear. We supposed its diffusion based physiology is the main reason (introduced in Chapter 1), through which the coral consistently and dynamically receives the inside symbiosis-derived as well as the outside environmental-derived oxidative stresses. For protection purpose, the coral

needs diversified antioxidants to deal with these potential stresses in different levels and cases.

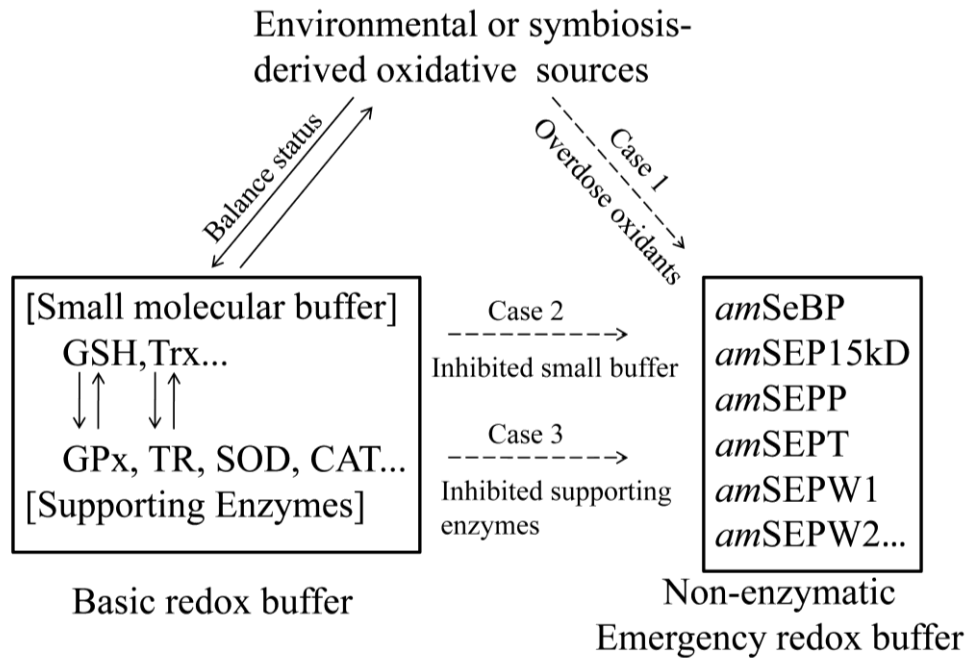


Figure 3.3 Hypothetical antioxidant network of *A. millepora*. The listed non-enzymatic selenium containing proteins may act as an emergency redox buffer in cases as below. Case 1: the oxidants significantly overdose the basic redox buffer which includes the small molecular buffer and the supporting enzymes. Case 2: the basic small molecular buffer were reduced or interfered. Case 3: The supporting redox enzymes for the basic redox buffer may be affected by the environmental factors such as temperature and chemicals.

## Chapter 4

### Two members of the 56 kDa selenium binding protein family from the coral *Acropora millepora*

#### 4.1 Introduction

SeBPs (selenium binding proteins) are believed to be fundamental cytosolic proteins that specifically bind selenium but which do not contain the amino acid selenocysteine (Sani et al., 1988). Based on molecular weight, two distinct types of SeBP are recognized in mammals (Behne and Kyriakopoulos 2001). Both types were originally identified in extracts of mouse liver; a 14 kDa SeBP protein (Bansal et al., 1989) of somewhat restricted distribution, and a 56 kDa SeBP (Bansal et al., 1990) which is often referred to as SeBP1 in the case of the human protein, but which is highly conserved among invertebrates, plants and mammals (Ishii et al., 1996<sup>a</sup>; Song et al., 2006; Bevan et al., 1998; Fliemetakis et al., 2002). In mammals, the 56 kDa SeBP is expressed predominantly in organs and tissues of endodermal origin, such as liver, lung, colon, and prostate, may be important for both xenobiotic metabolism and anti-carcinogenic growth regulation (Yang and Sytkowski 1998; Chen et al., 2002; Kim et al., 2006). Other studies demonstrated that the expression of the rat orthologue of human SeBP1 (known as the 54kDa SeBP in rat) changed significantly following administration of xenobiotics (Ishii et al., 1996<sup>b</sup>; Ishida et al., 1998; Chang et al., 1997), which is consistent with roles in xenobiotic metabolism and detoxification. The 56 kDa SeBP has also been suggested to function in redox modulation (Jamba et al., 1997; Ishii et al., 1996<sup>a</sup>), protein transport (Porat et al., 2000) and cell outgrowth (Miyaguchi 2004). However, the mechanism by which the 56 kDa SeBP carries out its roles remains unknown.

Structural analysis of the SeBPs is in its infancy. *In vitro* studies of the human 56 kDa SeBP suggest that the selenium, which is most likely bound through selenosulfide bonds, is critical for SeBP function (Jeong et al., 2009). The pentameric SeBP of *Methanococcus vannielii* binds inorganic selenite through selenosulfide bonds with the thiol groups of four cysteine residues (Suzuki et al., 2008; Patteson et al., 2005). By contrast, the 56 kDa SeBP of *Sulfolobus tokodaii* (Yamada, 2ECE in PBD, unpublished) is a monomer. At this stage the mode of selenium binding by SeBPs is unclear; much more extensive structural analyses are required to clarify this.

In Chapter 2 of this thesis we reported the identification of cnidarian SeBPs having high sequence similarity with the mammalian 56 kDa SeBP. The high level of sequence similarity observed in the metazoan proteins implies that their functions may be conserved even in morphologically simple animals. We hypothesized that the two 56 kDa SeBPs in *A. millepora* play important redox regulation roles; this was investigated in Chapter 3. In this chapter we report two SeBP sequences from *A. millepora*, map these onto the known structure, and examine their expression levels in different developmental stages. In addition, one of the *A. millepora* SeBPs (*amSeBP*) was expressed in *E. coli* and the recombinant protein was shown to be recognized by a commercial mouse anti-human SeBP monoclonal antibody. This antibody was used to localize the *amSeBP* protein in *A. millepora* planulae and in adult histology sections.

## **4.2 Materials and methods**

### ***4.2.1 Sequence analysis and protein modeling***

The 56 kDa SeBP protein sequences of human (AAH09084), lancelet *Branchiostoma floridae* (EEA68173), fly *Drosophila melanogaster* (AAF54900), sea anemone *Nematostella vectensis* (EDO41029), thale cress *Arabidopsis thaliana* (AAK32898) and archaea *S. tokodaii* (BAB65016) were obtained from the public database at NCBI

(National Center for Biotechnology Information). The complete coding sequences of two *A. millepora* SeBPs, *amSeBP17* (JF970199), *amSeBP23* (JF970200), were obtained by 5'RACE based on incomplete data from published EST studies (Kortschak et al., 2003), both sequences can be found in supplementary Table 1. Protein sequence alignments were conducted using ClustalW (Thompson et al., 1994), paying particular attention to cysteine residues likely to be critical to the structure of the protein.

The human SeBP (AAH09084) and coral *amSeBP23* sequences were mapped onto the known structure of the *S. tokodaii* SeBP (Yamada, unpublished; PDB identifier 2ECE) using the Geno3D web server (Combet et al., 2002). The *S. tokodaii* / human and *S. tokodaii* / coral structures were performed using the Superpose web server (Maiti et al., 2004). Three-dimensional diagrams were constructed and conserved cysteine residues characterized with the aid of the Swiss-Pdb Viewer 4.0.1 (Guex and Peitsch 1997).

#### **4.2.2 Temporal transcript levels of *amSeBP17* and *amSeBP23* genes**

Different developmental stages of *A. millepora* and samples of whole adult tissue were frozen in liquid nitrogen. Total RNA was extracted using the TRIZOL™ reagent (Invitrogen, USA) following published protocols (Seneca et al., 2009). RNA quality was determined by electrophoresis and concentrations were determined spectrophotometrically. One microgram of total RNA was used for first-strand cDNA synthesis with the SuperScript™ System for RT-PCR (Invitrogen, USA). Aliquots of single-strand cDNA were diluted ten times for reaction. The primer sequences, and the expected fragment size for *amSeBP17* gene, *amSeBP23* gene and parallel reference *amACTB* (Beta Actin) gene were as follows:

*amSeBP17F* (5'- GGACAGGTGTTTATTGGTGGCA-3'),

*amSeBP17R* (5'- ATCACCACCAGGATAGCGCAC-3'), 357bp;

*amSeBP23F* (5'-ACCAAGCCTGCTCCAATGG-3'),

*amSeBP23R* (5'-ATCAAACCTGGCATCTCGGG-3'), 389bp;

*amACTBF* (5'-TGTGATGGTTGGTATGGGTC-3'),

*amACTBR* (5'-ACCCTCGTAGATGGGAACT-3'), 378bp.

In experimental PCR conditions (94°C for 10 min, then cycled 94°C for 50 sec/56°C for 40 sec/70°C for 40 sec), *amSeBP17* and *amSeBP23* RT-PCR products can be observed after 25 cycles, so we chose 26 cycles to obtain the semi-quantitative results and analyzed the products by agarose electrophoresis.

#### **4.2.3 Expression and purification of recombinant *amSeBP23* in *E. coli***

A 1.3 kb fragment of *amSeBP23* containing a *Bam*HI site at the 5' end and *Xho* I site on the 3' terminus was generated from cDNA with the inner nest primers shown in Fig. 4.3A. To improve digestion efficiency, an overlapping set of primers ("outside nest primers"; see Fig. 4.3A) were used to reamplify the initial PCR product. After *Bam*HI / *Xho* I digestion, the 1.3 kb fragment encoding 431 amino acids of *amSeBP23* was ligated into *Bam*HI / *Xho* I digested pGEX-4T-2 expression vector (Amersham Biosciences). After the sequence of the insert was confirmed, the recombinant plasmid was used to transform *E. coli* cell strain BL21.

The transformed cells were grown in LB media with 100 mg/liter ampicillin at 37 °C to OD<sub>600</sub>=0.5 and then induced the expression of recombinant *amSeBP23* with 1mM isopropyl-β-D-thiogalactopyranoside. The cells were incubated at 30 °C for additional 48 hours. No additional selenium nutrition was added to the incubation medium. Cells were harvested by centrifugation (4000 g for 15 mins at 4 °C) and the pellet from 1 liter cell culture was re-suspended in 100 ml PBS. Total protein was extracted by sonication (in ice bucket 4 × 10 sec until the cloudy cell suspension becomes translucent). The recombinant *amSeBP23* was purified by chromatography on a glutathione Sepharose 4B column (Pharmacia Biotech), which has a high affinity for the GST tag in the recombinant *amSeBP23*. The size of the recombinant product was analyzed by one dimensional SDS-PAGE.

#### **4.2.4 Western blotting**

Protein concentrations were analysed using the Bradford method (Bradford 1976). Bovine serum albumin (BSA), which has similar molecular weight to the recombinant *amSeBP23*, was used to generate the Bradford standard curve. Twenty micrograms of purified recombinant *amSeBP23* were loaded to each of three lanes for SDS-PAGE, protein within the resulting gel was then transferred to Hybond C nitrocellulose membrane (Amersham Biosciences) by electroblotting. In parallel, crude extracts of induced *E. coli* BL21 expressing *amSeBP23* (loaded at 60 micrograms per lane) were subjected to SDS-PAGE and blotting, to allow the specificity of the antibody to be checked. Membranes were blocked by incubation with 3% BSA in PBT (phosphate-buffered saline with 0.5% Tween 20) for 1 hour at room temperature. Membrane strips corresponding to the gel lanes were then incubated with mouse anti-human SELENBP1 monoclonal antibody (MBL, Japan) at various dilutions (1:1000, 1:500, 1:250 in PBT with 3% BSA) for 1 h at room temperature. After incubation, the strips were washed five times with PBT and incubated with horseradish peroxidase (HRP)-conjugated goat anti-mouse secondary antibody (1:5000 in PBT with 1% BSA, Sigma) for 1 hour at room temperature. Unbound secondary antibody was removed by washing at least six times in PBT, after which the signal was detected using 3', 3'-diaminobenzidine (DAB tablets, Sigma).

#### **4.2.5 Immunohistochemistry**

*A. millepora* planulae were fixed in Lavdowsky's fixative (50% ethanol, 3.7% formaldehyde, 4% acetic acid) for 5 min, then washed repeatedly in MFSW (Millipore-filtered sea water), dehydrated in a graded ethanol/ddH<sub>2</sub>O series (20%, 50%, 70%), and stored in 70% ethanol at -20 °C until further use. Before exposure to the primary antibody, the larvae were treated with xylene for 1 hour, washed several times in PBT and then blocked by incubation in 2% bovine serum albumin (BSA) in PBT for 5 min. After blocking, the larvae were incubated with mouse anti-human SELENBP1 monoclonal antibody (1:250, MBL, Japan) for 36 h at 4 °C. Unbound

primary antibody was removed by washing at least six times in PBT prior to incubation with HRP-conjugated goat anti-mouse antibodies (1:500, Sigma) for 36 h at 4 °C. Unbound secondary antibody was removed by washing the larvae at least six times in PBT, after which HRP activity was detected using the nickel chloride-enhanced (0.03%) diaminobenzidine (DAB, Sigma) solution and 0.02% H<sub>2</sub>O<sub>2</sub>. Color development was stopped by washing repeatedly with PBT. Ten µm sections of frozen material were also made to clearly observe the staining.

Sections (4 µm) of adult *A. millepora* were generated as previously described (Ainsworth and Guldborg 2009). Slides were deparaffinized by washing three times with xylene (5 min per wash), then three times in ethanol (5 min per wash) to remove residual xylene. Slides were washed several times by PBS before being treated with 3% v/v H<sub>2</sub>O<sub>2</sub> for 10 min at room temperature to block endogenous peroxidase activity. Slides were then washed 3 times in PBS before being blocked by 3% BSA in PBS for 5 minutes. After blocking, the slides were incubated with mouse anti-human SELENBP1 monoclonal antibody (1:250, MBL, Japan) for 2 hours at room temperature; in parallel, controls were processed in which the primary antibody was replaced with PBS. Unbound primary antibody was removed by washing 4 times in PBS, after which residual PBS was gently wiped off the slides and HRP-conjugated goat anti-mouse antibodies (1:500, Sigma) applied. After 10 min incubation, unbound secondary antibody was removed by washing 3 times in PBS. HRP activity was detected using nickel chloride-enhanced (0.03%) diaminobenzidine (DAB, Sigma) solution with 0.02% H<sub>2</sub>O<sub>2</sub>. Color development was monitored under the microscope, and stopped (usually 15-20 minutes later) by 3 washing three times with distilled water. A series of washes were then performed first with PBS, then ethanol and finally xylene to dehydrate and preserve the sections.

## 4.3 Results

### 4.3.1 Sequence analysis and protein modeling

As can be seen in the sequence alignment shown as Fig. 4.1a, the SeBP sequences from a diverse range of eukaryotes showed substantial sequence similarity with the mammalian 56 kDa SeBP (Behne and Kyriakopoulos 2001) and can be aligned with the *Sulfolobus* sequence whereas the low molecular weight SeBP of *M. vanniellii* (Self et al., 2004) has no significant similarity with these. Due to the importance of cysteine in terms of both the structure and Se-binding properties of SeBPs (Suzuki et al., 2008), Fig 4.1a focuses on Cys-containing regions of the SeBPs sequences - the five regions shown contain cysteine residues shared by at least 6 of the 8 sequences. Four cysteine residues were conserved across all of the sequences; Cys80, 83, 141, 466 (labeled red in Fig. 4.1) in human SeBP correspond to Cys82, 85, 143,466 (labeled red in Fig. 4.1) in coral *amSeBP23* as well as Cys81, 86, 145 and 460 (labeled red in Fig. 4.1) in the *S. tokodaii* SeBP. The CSSC and HxxH motifs are associated with the four absolutely conserved cysteine residues (Fig. 4.1a). A fifth cysteine residue (indicated by yellow color in Fig. 4.1a) was present in each of the sequences except those from *Arabidopsis* and *Drosophila* and is shown in yellow in Fig. 4.1a; Cys31 of human SeBP, corresponds to Cys33 of coral SeBP23 and Cys32 of *S. tokodaii* SeBP. The cysteine residue indicated by pink color in Fig. 4.1a is not present in the *Arabidopsis* and *Sulfolobus* sequences but is present in each of the other sequences examined - in the alignment shown (Fig 4.1a) Cys268 of human SeBP corresponds to Cys268 in the coral SeBP23 and these are shown in pink.

Both coral *amSeBP23* (Fig. 4.1b A) and human SeBP1 (Fig. 4.1b C) can be mapped convincingly onto the crystal structure of *S. tokodaii* SeBP (Fig. 4.1b B, 2ECE, Yamada et al., unpublished), suggesting a monomer structure for each of these proteins; note that this structure is quite different from that of the *M. vanniellii* SeBP which is a pentamer in which each subunit contains a single cysteine residue (Suzuki

et al., 2008). The four cysteine residues in *S. tokodaii* SeBP that are conserved with the metazoan sequences are likely to form disulfide bonds (Fig. 4.1a, 4.1b B, red, Cys81 with 145, Cys86 with 460) that are embedded in the center of the protein structure. Whereas in the human SeBP1 model the corresponding cysteine residues are all also deeply embedded in the protein (Fig. 4.1a, 4.1b C, in red), this is the same in the *amSeBP23* model, where Cys82, 85, 143, and 466 (Fig 4.1a, 4.1b A; in red) is predicted to be embedded in the protein. A fifth cysteine residue present in each of the three proteins modeled (Cys31 of human SeBP, Cys33 of *amSeBP23* and Cys32 of *S. tokodaii* SeBP; Fig 4.1b, in yellow) is likely to be partially exposed on the surface of each protein. The fifth cysteine residue together with its neighboring amino acid residues may interact electrostatically with incoming chemical groups. Cys268 in the human SeBP and coral *amSeBP23* sequences is also partially exposed on the protein surface in the corresponding models (Fig. 4.1b A and C, in pink) but no counterpart is present in the *Sulfolobus* sequence hence it is more difficult to speculate on its likely function.

<i>H. sapiens</i> AAH09084	YLP <b>C</b> IYR (Cys31)	SGWNT <b>CSSC</b> F (Cys80, 83)	<b>HxxH</b> HTSH <b>C</b> LGSGE (Cys141)	QGFV <b>C</b> ALIS (Cys268)	RYPG <b>C</b> D <b>CSSD</b> IWI (Cys466)
<i>B. floridae</i> EEA6817	YLP <b>C</b> IYR (Cys50)	TGWNA <b>CSSC</b> F (Cys99, 102)	HTTH <b>C</b> LGSGE (Cys160)	QGYV <b>C</b> ALIS (Cys288)	RYPG <b>C</b> D <b>CSSD</b> IWL (Cys470)
<i>A. millepora</i> JF970200 <small>(omSeBP2)</small>	YLP <b>C</b> IYA (Cys33)	SGWNA <b>CSSC</b> H (Cys82, 85)	HTAH <b>C</b> LGSGE (Cys143)	QGFV <b>C</b> AL <b>Q</b> (Cys268)	RYPG <b>C</b> D <b>C</b> SFDIWL (Cys466)
<i>A. millepora</i> JF970199 <small>(omSeBP7)</small>	YLP <b>C</b> IRT (Cys32)	SGWNA <b>CSSC</b> Y (Cys81, 84)	HTTH <b>C</b> LGSGE (Cys142)	QGF <b>T</b> <b>C</b> ALIS (Cys268)	RYPG <b>C</b> D <b>CSSD</b> IWL (Cys466)
<i>N. vectensis</i> EDD04102	YLP <b>C</b> IHN (Cys25)	TGWN <b>A</b> <b>CSSC</b> Y (Cys74, 77)	HTTH <b>C</b> LGSGE (Cys135)	QGF <b>T</b> <b>C</b> ALIS (Cys262)	RYPG <b>C</b> D <b>CSSD</b> IWL (Cys460)
<i>A. thaliana</i> AAK32898	YV <b>T</b> ALYS	TGWN <b>S</b> <b>CSSC</b> H (Cys94, 97)	HTSH <b>C</b> LGSGD (Cys155)	TGYV <b>G</b> SALS	RYPG <b>C</b> D <b>C</b> TSDIWI (Cys481)
<i>D. melanogaste</i> AAF54900	Y <b>T</b> V <b>T</b> V <b>Q</b> P	SGWNA <b>CSSC</b> Y (Cys81, 84)	HTTH <b>C</b> LANGN (Cys147)	EGFV <b>G</b> <b>C</b> ALN (Cys274)	RYPG <b>C</b> D <b>C</b> TSDIWL (Cys476)
<i>S. tokodaii</i> BAB65016	YV <b>A</b> CL <b>V</b> T (Cys32)	FGWNA <b>CSSA</b> L <b>C</b> (Cys81, 86)	HTV <b>H</b> <b>C</b> -PDA (Cys145)	M <b>G</b> F <b>I</b> MMVVS	RLSG <b>G</b> D <b>A</b> SSDSY <b>C</b> Y (Cys460)

Fig 4.1. The sequence analysis and protein modeling of the 56 kDa SeBP. (4.1a) The location of conserved cysteine residues and CSSC, HxxH motifs in the amino acid sequence alignment of SeBPs. The four highly conserved cysteine residues (in red) are found in all the SeBPs studied and are likely to form two disulfide bonds; less conserved cysteine residues (in yellow and pink) are conserved in most 56 kDa SeBPs studied. (4.1b, see next page) The location of conserved cysteine residues (in red, yellow and pink) in the tertiary structure of the 56 kDa SeBPs from *S. tokodaii* (Fig. 4.1b B, PDB: 2ECE), the coral *A. millepora* (Fig. 4.1b A) and the human (Fig. 4.1b C).

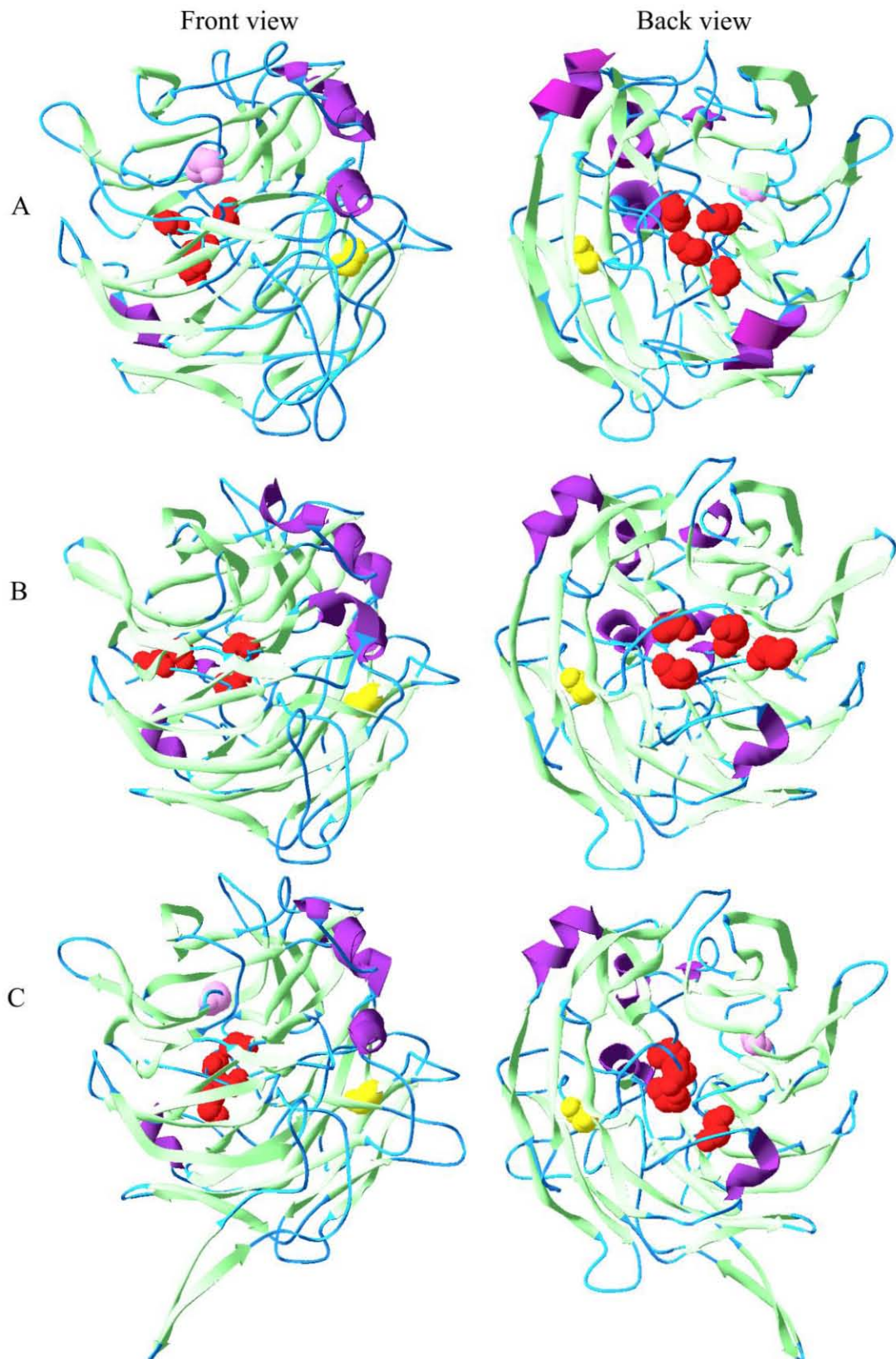


Fig 4.1 (4.1b) The location of the highly conserved cysteine residues (in red) and less conserved cysteine residues (in yellow or pink) in the tertiary structure of the 56kD SeBPs from A: *amSeBP23* from coral *A. millepora*; B: the 56kD SeBP from *Sulfolobus tokodaii* (PDB: 2ECE); C: Human 56kD SeBP. The structures are present both from front view (left) and back view (right).

### 4.3.2 Characterization of *amSeBP17* and *amSeBP23* transcripts

Semi-quantitative estimates of *amSeBP17* and *amSeBP23* transcript levels were derived for major developmental stages of *A. millepora* based on previous descriptions of the development (Ball et al., 2002). The RT-PCR results (Fig. 4.2) showed that *amSeBP17* and *amSeBP23* transcripts were present in all of the major developing stages examined. *amSeBP17* transcription peaked in the pre-settlement phase but was otherwise relatively low. Somewhat stronger signals were observed for *amSeBP23* and in this case expression peaked in earlier planulae. In both cases, expression in adult corals was very low.

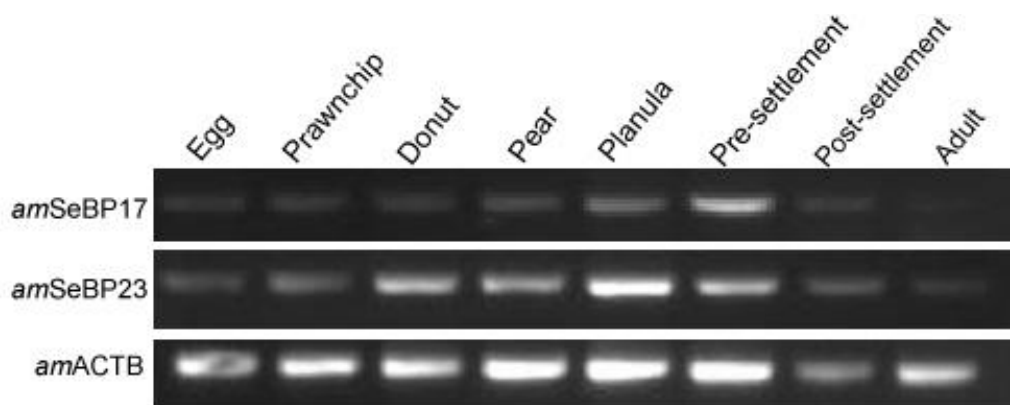


Fig. 4.2. Levels of *amSeBP17* (JF970199) and *amSeBP23*(JF970200) transcripts during the major developing stages (egg, prawnchip, donut, pear, planula, pre-settlement, post-settlement, adult) of *A. millepora*. Reference: *amACTB* (Beta Actin).

### 4.3.3 Production of recombinant *amSeBP23* and its recognition on western blots by heterologous antibody.

The *amSeBP23* (JF970200) open reading frame (ORF) encodes a polypeptide of 472 amino acid residues. A recombinant protein was generated corresponding to 431 amino acids (from Ser10 to Phe440) of *amSeBP23* fused to an N-terminal GST tag. This recombinant protein contained five cysteine residues (Cys33, 82, 85, 143, 268; Fig. 4.3 A) conserved with other SeBPs. The predicted molecular weight of the

recombinant protein is 72 kDa, 47 kDa of which corresponds to *amSeBP23* (the GST tag is about 25 kDa). The observed molecular weight of the recombinant protein as determined by SDS-PAGE electrophoresis was about 70 kDa (Fig. 4.3 B) which is consistent with that predicted.

Commercial monoclonal antibody to anti-human SeBP recognized the recombinant *amSeBP23* in western blotting experiments. Under standard conditions, the antibody recognized recombinant protein at primary antibody dilutions as low as 1:1000 (Fig. 4.3 C) and was highly specific towards the recombinant *amSeBP23* in crude protein extracts from *E.coli* (Fig. 4.3 C: lane 4). On the basis of these results the antibody was used in immunohistochemical studies described below.

A

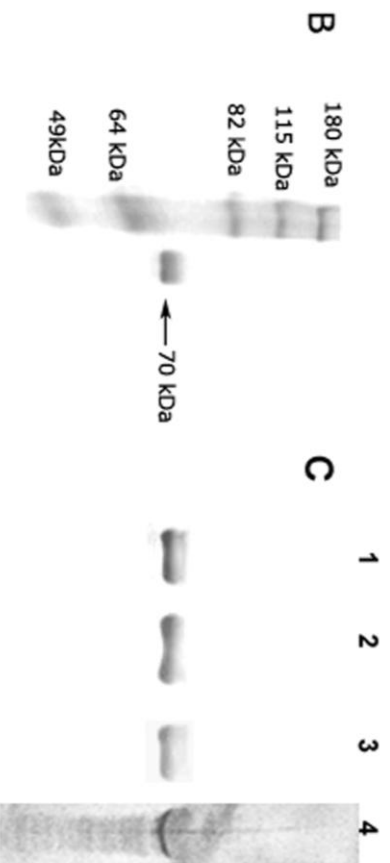
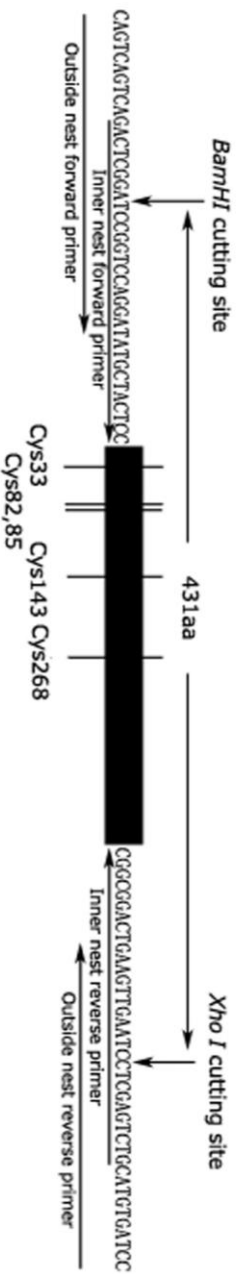


Fig. 4.3. Cloning strategy for the production of recombinant *amSeBP23* and western blotting experiments demonstrating the specificity of mouse anti-human SelenBP1 monoclonal antibody. (A) A 1.3 kb fragment of *amSeBP23* containing a *BamHI* site at the 5' end and *Xho I* site on the 3' terminus was generated from cDNA with the nest primers, the fragment coded 431 amino acids of *amSeBP23* (from Ser10 to Phe440) which included five conserved cysteine residues Cys33, 82, 85, 143, 268. (B) Coomassie blue stained SDS-PAGE gel showing the purity of recombinant *amSeBP23* eluted from the affinity column. A single band was detected at a molecular weight of about 70kD, corresponding to a 45kD fragment of *amSeBP23* (431 amino acids) and 25kD GST-tag. (C) Western blotting analysis showing the sensitivity and specificity of the mouse anti-human SelenBP1 monoclonal antibody; lane 1: purified *amSeBP23* with 1:250 first antibody; lane 2: purified *amSeBP23* with 1:500 first antibody; lane 3: purified *amSeBP23* with 1:1000 first antibody; lane 4: Total protein of *E. coli* (BL21) expression *amSeBP23* with 1:500 first antibody.

#### **4.3.4 Localization of immunoreactive *amSeBP***

SeBP immunostaining was clearly detected (Fig. 4.4 A) in planula larvae, which is consistent with the semi-quantitative PCR data for *amSeBP17* and *amSeBP23* shown as Fig. 4.2. Staining appeared to be associated with a subset of transectodermal cells that are pear shaped in appearance, the small end of the pear being proximal to the endoderm (Fig. 4.4 B). In some cases, the stained cells appeared to be clumped (Fig. 4.4 C, D).

In sections of adult *A. millepora* tissue, staining appeared to be associated with the tissue surrounding the endosymbiotic dinoflagellates (Fig. 4.5 A, B), which are located in the gastrodermis (endoderm). Weak staining was also associated with the epithelium layer corresponding to the larval ectoderm, which is consistent with the staining pattern of planulae. In all cases, negative controls showed no immunoreactive signals either in the gastrodermis or the epithelium layer (Fig. 4.5 C, D).

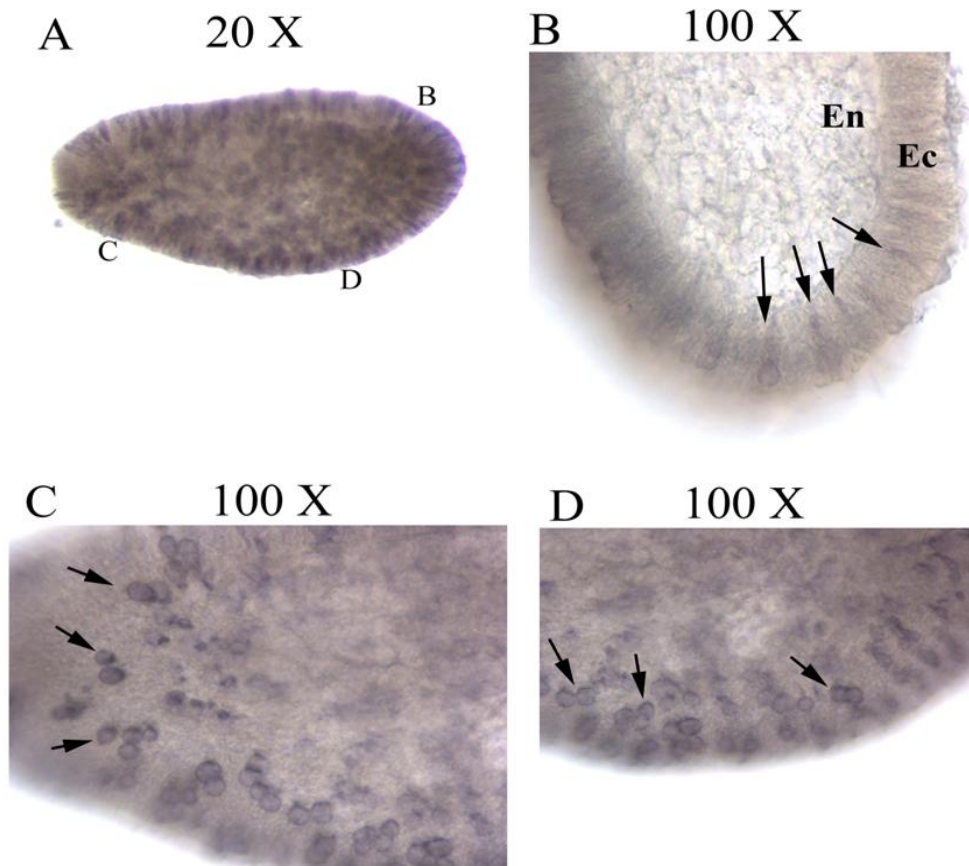


Fig. 4.4. Immunolocalisation of *amSeBP* in *A. millepora* at the early planula stage. A: Overview of immunolocalisation of *amSeBP* at the early planula stage. B: longitudinal section of A shows the staining (indicated by the black arrows) is restricted to a certain type of cells in the ectoderm (Ec); no staining is observed in the endoderm (En). C, D: in some cases the stained cells (indicated by the black arrow) appeared to be clumped.

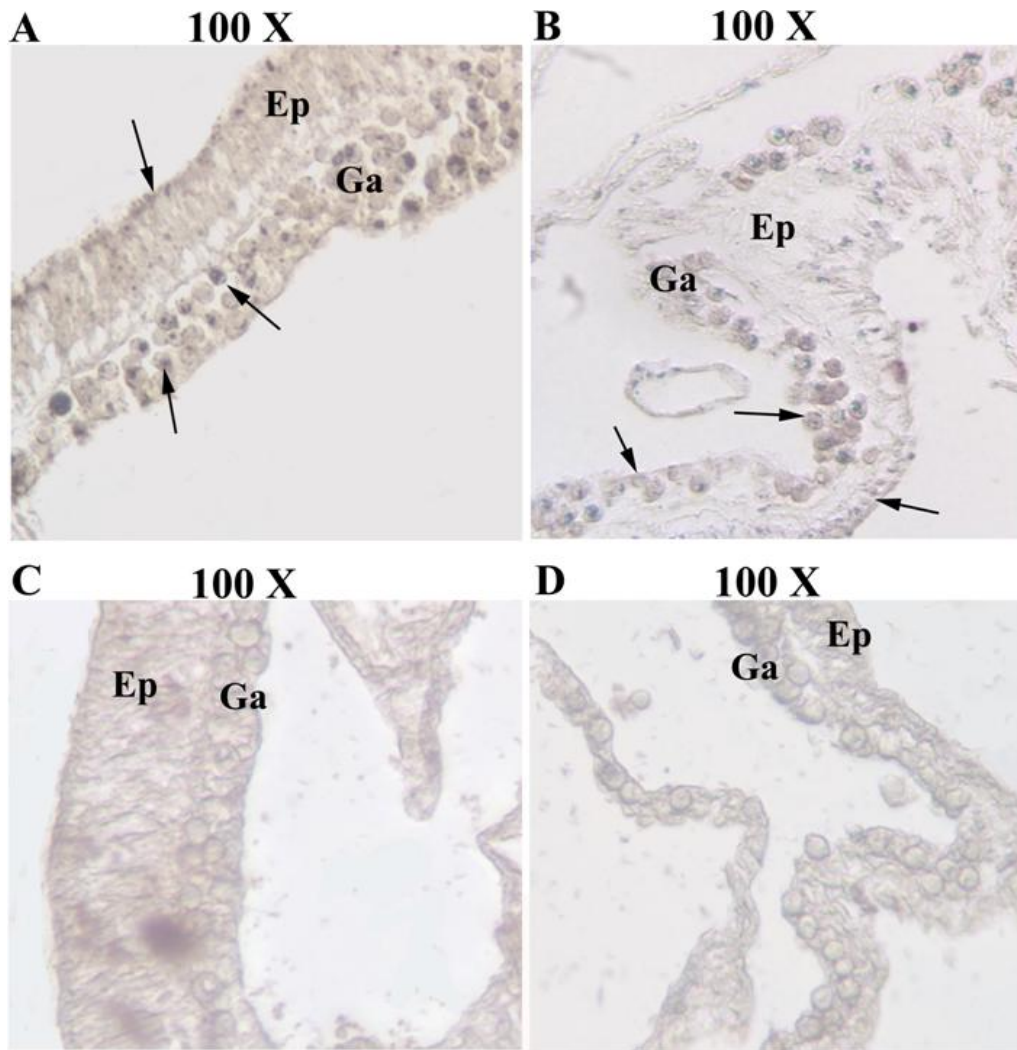


Fig. 4.5 Immunolocalisation of *amSeBP* in section of adult *A. millepora*. A, B: strong staining observed in gastrodermis (Ga) surrounding the symbiotic dinoflagellates and weak staining observed in the epithelium layer (Ep). C, D: no staining observed in the case of control slides (no primary antibody).

## 4.4 Discussion and Hypothesis

### *4.4.1 Conserved cysteine residues and nearby motifs form the redox centre of the 56 kDa SeBP*

In this study, two coral members of the 56 kDa SeBP protein family were identified and characterized. The high similarity observed between *amSeBP17*, *amSeBP23* and the metazoan/plant members of this protein family (Fig. 4.1a) is consistent with previous studies (Song et al., 2006; Bevan et al., 1998; Fletmetakis et al., 2002). Alignment of 56 kDa SeBP sequences implies that a number of cysteine residues and adjacent motifs are highly conserved (Fig. 4.1a) and may therefore be functionally significant. The CSSC motif which contains two cysteine residues (Cys82 and Cys85 of *amSeBP23*) and is present in all of the examined SeBP sequences is also a characteristic feature of many proteins that participate in oxidation/reduction metabolism *in vivo* (Meyer et al., 1999). The HxxH (His139 and His142 of *amSeBP23*) motif located proximal to another conserved cysteine residue (Cys143 of *amSeBP23*) and the CSSC motif are potential binding sites for selenium and other metals (Jamba et al., 1997; Fletmetakis et al., 2002).

Currently, the only X-ray crystal structure that has been reported for a member of the 56 kDa SeBP family is that for *S. tokodaii* (PDB: 2ECE, from Yamada et al., unpublished). Adopting this structure as the template (Fig. 4.1b B), homology modeling was carried out for *amSeBP23* and human SeBP1 and the results are shown as Fig. 4.1b A, C; the modeled structures are hemispherical monomers showing high similarity with 2ECE. In the modeled structures of human SeBP1 and 2ECE, four of the conserved cysteine residues (denoted in red, Fig. 4.1) are embedded in the centre of the cycle side, and likely to form two disulfide bonds (Fig. 4.1), while in the modeled structure of *amSeBP23*, four conserved cysteine residues (in red, Fig. 4.1) are embedded in the centre as well. A similar internal clustering of cysteine residues is

seen in the tertiary structure of the *M. vanniellii* SeBP (Suzuki et al., 2008) which is a symmetric pentamer and can bind selenite through four clustered cysteine residues. The potential selenium binding motifs CSSC and HxxH are also grouped in the central area, suggesting that the structurally clustered cysteine residues (in red, Fig. 1) and nearby motifs may form the redox centre of the 56 kDa SeBP and are potentially responsible for selenium binding and redox functions. In the 2ECE model, the bound selenium, which has higher reduction properties than sulfur, may potentially compete and affect the disulfide bonds which are formed by the clustered cysteine residues in the redox centre; moreover, the bound selenium may be associated with as many as four cysteine residues (Suzuki et al., 2008), whereas disulfide bonds only involve two cysteine residues. The bound selenium may thus be required for maintenance of the active form of SeBP. Recent work (Jeong et al., 2009) supports the hypothesis that bound selenium may act as a key structural and functional element. In addition to those which may constitute the redox centre, several other cysteine residues are broadly conserved in SeBP proteins, and these are close to the surface in the 56 kDa SeBP structure (in pink and yellow, Fig. 4.1b). These unpaired cysteine residues are likely to be more accessible to the incoming chemical groups and may be critical to the reaction mechanism.

#### ***4.4.2 amSeBP expression suggests high metabolic rates in A. millepora planula and pre-settlement stages***

Previous studies have demonstrated the expression of 56 kDa SeBP during development in both animals (Sawada et al., 2004; Kim et al., 2006) and plants (Flemetakis et al., 2002; Dutilleul et al., 2008; Hugouvieux et al., 2009) and that expression is particularly high in the most actively growing stages and tissues with high metabolic rates. In the work described here both *amSeBP17* and *amSeBP23* were expressed most highly during planula and pre-settlement stages, when lipid metabolism predominates. Interestingly, correlated to the *amSeBP* transcripts levels (Fig. 4.2), strong SeBP immunoreactive signals were observed in the ectodermal cells of *A. millepora* planula (Fig. 4.4). The *amSeBP* staining is associated with a specific

ectodermal cell type in the planula, the morphology of which is very similar to those shown to express lipase (Shinzato et al., 2008) and which are presumably responsible for oxidation of storage lipids during larval development. The exact physiological roles of the SeBPs in development remain unclear, but one can imagine a need for tight control of redox balance in cells in which high rates of lipid oxidation occur. Potentially, the *am*SeBPs may be involved in mediating redox regulation by balancing the oxidants and buffering the oxidation/reduction status, as described in Chapter 3 and other studies (Dutilleul et al., 2008; Desikan et al., 2001).

#### ***4.4.3 amSeBPs, may be involved in transport or metabolism between the host A. millepora and the Symbiodinium***

In higher animals, intracellular membrane compartments such as mitochondria and nuclei in liver cells are typically enriched in selenium-containing proteins (Chen et al., 1999). Cytosolic 56 kDa SeBP (human SeBP1) is thought to regulate intracellular protein transport among these subcellular compartments because antibody against human SeBP1 significantly blocked intra-Golgi transport of protein *in vitro* (Porat et al., 2000). Moreover, expression of the 56 kDa SeBP ortholog LjSBP was associated with membrane biogenesis during the establishment of symbiotic nodules in the plant *Lotus japonicus* (Flemetakis et al., 2002). The preliminary immunolocalisation data (Fig. 4.5) suggest that the *am*SeBPs may be enriched at the larval surface or at the *Symbiodinium* interface in the gastrodermis layer of adult *A. millepora*, raising the intriguing possibility of analogous functions in host/symbiont communication.

An alternative hypothesis is that SeBP may be involved in mediating redox metabolism in tissue proximal to these intracellular symbionts (Flores-Ramírez et al., 2007; Seneca et al., 2009); the selenium may effectively buffer the oxidation/reduction environment proximal to the symbionts (Jamba et al., 1997; Dutilleul et al., 2008; Desikan et al., 2001), thus protecting intracellular membranes from oxidative damage. Unfortunately, the preliminary data presented here do not enable subcellular localisation of the *am*SeBPs. It would be interesting to apply higher

resolution techniques to investigate the idea that *amSeBP* may be specifically associated with the intracellular membranes between the coral host cell and the symbiont.

## Chapter 5

### ***In vitro* selenite binding by a recombinant form of the *Acropora millepora* selenium binding protein (*ramSeBP*) produced in *Escherichia coli***

#### **5.1 Introduction**

Despite the ubiquity and level of conservation seen in the 56 kDa SeBP, the nature of the selenium binding site, the mode of binding and many other aspects of the structure of the protein remain unclear. It has recently been suggested (Jeong et al., 2009) that selenite is bound to the 56 kDa SeBP via a covalent Cys(S)-Se bond, but binding constant data were not provided. Structural studies of the low molecular weight SeBP of *M. vanniellii* have revealed that it is a symmetric pentamer that binds inorganic selenite through four cysteine thiol groups (Suzuki et al., 2008; Patteson et al., 2005). However, protein modelling based on the known structure of the *S. tokodaii* SeBP indicate that the 56 kDa proteins are typically monomeric (Yamada et al., unpublished), whereas the *M. vanniellii* SeBP is a homopentamer (Suzuki et al., 2008; Patteson et al., 2005). Whether or not the 56 kDa SeBP binds selenite through Cys(S)-Se bonds remains to be seen.

The common quantitative method to determine the “protein-bound” selenium is through inductively coupled plasma mass spectrometry (ICP-MS) which has been successfully applied to assay the protein-bound selenium in *S. tokodaii* SeBP (Suzuki et al., 2008; Patteson et al., 2005) and selenium in human serum selenoalbumin (Jitaru et al., 2010). Also the traditional <sup>75</sup>Se labelling and gamma spectrometry are quite often used to quantitatively assay the <sup>75</sup>Se in the selenium-containing compounds and proteins (introduced in Chapter 1). The latter method has advantages to assay low

volume samples due to its high accuracy and sensitivity.

In Chapter 4 it was demonstrated that the 56 kDa SeBPs present in the reef building coral *A. millepora* are most likely monomeric, with structures similar to their *S. tokodaii* and human counterparts. The recombinant *A. millepora* selenium binding protein (*ramSeBP*) described in Chapter 4 contains the cysteine residues that are conserved in most 56 kDa SeBPs, and in this chapter we describe experimental determination of the binding selenite in *ramSeBP* by using both traditional mass spectrometry and  $^{75}\text{Se}$  gamma spectrometry. Dithiothreitol (DTT), which is able to reduce thiol groups in Cys residues, was also included in binding assays to research if the cysteine thiol groups are important for the  $\text{SeO}_3^{2-}$  binding ability of *ramSeBP*.

## 5.2 Experimental methods

### 5.2.1 Large (milligram) scale *ramSeBP*/selenite binding assay

Soluble *ramSeBP* (70 kDa with GST tag) was prepared as described in Chapter 4. Approximately 2 mg of purified *ramSeBP* was bound to a glutathione Sepharose 4B affinity column (Pharmacia Biotech) with a bed volume of 400  $\mu\text{l}$ . A 2 ml aliquot of 0.15 mM sodium selenite (Sigma, USA; equivalent to 11.5 mg/l  $\text{Se}^{4+}$ ) in PBS (pH 7.4), was then applied to the column and incubated for 1h at room temperature. Unbound selenite was then removed by washing the column three times with 4 ml (10X bed volume) aliquots of PBS. Recombinant protein with bound selenium was then eluted from the column by applying 400  $\mu\text{l}$  of elution buffer (20 mM glutathione in PBS, pH 7.4) to the column and incubating it for 10 minutes at room temperature, before allowing the column to drain and then assaying the flow-through for protein content using the Bradford method (Bradford, 1976) and for selenium content (ppb grade) by ICP Mass Spectrometry (combined ICP-AES & ICP-MS, Varian 820, Australia). The elution process was repeated 3 more times, at which stage no protein could be detected in the flow through using the Bradford assay. In parallel, an aliquot of the

GST fragment encoded by the non-recombinant pGEX-4T-2 vector was generated (expressed in *E.coli* BL21, process described in chapter 4) and processed in exactly the same way as the SeBP construct, to act as a control for selenium binding to the GST part of the recombinant protein. A further control was provided by incubating *ramSeBP23* in selenite-free PBS, allowing us to test the possibility that selenium might be bound during the generation of the recombinant protein in *E. coli*.

### **5.2.2 HPLC (High-Performance Liquid Chromatography) assay of low levels (microgram) of *ramSeBP***

Low levels of *ramSeBP23* which were hard to be quantified using the standard Bradford assay were monitored in the eluate from a BioSep-SEC-S3000 column (300 mm × 7.8 mm, 5 µm, Phenomenex) on a Shimadzu HPLC system with a SPD-420A prominence Diode Array Detector. The column was equilibrated and eluted with 0.1 M sodium phosphate buffer (PBS) pH 6.8 at a flow rate of 1 ml/min. To obtain a standard curve a stock solution of *ramSeBP23* was diluted in PBS (pH 7.4), 20 µl aliquots of diluted protein (containing 0.12, 0.25, 0.5, 1, 2 and 4 µg *ramSeBP23*) were injected into the BioSep HPLC column, and the column eluate were scanned from 190 to 800 nm using the diode array detector. Protein content was assayed as the area under the 206 nm absorption maximum (calculated using the Shimadzu LS Postrum analysis software), allowing the generation of a standard curve.

### **5.2.3 Dithiothreitol (DTT) treatment**

In order to approve the importance of cysteine thiol groups for the binding of selenite, we treated the *ramSeBP* with DTT which can affect and reduce the cysteine residues. Stock of recombinant SeBP23 (20 µg) was thoroughly mixed with 300 µl DTT (Sigma, USA) solutions (2 mM DTT in PBS, pH 7.4), and the progress of the reaction was monitored over time (0, 1, 2, 3 to 24 hours) by withdrawing 20 µl aliquots of the reaction mixture and assaying these using the HPLC system described above (section 5.2.2).

#### 5.2.4 Small (microgram) scale ramSeBP/selenite ( $^{75}\text{SeO}_3^{2-}$ ) binding assay

Aliquots of untreated (6.5  $\mu\text{g}$ ; HPLC elution peak at 10.28 min) and reduced ramSeBP23 (6.0  $\mu\text{g}$  treated for 3 hours with DTT; HPLC elution peak at 10.70 min) were (separately) treated with 270 ng of  $^{75}\text{Se}^{4+}$  in a total volume of 40  $\mu\text{l}$  of sodium phosphate buffer (PBS, pH 7.4), mixed for 5 seconds and then incubated at 23  $^{\circ}\text{C}$  for 1 hour. The reaction was monitored at 23  $^{\circ}\text{C}$  by instant thin layer chromatography (ITLC-SG, Pall Corporation). The mobile phase (0.15 M ammonium acetate, pH 4.5) effectively separated the  $^{75}\text{Se}^{4+}$  bound by the ramSeBP23, refractive index ( $R_f$ )  $<0.2$ , from free  $^{75}\text{Se}^{4+}$  ( $R_f$ )  $>0.8$ . The processed ITLC-SG strips were cut into 2 cm sections and associated radioactivity measured in Wallac Wizard 1480 gamma counter (Fig. 5.1). The amount  $^{75}\text{Se}^{4+}$  bound by the ramSeBP23 was calculated for each reaction (1 k CPM  $^{75}\text{Se}^{4+}$  equals 6.1 ng  $^{75}\text{Se}^{4+}$ ). In order to verify that the GST-tag has no affinity for  $^{75}\text{Se}^{4+}$ , a control experiment was performed using 10  $\mu\text{g}$  of 25 kDa GST-tag. All other manipulations were the same as for ramSeBP23.

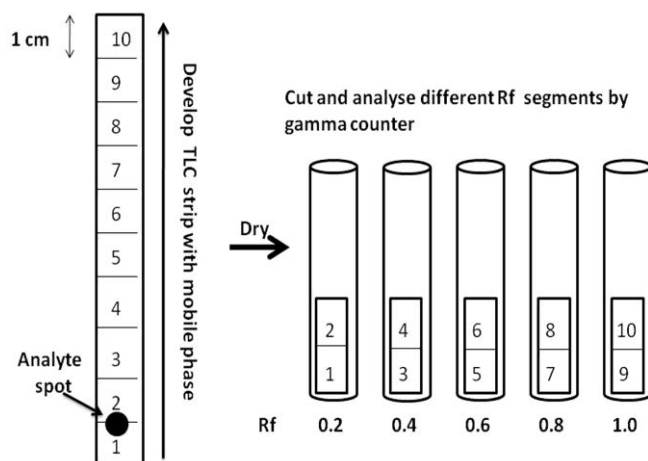


Fig.5.1 ITLC assay. Samples were spotted on the bottom analyte spot at Rf (Retention Factor) 0.2 and developed in mobile phase (0.15M Ammonium acetate) until to the top Rf 1.0. After drying, the ITLC strips were cut into 2 cm segments and associated radioactivity measured in a gamma counter in Kimble tubes.

## 5.3 Results

### 5.3.1 Selenite binding ability of high level *ramSeBP23* in vitro

After pre-incubation with selenite ( $\text{SeO}_3^{2-}$ ), significant ( $P < 0.001$ , compared to negative samples without selenite pre-incubation, tested by Tukey method,  $\alpha = 0.05$ ) levels of selenium (1100  $\mu\text{g/l}$  – 4700  $\mu\text{g/l}$ ) were associated with the recombinant protein eluting from the column (Fig. 5.2 A). In contrast, when selenite pre-incubation was not carried out, very little selenium ( $< 100 \mu\text{g/l}$ ) was detected in the fractions containing *ramSeBP23* (Fig. 5.2 B), proving that selenite was not bound during the production of the recombinant protein. To establish that selenite was not bound by the GST portion of the recombinant protein, non-recombinant GST was pre-incubated with sodium selenite in parallel with the treatment of the recombinant protein. As can be seen in Fig 5.2 C, selenium was not significantly ( $P > 0.01$ , compared to negative samples without selenite pre-incubation, tested by Tukey method,  $\alpha = 0.05$ ) associated ( $< 100 \mu\text{g/l}$ ) with the GST protein, indicating that selenite-binding was associated with the *amSeBP23* part of the recombinant protein rather than with the GST tag. As summarized in Table 5.1, the ratio of bound selenium to *ramSeBP23* was determined as approximately 1.8:1, and was consistent across the four elution volumes collected.

It is also interesting to note that selenium binding had an apparent effect on the *ramSeBP23* elution time. Protein without obvious selenium eluted more rapidly from the column (Fig. 5.2 B C) than did *ramSeBP23* with bound selenium (Fig. 5.2 A).

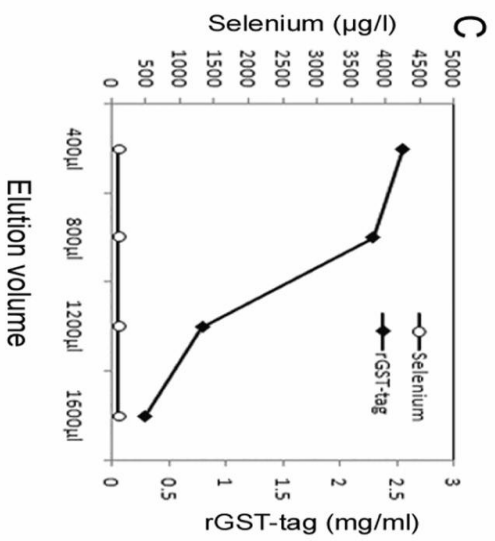
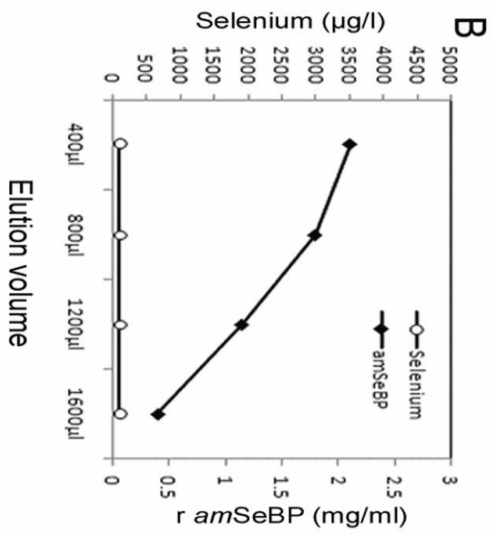
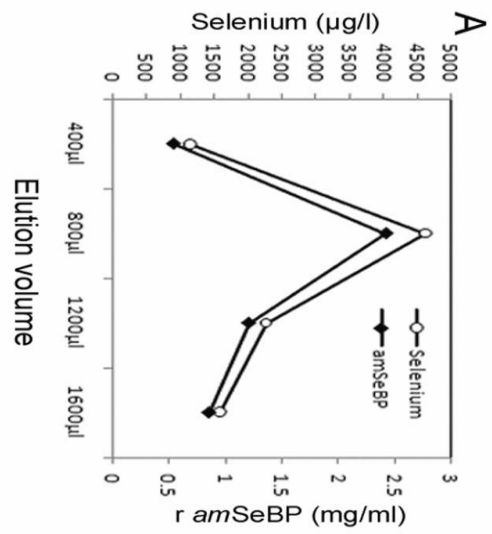


Fig 5.2. Selenium and protein content in the flow through mixtures of the affinity column. A: *r amSeBP23* with selenite ( $\text{SeO}_3^{2-}$ ); B: *r amSeBP23* without selenite ( $\text{SeO}_3^{2-}$ ); C: control protein GST-tag with selenite ( $\text{SeO}_3^{2-}$ ). Selenium content in B, C is  $<100 \mu\text{g/l}$ , similar with negative control.

Table 5.1 The binding ratio between selenium and *ramSeBP* in Fig. 5.2 A.

Elution volume	Selenium ( $\mu\text{g/l}$ )		<i>ramSeBP</i> (mg/ml)	Selenium: <i>ramSeBP</i> ( $\mu\text{mol}:\mu\text{mol}$ )	
	Mean	SD		Mean	SD
0 - 400 $\mu\text{l}$	1160	45	0.55	1.97	0.08
400 - 800 $\mu\text{l}$	4620	74	2.42	1.78	0.03
800 - 1200 $\mu\text{l}$	2280	101	1.21	1.75	0.08
1200 - 1600 $\mu\text{l}$	1590	93	0.86	1.72	0.10

SD: standard deviation

### 5.3.2 HPLC of native and DTT modified *ramSeBP23*

Chromatography revealed a single sharp 206 nm protein peak (10.287 min, Fig. 5.3A) even when as little as 0.12  $\mu\text{g}$  native *ramSeBP23* was loaded onto the column. The area under the 206 nm peak showed a linear relationship with protein loaded over the range 0.12 - 4  $\mu\text{g}$  of native *ramSeBP23* (Fig. 5.3B).

The effect of DTT treatment on *ramSeBP23* was analysed by HPLC. Irrespective of the period of reaction, DTT treatment of native *ramSeBP2* resulted in the detection of a second 206 nm peak behind the native protein peak (Fig. 5.4). The new peak at a retention time of 10.699 min corresponds to a modified (reduced) form of *ramSeBP23*. As can be seen in Fig 5.4, most native *ramSeBP23* was modified to the reduced form within one hour of DTT treatment, and after three hours, the native *ramSeBP23* was fully transformed (Fig. 5.4).

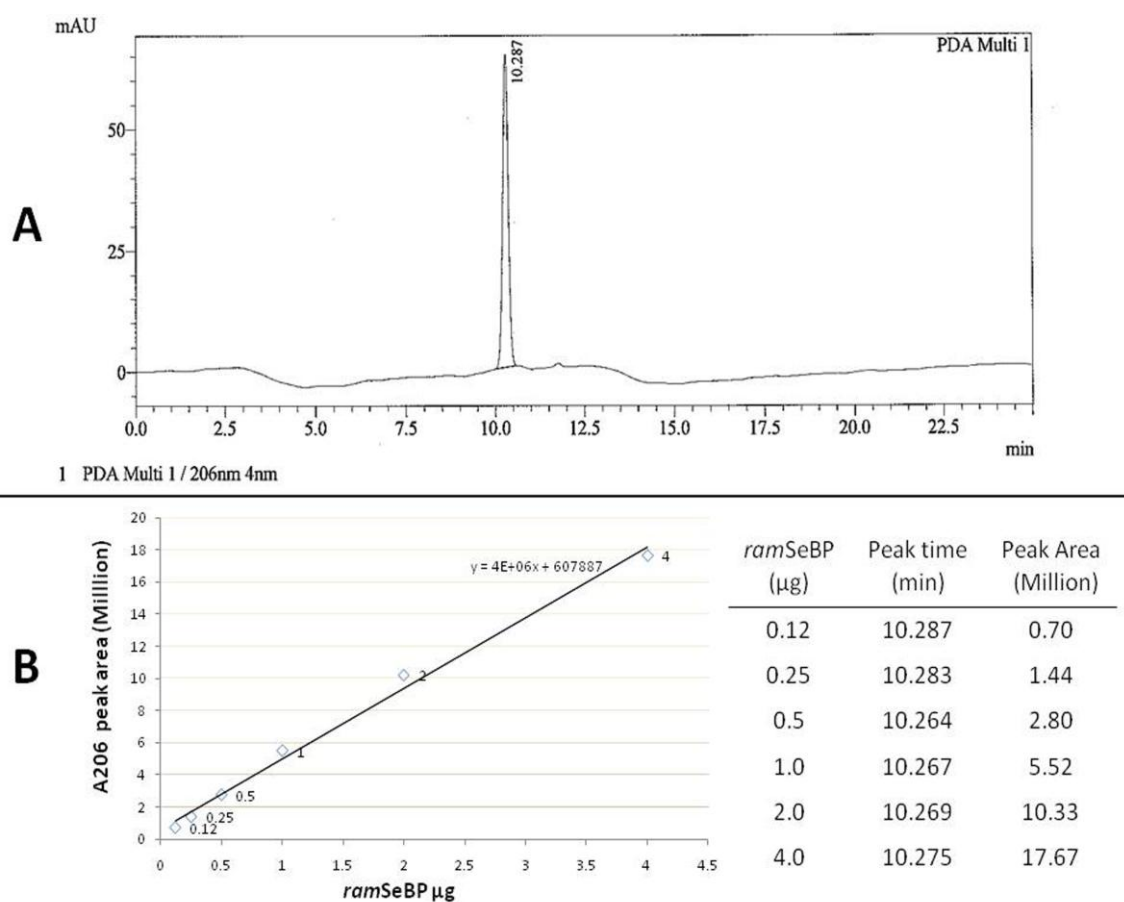


Fig. 5.3 Chromatography A206 nm peak area/protein content curve. A: Chromatography profiles of native *ramSeBP*, injection 0.12 µg; B: Chromatography A206 nm peak area towards 0.12, 0.25, 0.5, 1.0, 2.0, 4.0 µg *ramSeBP23* injection.

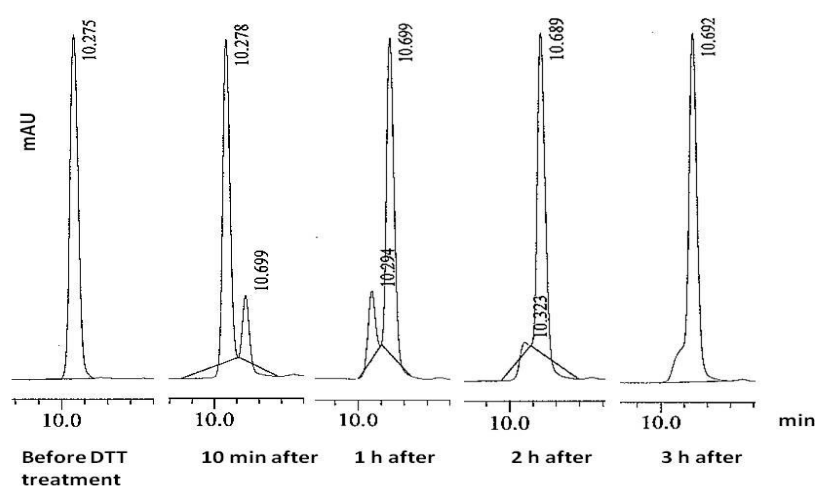


Fig. 5.4 Chromatography profiles of *ramSeBP* after different periods of DTT treatment

### 5.3.3 $^{75}\text{SeO}_3^{2-}$ binding ability of low level native and DTT-modified ramSeBP23 in vitro

After the ITLC strips were cut and checked by gamma counter, the control protein (25 kDa GST) showed no significant binding towards  $^{75}\text{Se}^{4+}$  at Rf 0.2 (Table 5.2), similar to the blank control. In comparison,  $^{75}\text{Se}$  was found in both native and DTT treated ramSeBP23 at Rf 0.2, the amount of Se and protein were translated from CPM and the peak area of A206 nm to ng  $^{75}\text{Se}$  and  $\mu\text{g}$  protein. The results indicate native ramSeBP23 can bind approximately 1.2  $^{75}\text{Se}$  per ramSeBP23. While following DTT-treatment, the binding ratio increased to approximately 4.0  $^{75}\text{Se}$  per ramSeBP23.

Table 5.2 The binding ratio between  $^{75}\text{Se}$  and ramSeBP in ITLC binding assay

Proteins	Rf 0.2			$^{75}\text{Se}^{4+}$ : protein ( $\mu\text{mol}$ : $\mu\text{mol}$ )	
	$^{75}\text{Se}^{4+}$ (CPM)	$^{75}\text{Se}^{4+}$ (ng)	Protein content ( $\mu\text{g}$ )	Mean	SD
Blank control	10 $\pm$ 5	NA	NA	NA	NA
25 kDa GST	13 $\pm$ 5	NA	1.00	NA	NA
Native ramSeBP23	150 $\pm$ 20	0.82 $\pm$ 0.12	0.65*	1.18	0.17
DTT treated ramSeBP23	414 $\pm$ 50	0.53 $\pm$ 0.31	0.60*	3.94	0.48

\*, Calculated from the u.v. 206 nm peak area/protein content curve shown in Fig. 5.3.

CPM: Counts per minute. NA: Not available. SD: standard deviation

## 5.4 Discussion and Hypothesis

### 5.4.1 The potential selenite binding sites of the ramSeBP23

Based on computational modelling (described in Chapter 4), the ramSeBP23 (monomer) protein contains five cysteine residues (Cys33, 82, 85, 143, 268) that are conserved in most 56 kDa SeBP family members, and three of these (Cys82, 85, 143) are likely to be clustered together in the 3D structure. Based on the structural alignment, the HxxH (His139, 142) motif located close to Cys143, together with the CSSC motif (Cys82, 85) are likely to constitute the selenium binding sites and redox centre of the 56 kDa SeBP (Jamba et al., 1997; Flemetakis et al., 2002). In the case of

the pentameric *M. vanniellii* SeBP, it has been reported that the clustering of a number of cysteine residues within the 3D structure (i.e. one Cys residue per monomer) facilitates selenite binding *in vitro* (Suzuki et al., 2008). In the case of SeBP23, two other cysteine residues (Cys-33, 268) may also be involved in Se binding because they are exposed on the protein surface and occur proximal to histidine residues. The occurrence and distribution of multiple reactive cysteine and histidine residues are consistent with the non-enzymic binding of selenite in SeBP: the formation of selenotrisulfides (RS-Se-SR) in the redox centre (Cys82, 85, 143) or selenopersulfide (RS-Se<sup>-</sup>) in the case where additional reductants are involved. Overall, the mechanism of selenite binding in SeBP is likely to be similar to its interaction with GSH (glutathione) and GAPDH (Kessi and Hanselmann 2004; Ogasawara et al., 2005).

#### ***5.4.2 The selenite binding towards ramSeBP23 is depending on the redox status***

No significant levels of selenium were bound (Fig. 5.2B) during the production and purification of the *ramSeBP23* protein. Estimates of the amount of selenium bound differed somewhat between the assay systems; the small scale assay implied approximately 1.2 mol of Se per mol of *ramSeBP23* (Table 5.2), while the corresponding figure was 1.7 Se per *ramSeBP23* in the large scale assay (Table 5.1). We consider that the estimate from the large scale assay is likely to be less accurate due to potential interference by the protein with the mass spectrometry-based assay. By comparison, quantification the <sup>75</sup>Se by gamma spectrometry is likely to be more accurate and sensitive than mass spectrometry. According to the binding rate of the native *ramSeBP23*, we suggest that one selenium molecule is bound in the redox centre of the native *ramSeBP23* in the form of selenotrisulfide (RS-Se-SR, R= Cys-82, 85, or 143), similar with the *M. vanniellii* SeBP that binds inorganic selenite through clustered cysteine thiol groups (Suzuki et al., 2008; Patteson et al., 2005), which is relatively stable because of the central location and the assistance from nearby HxxH / CSSC motifs (Fig. 4.1, in Chapter 4). We hypothesise that the remaining selenium (0.2 to 0.7 Se per *ramSeBP23*) may be bound at the protein surface (possibly

associated with Cys-33, 268), where its association may be dependent on the redox environment and therefore not stable. After 3 hours incubation, low concentrations of reductant (DTT) (Fig. 5.4) transformed all of the sulfhydryl groups in cysteine residues to thiols (Cys-SH). In this situation each *ram*SeBP23 may bind as many as four  $^{75}\text{Se}^{4+}$  in the form of selenopersulfide (RS-Se $^-$ ).

#### ***5.4.3 The amSeBP is an ideal selenium stock protein***

Unlike selenoproteins, in which the selenium is irreversibly incorporated, the 56kDa SeBP can selectively bind selenium through multiple cysteine and histidine residues. The binding process is non-enzymic and reversible depending on the redox status of the system (Kessi and Hanselmann 2004; Patteson et al., 2005), so the 56 kDa SeBP is an adjustable molecular for storage or supply of selenium *in vivo*. When the redox status *in vivo* is reductive, the reduced cysteine residues of the 56 kDa SeBP can capture selenite in the form of either selenotrisulfide (RS-Se-SR) or selenopersulfide (RS-Se $^-$ ). In this scenario, the binding between selenite and the thiol group will release the superoxide anion (O $_2^-$ ) (Kessi et al., 2004) which is not stable and can be easily balanced by the reductive environment *in vivo*. But when the redox status *in vivo* is not reductive, the cysteine residues not in the reduced form will suspend the binding towards the free selenite, avoid generation too much oxidative chemicals which will be toxic if they exceed the reduction ability of the environments. We hypothesise that the positions of the cysteine residues and the overall 3D structure of the protein are important for the adjustable Se binding function of the 56 kDa SeBP, and that this might underlie the high level of sequence as well as protein structure conservation seen in this protein family.

In the known invertebrates which have been studied their selenium repertoires, the coral *A. millepora* has the most abundant selenium containing proteins (Chapter 1). In connection with this complex selenium repertory, the coral must have an advanced

intermediary selenium buffer system which can balance between the selenium sources and demands *in vivo*. In this case, if the *A. millepora* SeBP acts as selenium stock buffer towards selenite, it can strongly support the advanced selenium network *in vivo*. Moreover, the localization studies in Chapter 4 have implied that the *A. millepora* SeBP potentially mediate the communication between the host and the *Symbiodinium*, which indicated the selenium metabolism is not only needed for the host coral, but also for the *Symbiodinium*, and the selenite bound *A. millepora* SeBP plays important roles in the symbiosis physiology through supplying the selenium sources for the *Symbiodinium*. However, more studies and methods with higher resolutions and sensitivities need to be performed to support this hypothesis.

## Chapter 6

### General conclusion

#### *6.1 To be or not to be: evolutionary insight into ancestral Se components*

Evolutionary and phylogenetic analyses of the cnidarian data (chapter 2) reveal the presence of a complex repertoire of selenium components that includes not only the selenocysteine incorporation apparatus, but also homologs of the GPx and TR family members and most other mammalian selenoproteins and selenium binding proteins. The results indicate that most of the selenium components known from bilaterian animals diverged before the bilaterian-cnidarian split.

One interesting general evolutionary trend, however, is that many of the selenoprotein homologs from the model invertebrates lack Sec residues compared to their mammalian counterparts (Kanzok et al., 2001; Lacey and Hondal 2006) – selenocysteine residues are either directly lost or replaced by cysteine. The extent of this ‘Sec drop out’ phenomenon differs dramatically across the model organisms included in my study. In particular, the lancelet, nematode worm and fruit fly have undergone extensive loss of Sec residues whereas the cnidarians *Hydra*, *Nematostella* and *Acropora* retain complex Sec-containing selenoproteins. Aquatic marine animals show us both ends of the spectrum in terms of Sec evolutionary trends: cnidarians have retained many Sec residues whereas the lancelet has dramatically lost the Sec residues from “selenoproteins”. These results indicate that the environmental Se source is unlikely to be the main factor underlying selenoprotein evolution. Rather, we suggest that the main reason cnidarians have in many cases maintained the Sec content of proteins is that there are physiological advantages in doing so.

The ‘Sec drop out’ phenomenon does not mean that the selenium utilization is

unimportant for those animals which have retained few Sec containing components, because selenium binding proteins are highly conserved in all of the model animals studied, leading us to conclude that, in common with their mammalian counterparts, these conserved ancestral Se components play important roles in a variety of physiological processes.

## **6.2 The nonenzymatic Se components: candidate antioxidants in *Acropora millepora***

Unlike the selenoenzymes (GPx, TR etc), most of which have well-established catalytic functions (chapter 2), most of the non-enzymatic Se components have no clear biochemical roles. In *A. millepora*, we found that transcription of the genes encoding many of the non-enzymatic selenium containing proteins, including *amSeBP*, *amSEP15kD*, *amSEPP*, *amSEPT* and *amSEPW* (W1, W2) can be triggered by oxidative stress. Up-regulation of genes encoding these redox-sensitive Se components was associated with two kinds of experimental conditions: (1) where oxidants overwhelm the basic redox buffering system, and (2) where the basic redox buffers or their supporting enzymes were inhibited (chapter 3). We conclude that these redox-sensitive selenium-containing proteins may constitute an emergency antioxidant defense system that is able to backup the basic redox system; non-enzymatic proteins may be more stable under extreme conditions. In the coral *Acropora*, it appears that the selenoenzymes and non-enzymatic selenoproteins, together with other antioxidants, constitute a complex antioxidant network, enabling it to deal with a wide variety of physiological challenges. Our study (chapter 3) has addressed only the basic expression profiles of these non-enzymatic selenium elements in *A. millepora* under oxidative conditions. Further biochemical research is needed towards understanding the individual functions of these non-enzymatic selenium components.

### **6.3 The 56kD SeBP in *Acropora millepora*: not simple, not well known**

SeBP is one of the most highly conserved Se containing proteins, but is not well characterized in terms of structure, the mechanism of Se-binding and functions. In Chapters 4 and 5 of this thesis, the sequence, structure, transcription and selenium (selenite)-binding properties of the *A. millepora* 56kD *amSeBP* were reported. The major findings can be summarized as follows: (1) based on sequence analysis and structural comparisons, the candidate redox centre, which consists of several highly conserved cysteine residues and proximal CSSC and HxxH motifs, is located at the core of the predicted *amSeBP* tertiary structure. (2) *amSeBP* is ubiquitous expressed during development, but up-regulated in the active growing stages which have higher metabolic rates. (3) Binding assays indicate that recombinant *amSeBP* binds inorganic selenite *in vitro*, but the binding properties are dependent on the redox environmental. In addition, immunostaining suggests that *amSeBP* may be involved in transport or metabolism at the larval surface or at the *Symbiodinium* interface.

Despite these studies, the function of *amSeBP* in particular the 56 kDa SeBP family in general remain unclear. It is remarkable that so little is known about such an ancient conserved protein. Functional analyses in manipulable model organisms should be a high priority because these are likely to be particularly informative, and site-directed mutagenesis in association with crystallography may be helpful in understanding the mechanism of selenium binding.

### **6.4 Future directions**

The major contribution of this study is the revealing of complex selenium containing proteins in the early-diverging metazoan animals (poriferan and cnidarians) and further characterization some of them in the coral *A. millepora*, which is not systematically studied before. After filling this research gap, a clearer profile of the selenium utilization in the metazoan animals along the evolutionary line is taking shape. Moreover, the results of this thesis infer several challenging questions which

may interest not only the Se biochemists but also the coral biologists for the future studies.

First, can the coral *A. millepora* be set up as a comparative model to research the Se biochemistry? Up to now, 21 selenoproteins were identified in *A. millepora*, which is comparable with mammals (25 selenoproteins), but the coral morphology is much simpler. Comparison of the sequence and structure information, spatiotemporal distribution, regulation, and specific activities of these selenium-containing proteins will benefit to reveal their practical physiological roles and evolution, some of which remain poorly documented. For example, the mammalian selenoprotein T was recently found to have potential roles in nerve tissues (Tanguy et al., 2011); comparatively, selenoprotein T was also found in adult *A. millepora*, even though its expression level was quite low (results described in Chapter 3). Future studies aiming to explore the spatiotemporal distribution and regulation pattern of *A. millepora* selenoprotein T may contribute to better understanding the role of selenoprotein T in the unclear *A. millepora* nerve system. Similarly, a number of mammalian selenium-containing proteins are believed to play important roles in immunity through adjusting the signal pathways or chemical flux (reviewed by Huang et al., 2011). It would be interesting if we could get similar conclusion for these selenium-containing proteins in *A. millepora* immune system, which is still largely unknown for us in the molecular level.

The second question may interest the coral biologists: is the selenium utilization essential for the symbiosis in corals? I point this question here not only because the symbiosis is a specific physiological activity for corals comparing other research models in the Se biochemistry field, but also because the corals are under serious threats of retardation and the bleaching (loss of the symbiotic algae) is becoming worldwide ecological problems. Parts of the results in this thesis have indicated that some selenium-containing proteins are redox-sensitive (in Chapter 3) in *A. millepora*. Among these proteins, finding of one candidate (*amSeBP*) in host/*Symbiodinium*

interface (in Chapter 4) provides an initial insight for the potential involvement of selenium-containing proteins in symbiosis through: 1). dealing with the symbiont-derived oxidants, or 2). transporting and supplying the Se nutrition which is needed by *Symbiodinium*. In the future studies more advanced and sensitive methods need to be utilized to verify this hypothesis and further research the molecular mechanism of these selenium bio-markers, in coral symbiosis.

# References

- Abrego D, Ulstrup KE, Willis BL, van Oppen MJ. Species-specific interactions between algal endosymbionts and coral hosts define their bleaching response to heat and light stress. *Proceedings of the Royal Society B: Biological Sciences*. 2008; 275(1648):2273–82
- Adams ML, Lombi E, Zhao F-J and McGrath SP, Evidence of low selenium concentrations in UK bread-making wheat grain. *Journal of the Science of Food and Agriculture*. 2002; 82:1160–1165
- Allemand D, Ferrier-Pagès C, Furla P, Houlbrèque F, Puvarel S, Reynaud S, Tambutté É, Tambutté S, Zoccola D. Biomineralisation in reef-building corals: from molecular mechanisms to environmental control. *Comptes Rendus Palevol*. 2004; 3(6-7):453–467
- Ainsworth TD, Guldborg OH. Bacterial communities closely associated with coral tissues vary under experimental and natural reef conditions and thermal stress. *Aquatic Biology*. 2009; 4:289–296
- Arai M, Imai H, Sumi D, Imanaka T, Takano T, et al. Import into mitochondria of phospholipid hydroperoxide glutathione peroxidase requires a leader sequence. *Biochemical and Biophysical Research Communications*. 1996; 227:433–39
- Arthur JR, McKenzie RC, Beckett GJ. Selenium in the immune system. *The Journal of Nutrition*. 2003; 133(5 Suppl 1):1457S-9S
- Ball EE, Hayward DC, Reece-Hoyes JS, Hislop NR, Samuel G, Saint R, Harrison PL, Miller DJ. Coral development: from classical embryology to molecular control. *The International Journal of Developmental Biology*. 2002; 46(4):671–678
- Ball EE, Hayward DC, Saint R, Miller DJ. A simple plan — cnidarians and the origins of developmental mechanisms. *Nature Reviews Genetics*. 2004; 5: 567–577
- Baird AH, Gilmour J, Kamiki T, Nonaka M, Pratchett M, Yamamoto H, Yamasaki H. Temperature tolerance of symbiotic and non-symbiotic coral larvae. *Proceedings of the 10th International Coral Reef Symposium*. 2006; Okinawa, Japan: ICRS.
- Bansal MP, Cook RG, Danielson KG, Medina D. A 14- Kilodalton Selenium-binding protein in mouse liver is fatty acid-binding protein. *The Journal of Biological Chemistry*. 1989b; 264:13780–4
- Bansal MP, Mukhopadhyay T, Scott J, Cook RG, Mukhopadhyay R, Medina D. DNA sequencing of a mouse liver protein that binds selenium: implications for selenium's mechanism of action in cancer prevention. *Carcinogenesis*. 1990;

- Bansal MP, Oborn CJ, Danielson KG, Medina D. Evidence for two selenium-binding proteins distinct from glutathione peroxidase in mouse liver. *Carcinogenesis* 1989a; 10:541–6
- Bay LK, Ulstrup KE, Nielsen HB, Jarmer H, Goffard N, Willis BL, Miller DJ, Van Oppen MJ. Microarray analysis reveals transcriptional plasticity in the reef building coral *Acropora millepora*. *Molecular Ecology*. 2009; 18(14):3062–75
- Behne D, Hilmert H, Scheid S, Gessner H, Elger W. Evidence for specific selenium target tissues and new biologically important selenoproteins. *Biochimica et Biophysica Acta*. 1988; 966:12–21
- Behne D, Höfer H, von Berswordt-Wallrabe R, Elger W. Selenium in the testis of the rat: studies on its regulation and its importance for the organism. *The Journal of Nutrition*. 1982; 112:1682–87
- Behne D, Kyriakopoulos A, Meinhold H, Kohrle J. Identification of type I iodothyronine 5'-deiodinase as a selenoenzyme. *Biochemical and Biophysical Research Communications*. 1990; 173:1143–49
- Behne D, Kyriakopoulos A, Scheid S, Gessner H. Effects of chemical form and dosage on the incorporation of selenium into tissue proteins in rats. *The Journal of Nutrition*. 1991; 121:806–14
- Behne D, Kyriakopoulos A. Mammalian selenium-containing proteins. *Annual Review of Nutrition*. 2001; 21:453–473
- Behne D, Pfeifer H, Röhlein D, Kyriakopoulos A. Cellular and subcellular distribution of selenium and selenium containing proteins in the rat. In *Trace Elements in Man and Animals 10*, 2000; pp. 29– 34. New York: Kluwer/Plenum
- Bénazet-Tambutti S, Allemand D, Jaubert J. Permeability of the oral epithelial layers in cnidarians. *Marine biology*. 1996; 126(1):43–53
- Berry MJ, Martin GW III, Low SC. RNA and protein requirements for eukaryotic selenoprotein synthesis. *Biomedical and Environmental Sciences*. 1997; 10:182–89
- Bevan M, Bancroft I, Bent E. Analysis of 1.9 Mb of contiguous sequence from chromosome 4 of *Arabidopsis thaliana*. *Nature*. 1998; 391(6666):485–8
- Bierkens JG. Applications and pitfalls of stress-proteins in biomonitoring. *Toxicology*. 2000; 153(1-3):61–72
- Bock A. Biosynthesis of selenoproteins— an overview. *BioFactors*. 2000; 11:77–78
- Bock A. Incorporation of selenium into bacterial selenoproteins. In *Selenium in Biology and Human Health*, ed. RF Burk, 1994; pp. 9–24. New York: Springer

- Bradford MM. A rapid and sensitive method for the quantitation of microgram quantities of protein utilizing the principle of protein-dye binding. *Analytical Biochemistry*. 1976; 72:248–54
- Budd GE. The earliest fossil record of the animals and its significance. *Philosophical Transactions of the Royal Society B-Biological Sciences*. 2008; 363(1496): 1425–1434
- Burk RF. Selenium, an antioxidant nutrient. *Nutrition in Clinical Care*. 2002; 5:47–9
- Calvin HI, Cooper GW, Wallace E. Evidence that selenium in rat sperm is associated with a cysteine-rich structural protein of the mitochondrial capsules. *Gamete Research*. 1981; 4:139–49
- Castellano S, Novoselov SV, Kryukov GV, Lescure A, Blanco E, Krol A, Gladyshev VN, Guigó R. Reconsidering the evolution of eukaryotic selenoproteins: a novel nonmammalian family with scattered phylogenetic distribution. *EMBO Reports*. 2004; 5(1):71–7
- Castellano S, Lobanov AV, Chapple C, Novoselov SV, Albrecht M, Hua D, Lescure A, Lengauer T, Krol A, Gladyshev VN, Guigó R. Diversity and functional plasticity of eukaryotic selenoproteins: identification and characterization of the SelJ family. *Proceedings of the National Academy of Sciences of the United States of America*. 2005; 102(45):16188–93
- Castellano S, Gladyshev VN, Guigó R, Berry MJ. SelenoDB 1.0 : a database of selenoprotein genes, proteins and SECIS elements. *Nucleic Acids Research*. 2008; 36(Database issue):D332–8
- Chang PW, Tsui SK, Liew C, Lee CC, Waye MM, Fung KP. Isolation, characterization, and chromosomal mapping of a novel cDNA clone encoding human selenium binding protein. *Journal of Cellular Biochemistry*. 1997; 64:217–24
- Chen C, Zhang P, Hou X, Chai Z. Subcellular distribution of selenium and Se-containing proteins in human liver. *Biochimica et Biophysica Acta*. 1999; 1427(2):205–215
- Chen G, Gharib TG, Huang CC. Proteomic analysis of lung adenocarcinoma: identification of a highly expressed set of proteins in tumors. *Clinical Cancer Research*. 2002; 8(7):2298–2305
- Chen X, Yang G, Chen J, Chen X, Wen Z, Ge K. Studies on the relations of selenium and Keshan disease. *Biological Trace Element Research*. 1980; 2(2):91–107
- Chu FF, Doroshov JH, Esworthy RS. Expression, characterization, and tissue distribution of a new cellular selenium-dependent glutathione peroxidase, GSHPx-GI. *The Journal of Biological Chemistry*. 1993; 268:2571–76
- Chu FF, Esworthy RS, Ho Y-S, Swiderek K, Elliot RW. Expression and

chromosomal mapping of mouse Gpx2 gene encoding the gastrointestinal form of glutathione peroxidase, GPX-GI. *Biomedical and Environmental Sciences*. 1997; 10:156–62

- Clark LC, Combs GF, Turnbull BW, Slate EH, Chalker DK, Chow J, Davis LS, Glover RA, Graham GF, Gross EG, Krongrad A, Lesher JL, Park HK, Sanders BB, Smith CL, Taylor JR. Effects of selenium supplementation for cancer prevention in patients with carcinoma of the skin. A randomized controlled trial. Nutritional Prevention of Cancer Study Group. *The Journal of the American Medical Association*. 1996; 276(24):1957–63
- Collins AG. Phylogeny of Medusozoa and the evolution of cnidarian life cycles. *Journal of Evolutionary Biology*. 2002; 15(3): 418–432
- Coles SL, Brown BE. Coral bleaching--capacity for acclimatization and adaptation. *Advances in Marine Biology*. 2003; 46:183–223
- Combet C, Jambon M, Del éage G, Geourjon C. Geno3D: automatic comparative molecular modelling of protein. *Bioinformatics*. 2002;18(1):213–214
- Croteau W, Whittemore SL, Schneider MJ, St Germain DL. Cloning and expression of a cDNA for a mammalian type III iodothyronine deiodinase. *The Journal of Biological Chemistry*. 1995; 270:16569–75
- Dash B, Metz R, Huebner HJ, Porter W, Phillips TD. Molecular characterization of phospholipid hydroperoxide glutathione peroxidases from *Hydra vulgaris*. *Gene*. 2006; 381:1–12
- Davey JC, Becker KB, Schneider MJ, St. Germain DL, Galton VA. Cloning of a cDNA for the type II iodothyronine deiodinase. *The Journal of Biological Chemistry*. 1995; 270:26786–89
- Dear TN, Campbell K, Rabbitts TH. Molecular cloning of putative odorant-binding and odorant-metabolizing proteins. *Biochemistry*. 1991; 30(43):10376–82
- Desikan R, A-H-Mackerness S, Hancock JT, Neill SJ. Regulation of the Arabidopsis transcriptome by oxidative stress. *Plant Physiology*. 2001; 127(1):159–172
- Donahue WF, Allen EW, Schindler DW. Impacts of coal-fired power plants on trace metals and polycyclic aromatic hydrocarbons (PAHs) in lake sediments in central Alberta, Canada. *Journal of Paleolimnology*. 2006; 35(1):111–128
- Dove S, Takabayashi M, Hoegh-Guldberg O. Isolation and partial characterization of the pink and blue pigments of Pocilloporid and Acroporid corals. *The Biological Bulletin*. 1995; 189:288–297
- Dove SG, Hoegh-Guldberg O, Ranganathan S. Major colour patterns of reef-building corals are due to a family of GFP-like proteins. *Coral Reefs*. 2001; 19:197–204
- Downs CA, Mueller E, Phillips S, Fauth JE, Woodley CM. A molecular biomarker system for assessing the health of coral (*Montastraea faveolata*) during heat

- stress. *Marine Biotechnology (NY)*. 2000; 2(6):533–44
- Downs CA, Fauth JE, Halas JC, Dustan P, Bemiss J, Woodley CM. Oxidative stress and seasonal coral bleaching. *Free Radical Biology and Medicine*. 2002; 33(4):533–543
- Driscoll DM, Copeland PR. Mechanism and regulation of selenoprotein synthesis. *Annual Review of Nutrition*. 2003; 23:17–40
- Dutilleul C, Jourdain A, Bourguignon J, Hugouvieux V. The Arabidopsis putative selenium-binding protein family: expression study and characterization of SBP1 as a potential new player in cadmium detoxification processes. *Plant Physiology*. 2008;147(1):239–251
- Esworthy RS, Swiderek KM, Ho YS, Chu FF. Selenium-dependent glutathione peroxidase-GI is a major glutathione peroxidase activity in the mucosal epithelium of rodent intestine. *Biochimica et Biophysica Acta*. 1998; 1381:213–26
- Flemetakis E, Agalou A, Kavroulakis N, Dimou M, Martsikovskaya A, Slater A, Spaink HP, Roussis A, Katinakis P. Lotus japonicus gene Ljsbp is highly conserved among plants and animals and encodes a homologue to the mammalian selenium-binding Proteins. *Molecular Plant-Microbe Interactions*. 2002; 15(4):313–22
- Floh éL, Günzler WA, Schock HH. Glutathione peroxidase: a selenoenzyme. *FEBS Letters*. 1973; 32:132–34
- Flores-Ram íez LA, Li ñán-Cabello MA. Relationships among thermal stress, bleaching and oxidative damage in the hermatypic coral, *Pocillopora capitata*. *Comparative biochemistry and physiology C Toxicology & pharmacology*. 2007; 146(1-2):194–202
- Fra ústo Da Silva JJR, Williams RJP. The biological chemistry of the elements. Clarendon Press, Oxford UK, 1997.
- Gasdaska PY, Berggren MM, Berry ML, Powis G. Cloning, sequencing and functional expression of a novel human thioredoxin reductase. *FEBS Letters*. 1999; 442:105–11
- Gasdaska PY, Gasdaska JR, Cochran S, Powis G. Cloning and sequencing of a human thioredoxin reductase. *FEBS Letters*. 1995; 373:5–9
- Gladyshev VN, Jeang KT, Wootton JC, Hatfield DL. A new human selenium-containing protein. Purification, characterization, and cDNA sequence. *The Journal of Biological Chemistry*. 1998; 273:8910–15
- Gladyshev VN, Krause M, Xu XM, Korotkov KV, Kryukov GV, Sun QA, Lee BJ, Wootton JC, Hatfield DL. Selenocysteine-containing thioredoxin reductase in *C. elegans*. *Biochemical and Biophysical Research Communications*. 1999;

259(2):244–9

- Giardi MT, Koblížek M, Masojedek J. Photosystem II-based biosensors for the detection of pollutants. *Biosensors & Bioelectronics*. 2001; 16(9-12):1027–33
- Gouy M, Guindon S, Gascuel O. SeaView version 4: A multiplatform graphical user interface for sequence alignment and phylogenetic tree building. *Molecular Biology and Evolution*. 2010; 27(2):221–24
- Griffith OW, Meister A. Potent and specific inhibition of glutathione synthesis by buthionine sulfoximine (S-n-butyl homocysteine sulfoximine). *The Journal of Biological Chemistry*. 1979; 254(16):7558–60
- Gu QP, Beilstein MA, Barofsky E, Ream W, Whanger PD. Purification, characterization and glutathione binding to selenoprotein W from monkey muscle. *Archives of Biochemistry and Biophysics*. 1999; 361:25–33
- Guder C, Philipp I, Lengfeld T, Watanabe H, Hobmayer B, Holstein TW. The Wnt code: cnidarians signal the way. *Oncogene*. 2006; 25:7450–7460
- Guex N, Peitsch MC. SWISS-MODEL and the Swiss-PdbViewer: An environment for comparative protein modeling. *Electrophoresis*. 1997; 18:2714–2723
- Guindon S, Gascuel O. A simple, fast, and accurate algorithm to estimate large phylogenies by maximum likelihood. *Systematic Biology*. 2003; 52(5):696–704
- Hamilton SJ, Lemly AD. Water-sediment controversy in setting environmental standards for selenium. *Ecotoxicology and environmental safety*. 1999; 44(3):227–35
- Hassan MQ, Stohs SJ, Murray WJ. Comparative ability of TCDD to induce lipid peroxidation in rats, guinea pigs, and Syrian golden hamsters. *Bulletin of Environmental Contamination & Toxicology*. 1983; 31:649–57
- Heinz GH, Hoffman DJ, Krynitsky AJ, Weller DMG. Reproduction in mallards fed selenium. *Environmental Toxicology and Chemistry*. 1987; 6:423-433.
- Hill KE, Lloyd RS, Yang J-G, Read R, Burk RF. The cDNA for rat selenoprotein P contains 10 TGA codons in the open reading frame. *The Journal of Biological Chemistry*. 1991; 266:10050–53
- Hirose M, Kinzie RA, Hidaka M. Early development of zooxanthella-containing eggs of the corals *Pocillopora verrucosa* and *P. eydouxi* with special reference to the distribution of zooxanthellae. *The Biological Bulletin*. 2000; 199:68–75
- Hughes TP, Baird AH, Bellwood DR, Card M, Connolly SR, Folke C, Grosberg R, Hoegh-Guldberg O, Jackson JB, Kleypas J, Lough JM, Marshall P, Nyström M, Palumbi SR, Pandolfi JM, Rosen B, Roughgarden J. Climate change, human impacts, and the resilience of coral reefs. *Science*. 2003; 301(5635):929–33
- Hugouvieux V, Dutilleul C, Jourdain A, Reynaud F, Lopez V, Bourguignon J.

- Arabidopsis putative selenium-binding protein1 expression is tightly linked to cellular sulfur demand and can reduce sensitivity to stresses requiring glutathione for tolerance. *Plant Physiology*. 2009; 151(2):768–781
- Huang Z, Rose AH, Hoffmann PR. The Role of Selenium in Inflammation and Immunity: From Molecular Mechanisms to Therapeutic Opportunities. *Antioxidants & Redox Signaling*. 2011. [doi:10.1089/ars.2011.4145]
- Ip C, Hayes C, Budnick RM, Ganther HE. Chemical form of selenium, critical metabolites and cancer prevention. *Cancer Research*. 1991; 51:595–600
- Irigaray JL, Braye F, Oudadesse H, Jallot E, Weber G, Amiribadi A, Tixier H. Diffusion of mineral elements evaluated by PIXE at the bone-coral interface. *Journal of Biomaterials Science, Polymer Edition*. 1996; 7(8): 741–749
- Ishida T, Tasaki K, Fukuda A, Ishii Y, Oguri K. Induction of a cytosolic 54 kDa protein in rat liver that is highly homologous to selenium-binding protein. *Environmental toxicology and pharmacology*. 1998; 6:249–55
- Ishii Y, Hatsumura M, Ishida T, Ariyoshi N, Oguri K. A coplanar PCB induces a selenium binding protein as a major cytosolic protein rat liver. *Chemosphere* 1996b; 32:509–515
- Ishii Y, Hatsumura M, Ishida T. Significant induction of a 54-kDa protein in rat liver with homologous alignment to mouse selenium binding protein by a coplanar polychlorinated biphenyl, 3,4,5,3',4'-pentachlorobiphenyl and 3-methylcholanthrene. *Toxicology Letters*. 1996<sup>a</sup>; 87(1):1–9
- Jamba L, Nehru B, Bansal MP. Redox modulation of selenium binding proteins by cadmium exposures in mice. *Molecular and Cellular Biochemistry*. 1997; 177(1/2):169–75
- Jeong JY, Wang Y, Sytkowski AJ. Human selenium binding protein-1 (hSP56) interacts with VDU1 in a selenium-dependent manner. *Biochemical and Biophysical Research Communications*. 2009; 379(2):583–588
- Jiang L, Liu Q, Ni J. In silico identification of the sea squirt selenoproteome. *BMC Genomics*. 2010; 11:289
- Jitaru P, Goenaga-Infante H, Vaslin-Reimann S, Fisicaro P. A systematic approach to the accurate quantification of selenium in serum selenoalbumin by HPLC-ICP-MS. *Analytica Chimica Acta*. 2010; 657(2):100–107
- Kaim W, Schwederski B. Bioinorganic chemistry: Inorganic elements in the chemistry of life. Wiley, Chichester UK, 1994.
- Kalcklosch M, Kyriakopoulos A, Hammel C, Behne D. A new selenoprotein found in the glandular epithelial cells of the rat prostate. *Biochemical and Biophysical Research Communications*. 1995; 217:162–70
- Kanzok SM, Fechner A, Bauer H, Ulschmid JK, Müller HM, Botella-Munoz J,

- Schneuwly S, Schirmer R, Becker K. Substitution of the thioredoxin system for glutathione reductase in *Drosophila melanogaster*. *Science*. 2001; 291(5504):643–6
- Kemp M, Go YM, Jones DP. Nonequilibrium thermodynamics of thiol/disulfide redox systems: A perspective on redox systems biology. *Free Radical Biology & Medicine*. 2008; 44:921–37
- Kessi J, Hanselmann KW. Similarities between the abiotic reduction of selenite with glutathione and the dissimilatory reaction mediated by *Rhodospirillum rubrum* and *Escherichia coli*. *The Journal of Biological Chemistry*. 2004; 279:50662–69
- Kim H, Kang HJ, You KT. Suppression of human selenium-binding protein 1 is a late event in colorectal carcinogenesis and is associated with poor survival. *Proteomics*. 2006; 6(11):3466–3476
- Kirby J, Maher W, Harasti D. Changes in selenium, copper, cadmium, and zinc concentrations in mullet (*Mugil cephalus*) from the southern basin of Lake Macquarie, Australia, in response to alteration of coal-fired power station fly ash handling procedures. *Archives of environmental contamination and toxicology*. 2001; 41(2):171–81
- Kortschak RD, Samuel G, Saint R, Miller DJ. EST analysis of the cnidarian *Acropora millepora* reveals extensive gene loss and rapid sequence divergence in the model invertebrates. *Current Biology*. 2003; 13(24):2190–2195
- Kryukov GV, Castellano S, Novoselov SV, Lobanov AV, Zehtab O, Guigó R, Gladyshev VN. Characterization of mammalian selenoproteomes. *Science*. 2003; 300(5624):1439–43
- Kryukov GV, Kryukov VM, Gladyshev VN. New mammalian selenocysteine-containing proteins identified with an algorithm that searches for selenocysteine insertion sequence elements. *The Journal of Biological Chemistry*. 1999; 274:33888–97
- Kusserow A, Pang K, Sturm C, Hroudá M, Lentfer J, Schmidt HA, Technau U, Haeseler AV, Hobmayer B, Martindale MQ, Holstein TW. Unexpected complexity of the Wnt gene family in a sea anemone. *Nature*. 2005; 433:156–160
- Kyriakopoulos A, Hammel C, Gessner H, Behne D. Characterization of an 18 kDa-selenium-containing protein in several tissues of the rat. *American Biotechnology Laboratory*. 1996; 14:22
- Lacey BM, Hondal RJ. Characterization of mitochondrial thioredoxin reductase from *C. elegans*. *Biochemical and Biophysical Research Communications*. 2006; 346(3):629–36
- Larkin MA, Blackshields G, Brown NP, Chenna R, McGettigan PA, McWilliam H, Valentin F, Wallace IM, Wilm A, Lopez R, Thompson JD, Gibson TJ, Higgins

- DG. Clustal W and Clustal X version 2.0. *Bioinformatics*. 2007; 23(21):2947–48
- Le SQ, Gascuel O. An improved general amino acid replacement matrix. *Molecular Biology and Evolution*. 2008; 25(7):1307–20
- Lee SR, Kim JR, Kwon KS, Yoon HW, Levine RL, et al. Molecular cloning and characterization of a mitochondrial selenocysteine-containing thioredoxin reductase from rat liver. *The Journal of Biological Chemistry*. 1999; 274(8):4722–34
- Lemly AD. Symptoms and implications of selenium toxicity in fish: the Belews Lake case example. *Aquatic Toxicology*. 2002; 57(1-2):39–49
- Lescure A, Gautheret D, Carbon P, Krol A. Novel selenoproteins identified in silico and in vivo by using a conserved RNA structural motif. *The Journal of Biological Chemistry*. 1999; 274:38147–54
- Lesser MP, Stochaj WR, Tapley DW, Shick JM. Bleaching in coral reef anthozoans: effects of irradiance, ultraviolet radiation, and temperature on the activities of protective enzymes against active oxygen. *Coral Reefs*. 1990; 8(4):225–232
- Lobanov AV, Fomenko DE, Zhang Y, Sengupta A, Hatfield DL, Gladyshev VN. Evolutionary dynamics of eukaryotic selenoproteomes: large selenoproteomes may associate with aquatic life and small with terrestrial life. *Genome Biology*. 2007; 8(9):R198
- Lobanov AV, Hatfield DL, Gladyshev VN. Reduced reliance on the trace element selenium during evolution of mammals. *Genome Biology*. 2008; 9(3):R62
- Lockitch G. Selenium: clinical significance and analytical concepts. *Critical reviews in clinical laboratory sciences*. 1989; 27(6):483–541
- Loflin J, Lopez N, Whanger PD, Kiousi C. Selenoprotein W during development and oxidative stress. *Journal of Inorganic Biochemistry*. 2006; 100(10):1679–84
- Low SC, Berry MJ. Knowing when not to stop. Selenocysteine incorporation in eukaryotes. *Trends in Biochemical Sciences*. 1996; 21:203–8
- Maiti R, Van Domselaar GH, Zhang H, Wishart DS. SuperPose: a simple server for sophisticated structural superposition. *Nucleic Acids Research*. 2004; 32(Web Server issue):W590–594
- Marshall JF, McCulloch MT. An assessment of the Sr/Ca ratio in shallow water hermatypic corals as a proxy for sea surface temperature. *Geochimica et Cosmochimica Acta*. 2002; 66(18):3263–3280
- Martin-Romero FJ, Kryukov GV, Lobanov AV, Carlson BA, Lee BJ, Gladyshev VN, Hatfield DL. Selenium metabolism in *Drosophila*: selenoproteins, selenoprotein mRNA expression, fertility, and mortality. *The Journal of Biological Chemistry*.

2001; 276(32):29798–804

- Mayfield AB, Hirst MB, Gates RD. Gene expression normalization in a dual-compartment system: a real-time quantitative polymerase chain reaction protocol for symbiotic anthozoans. *Molecular Ecology Resources*. 2009; 9:462–470
- Mazel CH, Lesser MP, Gorbunov MY, Barry TM, Farrell JH, Wyman KD, Falkowski PG. Green-fluorescent proteins in Caribbean corals. *Limnology and Oceanography*. 2003; 48:402–11
- McKenzie RC, Rafferty TS, Beckett GJ. Selenium: an essential element for immune function. *Immunology Today*. 1998; 19(8):342–45
- Mendelev N, Mehta SL, Witherspoon S, He Q, Sexton JZ, Li PA. Upregulation of Human Selenoprotein H in murine hippocampal neuronal cells promotes mitochondrial biogenesis and functional performance. *Mitochondrion*. 2011; 11(1):76–82
- Meyer Y, Verdoucq L, Vignols F. Plant thioredoxins and glutaredoxins: identity and putative roles. *Trends in Plant Science*. 1999; 4(10):388–394
- Miller DJ, Hayward DC, John S, Reece-Hoyes JS, Scholten I, Catmull J, Gehring WJ, Callaerts P, Larsen JE, Ball EE. Pax gene diversity in the basal cnidarian *Acropora millepora* (Cnidaria, Anthozoa): Implications for the evolution of the Pax gene family. *Proceedings of the National Academy of Sciences of the United States of America*. 2000; 97(9):4475–4480
- Miller DJ, Ball EE, Technau U. Cnidarians and ancestral genetic complexity in the animal kingdom. *Trends in Genetics*. 2005; 21(10): 536–539
- Miranda-Vizuete A, Damdimopoulos AE, Pedrajas JR, Gustafsson JA, Spyrou G. Human mitochondrial thioredoxin reductase. *European Journal of Biochemistry*. 1999; 261:405–12
- Miyaguchi K. Localization of selenium-binding protein at the tips of rapidly extending protrusions. *Histochemistry and Cell Biology*. 2004; 121(5):371–376
- Miyawaki A. Green fluorescent protein-like proteins in reef anthozoa animals. *Cell Structure and Function*. 2002; 27:343–47
- Morrison DG, Dishart MK, Medina D. Intracellular 58-kd selenoprotein levels correlate with inhibition of DNA synthesis in mammary epithelial cells. *Carcinogenesis*. 1988; 9:1801–10
- Motsenbocker MA, Tappel AL. A selenocysteine-containing selenium transport protein in rat plasma. *Biochimica et Biophysica Acta*. 1982; 719:147–53
- Muscatine L, Porter JW. Reef corals: mutualistic symbioses adapted to nutrient-poor environments. *Bioscience*. 1977; 27(7):454

- Ogasawara Y, Lacourciere GM, Ishii K, Stadtman TC. Characterization of potential selenium-binding proteins in the selenophosphate synthetase system. *Proceedings of the National Academy of Sciences of the United States of America*. 2005; 102(4):1012–1016
- Papina M, Meziane T, Woesik RV. Symbiotic zooxanthellae provide the host-coral *Montipora digitata* with polyunsaturated fatty acids. *Comparative Biochemistry and Physiology Part B: Biochemistry and Molecular Biology*. 2003; 135(3): 533–537
- Papp LV, Lu J, Holmgren A, Khanna KK. From selenium to selenoproteins: synthesis, identity, and their role in human health. *Antioxidants & Redox Signaling*. 2007; 9(7):775–806
- Patteson KG, Trivedi N, Stadtman TC. Methanococcus vannielii selenium-binding protein (SeBP): chemical reactivity of recombinant SeBP produced in *Escherichia coli*. *Proceedings of the National Academy of Sciences of the United States of America*. 2005; 102(34):12029–34
- Peterson PJ, Butler GW. Significance of selenocystathionine in an Australian selenium-accumulating plant, *Neptunia amplexicaulis*. *Nature*. 1967; 213:599–600
- Pfeifer H, Conrad M, Roethlein D, Kyriakopoulos A, Brielmeier M, Bornkamm GW, Behne D. Identification of a specific sperm nuclei selenoenzyme necessary for protamine thiol cross-linking during sperm maturation. *The FASEB Journal*. 2001; 15(7):1236–8
- Piniak GA. Effects of two sediment types on the fluorescence yield of two Hawaiian scleractinian corals. *Marine Environmental Research*. 2007; 64(4):456–468
- Porat A, Sagiv Y, Elazar Z. A 56-kDa Selenium-binding protein participates in intra-golgi protein transport. *The Journal of Biological Chemistry*. 2000; 275:14457–65
- Pushpa-Rekha TR, Burdsall AL, Oleksa LM, Chisolm GM, Driscoll DM. Rat phospholipid-hydroperoxide glutathione peroxidase. cDNA cloning and identification of multiple transcription and translation start sites. *The Journal of Biological Chemistry*. 1995; 270:26993–99
- Putnam NH, Srivastava M, Hellsten U, Dirks B, Chapman J, Salamov A, Terry A, Shapiro H, Lindquist E, Kapitonov VV, Jurka J, Genikhovich G, Grigoriev IV, Lucas SM, Steele RE, Finnerty JR, Technau U, Martindale MQ, Rokhsar DS. Sea Anemone Genome Reveals Ancestral Eumetazoan Gene Repertoire and Genomic Organization. *Science*. 2007; 317(5834):86–94
- Rayman MP. The importance of selenium to human health. *Lancet* 2000;356:233–41
- Read R, Bellow T, Yang J-G, Hill KE, Palmer IS, Burk RF. Selenium and amino acid

- composition of selenoprotein P, the major selenoprotein in rat serum. *The Journal of Biological Chemistry*. 1990; 265:17899–905
- Rosenberg P, Mautner HG, Nachmans D. Similarity of effects of oxygen sulfur and selenium isologs on acetylcholine receptor in excitable membranes of junctions and axons. *Proceedings of the National Academy of Sciences of the United States of America*. 1966; 55(4):835–838
- Rosenberg E, Koren O, Reshef L, Efrony R, Zilber-Rosenberg I. The role of microorganisms in coral health, disease and evolution. *Nature Reviews Microbiology*. 2007; 5:355–362
- Rotruck JT, Pope AL, Ganther HE, Swanson AB, Hafeman DG, Hoekstra WG. Selenium: biochemical role as a component of glutathione peroxidase. *Science*. 1973; 179:588–90
- Roveri A, Maiorino M, Ursini F. Enzymatic and immunological measurements of soluble and membrane-bound PHGPx. *Methods in Enzymology*. 1994; 233:202–12
- Rushmore TH, Morton MR, Pickett CB. The antioxidant responsive element. *The Journal of Biological Chemistry*. 1991;266:11632–9
- Saijoh K, Saito N, Lee MJ, Fujii M, Kobayashi T, Sumino K. Molecular cloning of cDNA encoding a bovine selenoprotein P-like protein containing 12 selenocysteines and a (His-Pro) rich domain insertion, and its regional expression. *Molecular Brain Research*. 1995; 30:301–11
- Sani BP, Woodard JL, Pierson MC, Allen RD. Specific binding proteins for selenium in rat tissues. *Carcinogenesis*. 1988; 9:277–84
- Sawada K, Hasegawa M, Tokuda L, Kameyama J, Kodama O, Kohchi T, Yoshida K, Shinmyo A. Enhanced resistance to blast fungus and bacterial blight in transgenic rice constitutively expressing OsSBP, a rice homologue of mammalian selenium-binding proteins. *Bioscience, Biotechnology, and Biochemistry*. 2004; 68(4):873–880
- Self WT, Pierce R, Stadtman TC. Cloning and heterologous expression of a *Methanococcus vannielii* gene encoding a selenium-binding protein. *IUBMB Life*. 2004; 56(8):501–507
- Seneca FO, Forêt S, Ball EE, Smith-Keune C, Miller DJ, van Oppen MJ. Patterns of Gene Expression in a Scleractinian Coral Undergoing Natural Bleaching. *Marine Biotechnology* (NY). 2010; 12(5):594–604
- Shand CA, Balsam M, Hillier SJ, Hudson G, Newman G, Arthur JR, Nicol F. Aqua regia extractable selenium concentrations of some Scottish topsoils measured by ICP-MS and the relationship with mineral and organic soil components. *Journal of the Science of Food and Agriculture*. 2010; 90(6):972–80

- Shchedrina VA, Novoselov SV, Malinouski MY, Gladyshev VN. Identification and characterization of a selenoprotein family containing a diselenide bond in a redox motif. *Proceedings of the National Academy of Sciences of the United States of America*. 2007; 104(35):13919–24
- Shinzato C, Iguchi A, Hayward DC, Technau U, Ball EE and Miller DJ. Sox genes in the coral *Acropora millepora*: divergent expression patterns reflect differences in developmental mechanisms within the Anthozoa. *BMC Evolutionary Biology*. 2008; 8:311
- Shisler JL, Senkevich TG, Berry MJ, Moss B. Ultraviolet-induced cell death blocked by a selenoprotein from a human dermatotropic poxvirus. *Science*. 1998; 279(5347):102–5
- Song LS, Zou HB and et al. The cDNA cloning and mRNA expression of a potential selenium-binding protein gene in the scallop *Chlamys farreri*. *Developmental and Comparative Immunology*. 2006; 30:265–273
- Squires JE, Berry MJ. Eukaryotic selenoprotein synthesis: mechanistic insight incorporating new factors and new functions for old factors. *IUBMB Life*. 2008; 60(4):232–5
- Stadtman TC. Selenocysteine. *The Annual Review of Biochemistry*. 1996; 65: 83–100
- Stadtman TC. Selenium biochemistry. Mammalian selenoenzymes. *Annals of the New York Academy of Sciences*. 2000; 899:399–402
- Sun QA, Wu Y, Zappacosta F, Jeang KT, Lee BJ, Hatfield DL, Gladyshev VN. Redox Regulation of Cell Signaling by Selenocysteine in Mammalian Thioredoxin Reductases. *The Journal of Biological Chemistry*. 1999; 274(35): 24522–30
- Sun Y, Ha PC, Butler JA, Ou BR, Yeh JY, Whanger PD. Effect of dietary selenium on selenoprotein W and glutathione peroxidase in 28 tissues of the rat. *The Journal of Nutritional Biochemistry*. 1998; 9:23–27
- Suzuki M, Lee DY, Inyamah N, Stadtman TC, Tjandra N. Solution NMR structure of selenium-binding protein from *Methanococcus vannielii*. *The Journal of Biological Chemistry*. 2008; 283(38):25936–43
- Takahashi K, Avissar N, Whitin J, Cohen H. Purification and characterization of human plasma glutathione peroxidase: a selenoglycoprotein distinct from the known cellular enzyme. *Archives of Biochemistry and Biophysics*. 1987; 256:677–86
- Tamura T, Stadtman TC. A new selenoprotein from human lung adenocarcinoma cells: purification, properties, and thioredoxin activity. *Proceedings of the National Academy of Sciences of the United States of America*. 1996; 93:1006–11
- Tanguy Y, Falluel-Morel A, Arthaud S, Boukhzar L, Manecka DL, Chagraoui A, Prevost G, Elias S, Dorval-Coiffec I, Lesage J, Vieau D, Lihmann I, Jégou B,

- Anouar Y. The PACAP-regulated gene selenoprotein T is highly induced in nervous, endocrine, and metabolic tissues during ontogenetic and regenerative processes. *Endocrinology*. 2011; 152(11):4322–35
- Technau U, Rudd S, Maxwell P, Gordon PMK, Saina M, Grasso LC, Hayward DC, Sensen CW, Saint R, Holstein TW, Ball EE, Miller DJ. Maintenance of ancestral complexity and non-metazoan genes in two basal cnidarians. *Trends in Genetics*. 2005; 21(12):633–639
- Thomas JP, Maiorino M, Ursini F, Girotti AW. Protective action of phospholipids hydroperoxide glutathione peroxidase against membrane-damaging lipid peroxidation. In situ reduction of phospholipids and cholesterol hydroperoxides. *The Journal of Biological Chemistry*. 1990; 265:454–61
- Thompson JD, Higgins DG, Gibson TJ. CLUSTAL W: improving the sensitivity of progressive multiple sequence alignment through sequence weighting, position-specific gap penalties and weight matrix choice. *Nucleic Acids Research*. 1994; 22(22):4673–80
- Tinggi U. Essentiality and toxicity of selenium and its status in Australia: a review. *Toxicology Letters*. 2003; 137(1-2):103–10
- Toppo S, Vanin S, Bosello V, Tosatto SC. Evolutionary and structural insights into the multifaceted glutathione peroxidase (Gpx) superfamily. *Antioxidants & Redox Signaling*. 2008; 10(9):1501–14
- Ure AM and Berrow ML. The elemental constituents of soils. Environmental Chemistry. Specialist Periodical Report, Royal Society of Chemistry, London, 1982; 2:94–204
- Ursini F, Heim S, Kiess M, Maiorino M, Roveri A, et al. Dual function of the selenoprotein PHGPx during sperm maturation. *Science*. 1999; 285:1393–96
- Ursini F, Maiorino M, Gregolin C. The selenoenzyme phospholipids hydroperoxide glutathione peroxidase. *Biochimica et Biophysica Acta*. 1985; 39:62–70
- Vandesompele J, De Preter K, Pattyn F, Poppe B, Van Roy N, De Paepe A, Speleman F. Accurate normalization of real-time quantitative RT-PCR data by geometric averaging of multiple internal control genes. *Genome Biology*. 2002; 3(7):RESEARCH0034.
- Van Oppen MJH, Mahiny AJ, Done TJ. Geographic distribution of zooxanthella types in three coral species on the Great Barrier Reef sampled after the 2002 bleaching event. *Coral reefs*. 2005; 24(3):482–487
- Vendeland SC, Beilstein MA, Chen CL, Jensen ON, Barofsky E, Whanger PD. Purification and properties of selenoprotein-W from rat muscle. *The Journal of Biological Chemistry*. 1993; 268:17103–7
- Watabe S, Makino Y, Ogawa K, Hiroi T, Yamamoto Y, Takahashi SY. Mitochondrial

- thioredoxin reductase in bovine adrenal cortex. Its purification, nucleotide/amino acid sequence, and identification of selenocysteine. *European Journal of Biochemistry*. 1999; 264:74–84
- Winterbourn CC, Hampton MB. Thiol chemistry and specificity in redox signaling. *Free Radical Biology & Medicine*. 2008; 45:549–61
- Yamada M, Yoshida H, Kuramitsu S, Kamitori S. Protein Data Bank: 2ECE. Unpublished.
- Yang M, Sytkowski AJ. Differential expression and androgen regulation of the human selenium-binding protein gene hSP56 in prostate cancer cells. *Cancer Research*. 1998; 58(14):3150–3
- Zhang Y, Fomenko DE, Gladyshev VN. The microbial selenoproteome of the Sargasso Sea. *Genome Biology*. 2005; 6(4):R37
- Zoccola D, Tambutté E, Ségas-Balas F, Michiels JF, Failla JP, Jaubert J, Allemand D. Cloning of a calcium channel  $\alpha 1$  subunit from the reef-building coral, *Stylophora pistillata*. *Gene*. 1999; 227(2):157–167
- Zoccola D, Tambutté E, Kulhanek E, Puverel S, Scimeca JC, Allemand D, and Tambutté S. Molecular cloning and localization of a PMCA P-type calcium ATPase from the coral *Stylophora pistillata*. *Biochimica et Biophysica Acta – Biomembranes*. 2004; 1663 (1-2):117–126
- Jeong JY, Wang Y, Sytkowski AJ. Human selenium binding protein-1 (hSP56) interacts with VDU1 in a selenium-dependent manner. *Biochemical and Biophysical Research Communications*. 2009; 379(2):583–588

## Supplementary file

Supplementary Table 1. Unpublished Se components of *A. millepora*

Code	Name	Amino acid sequence
am sepH (JF970195)	Selenoprotein H	MPRGRKRKEEITSSVGGDVAAEADEVKKSSEESPAKKRKGSDNNMTFKIEHCKSUQVYKRANANQLSSELMKAFPDAVVLINDTKPRFKEF
am sepI (JF970196)	Selenoprotein I	KGMYLTREELRGFDKYKYKSEDTSVPVSKYITHPFWNFVQFFPRWLAPNLLTFSGWSLLFMIYAVTCYYDPHFTASVGDDSKRLPSIWWLIFA FAHFTAHTFDGCDGKQARRTNSSSPLGELFDHGLDSSAAFLIPMSLFSLFHGHPGIVSLELYHIMLACLLGFFVAHWKEYNTGSLFLPWTYDAS QLAVVLVYLLTYFSGVDLWKIQLMPGPFCHVFRWTVYFTSAIVTVAMAVYNMYQGRISKTRGLTFYEGCRPMLSFVGLVALFYTWLLSPAGI LELQPRMFFTATGIVFSNITCRLIVSTMSGQRCQPFNVMLLPVCAIILVFPVQSAQVEVAILALYTAGVAVFHVHYGVFVVRELCDHLHINCFSIKK PUFNSFSWKNVQHVIWL
am sepR (JF970197)	Selenoprotein R	MVKNSDAEWKKKLTPEQFWVCRQKGTLPWSGEYLDLTKGIYKCVCCGSELFSSASKFUFSHKEDRTFHSALEMSSNSNLSPELSVVEKSD NSYGMMRVEVLCRQCDSHLGHVFSDRPHHQL
am sepS (JF970198)	Selenoprotein S	MEAPEETPPNSVPQNKAPNFVVDALTTGLGFFEQYGFVVFVFGAILLVLLWNKVKPYWKELLNKWERQREIDNFDPVKAASQQESLENARRRL QEQHNAKAARFMEDRMQEEEDKRRERIDDWDRHQEGKGYRSKNPKSP DDSSEAGNSTMPKKPKKPLRRSDYSPLSGGGSGFSYRPPRRGAGGGGUG
am eEFSec	Sec elongation factor	GRSNMATS NVLNFNIGVLGHIDSGKTALAKALSSIASTASFDKNPQSKERGITL DLGFSFRVPMPEHLKKYPYEV LQFTLVDCPGHASLIRTIIGG AQIIDMMMLVVDVTKGVQTQTAECVLIGEILCEKMVVXNKIDLLKEEKRXALIEKMSKLLXKTLQNTK FVGSPILAVSAKPGGPESPESESIGT QELVDLLSSMAYIPNRDPSGPLVYAVDHCFSIRGQGTVMGTILSGSVK VNDNIEIPSMKIXKKVKSMQMFKVPVTEASQGXRVGICV

am SECIS-BP	SECIS binding protein	GILKVQPPLAINEVENGASQDQSSQVKNMKRKKKKTGVTGEQVKDINTSIKRTQRPYLDWTMMQTPPEAKAQKNSKRKTILLSSSSMAPFVNH LVKRSSTNRAEVRKTPNALDSTAPLVKRGKERESPSRKKPSRVKRIILKEREKKKARETTEADNTDQSWDDNQIDVTCEVEAEAKDVIPQEISE NLSEEETAQGVSGKLPSPDDEIAAQIHSRRFREYCSQIPDKEVDLVTIELLKALVRFQDKQFHKDPTKAKQKRRLVGLREVTKHLKLRKLCVI ISSNVERIRSEGGLDETLSSIALCQENQVHLVFALKRQRLGKVLKVPVIVGIFNYNGADDHYNKLIELTQRTKQAYTEKWEETREKLESQQL PGTNMNDLENNQSCEADNTIDSVPENSDDDDEKVGGDNDSGSANEDRITGNDLTIEDV
am SeBP1 (JF970200)	Selenium binding protein	MDTANNCHSGPGYATPLEAMNGPREKLLYLPCIYANTGTEKPDYLATVDADPASPTYSKVIHRLPGPFCGDELHHSWGNACSSCHGDPN QKRNRMLVMPSLGSGRIYIFDVEITNPRAPSIYKIVEPEEVIDKTGLTFLHTAHCLGSGEIMISAMGNKEYEQEGGFVLLDGKTFDVKGRWETK PAPMGYDFWYQPRHNVMISSWEGAPSSFKAGFNPQDIAAGKYGSQHLVWDWTTRTMKQTIDLGVGTIPLEIRFLHDPDQPQGFVGCALQ SSLVRFMKEDKTWGAEKVCQVPSKKVEGWALPEMPLITDIVISLDDKYLYFSNWLHGDIRQYDISDTKSPKLVGGVFGGSITSDDLK VVEDSELSEQPEPCYVKGKRVGGPQMIQVSLDGKRLYVTTSLFSVWDNQFYFNLAKKGSMLLQVDIDTVNGGLKLNPDFCVDFGEEPE GPALAHEVRYPGGDCSFDIWL
am SeBP2 (JF970199)	Selenium binding protein	MATEGHCGCGPGYATPVDAMSGPREEIVYLPCIRTNGLDKPDYLATVDVNPRESFTYSQVIHRLPVPYKDELHHSWGNACSSCYGDSSK KRDRLIMPSLISSRIYIFDVGTDPRAPRIHKIISPEDVAQKTGLGFLHTTHCLASGEVMISLGGKPNGEEGGFVILDGKFDVKGRWECGQP APMGYDFWYQPRLNVMIWTEWELKALTQGFKVEDVETGKYGSRLHVDWTTTHALKQTIDLGVGTIPLEIRFLHDPDQPQGFVGCALSS TIVRFFQNEETWSAETVIKVPKVEGWALPDMPGLITDILISLDDKFLYFSNWLHGDIRQYDIRDPRNPRLVGGVFIGGSIVSDGPVKVVQ DSELSGQPAPCYVKGKRVGGPQMIQVSLDGKRLYVTTSLYVWDNQFYFNLAKKGSMLLQMDVDTVNGGLTLNRDFCVDFGEEPDGPC LAHEVRYPGGDCSSDIWLSKTRPAKL
am TR (JF970201)	Thioredoxin reductase	MAPIQDMIEQNINENTVMVFSKSTCPFCCKVKELFTSLNVSFYAMELDDLNCQSIQDKLKEKTGQRSVFNIFIRGNHVGADATIKLHQD GKLMNLIVPPTTEEYTYDLIVIGGGSGGLACSKAANLGKKVAVLDFVKPSPIGTTWGLGGTCVNVGCIPKLMHQAALLGHSMEDARMFG WEFDQKVEHKWATMRENVQNHIGSLNWAYRVELRDKKVLKYNATGLVNAHTVKAVDKRGRVTEMTAQNIVLATGLRPRYPDIPGAKEY GITSDDLFSLEHNPVKTMIGASYVALECAAGFLAGVGLDVTVLVRSILLRQFDQMAEKIGNDLENHGVHIQRPVPTKIELVEEGTPRKLRLV HYKFLETGEETSIECNTVMFAIGRDPCTKGIGLEDVGVKHPKSGKVIAGDNEQSSVSNIAIGDILEGKLELTPVAIHAGKLLAKRFLGGSNE LCDYVNVATTVFTPLEYGCIGLSEEDAIKYGDDNIEVYHSNYIPLEYTPVKRMAKECYAKLVCNKLDNERVIGFHIAGPNAGEVTQGYAVA IKLGATKQDFDRTVGIHPTVSEVFTTLSTTKRSGKDVSAGGCU

# Abbreviations

ACTB, Beta actin;

BCP, trimethylene chlorobromide;

BSA, Bovine serum albumin;

BSO, L-buthionine-[S,R]-sulfoxinmine;

CA, carbonic anhydrase;

CAT, catalase;

Cq, comparative quantity;

Cys, cysteine;

DAB, 3', 3'-diaminobenzidine;

DI, iodothyronine deiodinase;

DsbA, disulfide bond formation protein A;

DTT, dithiothreitol;

eEFSec, Sec-specific elongation factor;

EST, expressed sequence tag;

GAPD, Glyceraldehyde-3- phosphate dehydrogenase;

GBR, Great Barrier Reef;

GFP, green fluorescent protein;

GI-GPx, gastrointestinal GPx;

GOI, genes of interest;

GPx, glutathione peroxidases;

GSH, glutathione;

H<sub>2</sub>O<sub>2</sub>, hydrogen peroxide;

HPLC, high-Performance liquid chromatography;

HRP, horseradish peroxidase;

ICG, inner control gene;

ICP-MS, inductively coupled plasma-mass spectrometry;

IPTG, isopropyl- $\beta$ -D-thiogalactopyranoside;  
ITLC, instant thin-layer chromatography;  
LOI, loss on ignition;  
MC, 3-methylcholanthrene;  
MFSW, Millipore-filtered sea water;  
MsrA, methionine sulfoxide reductase;  
NADPH, nicotinamide adenine dinucleotide phosphate;  
NF, normalization factors;  
ORF, open reading frame;  
PBS, phosphate-buffered saline;  
PBT, phosphate-buffered saline with 0.5% Tween 20;  
PCB126, pentachlorobiphenyl;  
pGPx, Plasma GPx;  
PHGPx, Peroxidase Phospholipid hydroperoxide GPx;  
RDI, recommended dietary intake;  
ROS, reactive oxygen species;  
SDHA, Succinate dehydrogenase;  
SDS-PAGE, sodium dodecyl sulfate polyacrylamide gel electrophoresis;  
Se, selenium;  
SeBP, selenium binding protein;  
Sec, selenocysteine;  
SECIS, Sec insertion sequence;  
Sel, selenoprotein;  
SOD, superoxide dismutase;  
SPS, selenophosphate synthetase;  
TR, thioredoxin reductases;  
Trx, thioredoxin;  
UBC, Ubiquitin C;  
UTR, untranslated region;